Alma Mater Studiorum – Università di Bologna

Dottorato di Ricerca in **Biologia Cellulare Molecolare**

Ciclo **XXVI**

Settore Concorsuale di afferenza: **05/I1 Genetica e Microbiologia**
Settore Scientifico disciplinare: **BIO/18 Genetica**

Drosophila melanogaster as a model to study host-parasitoid interactions: the case of the polydnaviral protein *Tn*BVANK1

Presentata da: **Luca VALZANIA**

Coordinatore dottorato

Prof. **Vincenzo SCARLATO**

Relatore

Prof. **Giuseppe GARGIULO**

Esame finale anno 2014

Abstract ***4***

1-Introduction ***6***

1.1 Parasitoids 8

1.2 Polydnaviruses 10

1.3 The host-parasitoid association *Heliothis virescens-*

Toxoneuron nigriceps 12

1.4 The Braconidae polydnavirus associated with *T. nigriceps*

(*Tn*BV) 14

1.5 *TnBVank1* 17

1.6 *Drosophila melanogaster* as a model system 18

1.7 Overview of *Drosophila* development 19

1.8 The role of the steroid hormone ecdysone in *Drosophila*

melanogaster 21

1.9 The prothoracic gland: the site of ecdysteroidogenesis 28

1.10 Ecdysone biosynthesis 29

1.11 Cholesterol trafficking in steroidogenic cells 33

2-Research Aims ***36***

3-Materials and Methods ***38***

3.1 Fly food 39

3.2 Fly strains 39

3.3 Genetic crosses 41

3.4 Larval length measurements 42

3.5 20-hydroxyecdysone (20E) titration 42

3.6 Rescue experiments 42

3.7 Prothoracic gland and cellular size measurements 43

3.8 Immunofluorescence Microscopy 43

3.9 Antibodies 44

3.10 Terminal deoxynucleotidyl transferase-mediated dUTP Nick End Labeling (TUNEL) Analysis 46

3.11 Filipin and Oil Red O stainings 46

3.12 Colocalization analysis 47

3.13 Statistical analyses 47

4-Results ***48***

4.1 The expression of *TnBVank1* arrests development during larval stage three 49

4.2 *TnBVank1* expression in the prothoracic gland cells blocks the larva-to-pupa transition 52

4.3 *phm-Gal4>TnBVank1* larvae contain low levels of 20-hydroxyecdysone 54

4.4 The expression of *TnBVank1* affects the PG morphology 58

4.5 The expression of *TnBVank1* in the PG impairs the cytoskeletal network 64

4.6 *TnBVank1* expression causes increased accumulation of lipids in PG cells 68

4.7 The organization of the cholesterol trafficking pathway in PG cells 70

4.8 The endocytic pathway is altered in PG cells expressing *TnBVank1* 72

4.9 *Tn*BVANK1 is localized in multivesicular bodies 74

4.10 The role of ALIX in the endosomal trafficking 76

4.11 In PG cells *Tn*BVANK1 colocalizes with ALIX positive endosomes 77

4.12 ALIX knockdown in the PG cells impairs larval development and lipid endosomal trafficking 79

5-Discussion ***81***

6-References ***88***

Abstract

Parasitic wasps attack a number of insect species on which they feed, either externally or internally. This requires very effective strategies for suppressing the immune response and a finely tuned interference with the host physiology that is co-opted for the developing parasitoid progeny. The wealth of physiological host alterations is mediated by virulence factors encoded by the wasp or, in some cases, by polydnaviruses (PDVs), unique viral symbionts injected into the host at oviposition along with the egg, venom and ovarian secretions. PDVs are among the most powerful immunosuppressors in nature, targeting insect defense barriers at different levels.

During my PhD research program I have used *Drosophila melanogaster* as a model to expand the functional analysis of virulence factors encoded by PDV focusing on the molecular processes underlying the disruption of the host endocrine system. I focused my research on a member of the *ankyrin* (*ank*) gene family, an immunosuppressant found in bracovirus, which associates with the parasitic wasp *Toxoneuron nigriceps.* I found that ankyrin disrupts ecdysone biosynthesis by impairing the vesicular traffic of ecdysteroid precursors in the cells of the prothoracic gland and results in developmental arrest.

1-Introduction

Starting from the second half of the last century a responsible use of planet's natural resources to protect the environment for future generations has become a priority.

In this context, a major issue which must be drastically reduced is the indiscriminate use of pesticides to control food production. While the control of economically important pest insects is still largely based on the use of chemical insecticides, the use of biological control agents is a valid alternative. Bio-insecticides, natural molecules deriving from bacteria, viruses, plants and animals, are environmentally safe, biodegradable and have much higher specificity than chemical pesticides, which instead display a wide spectrum of negative effects on all organisms, including humans.

These considerations stimulated an increase of studies aimed at the identification, isolation, characterization and production of molecules that could be used as bio-insecticides. In particular, strong efforts have been directed towards investigations of the control strategies used by insect's natural enemies.

Among these enemies, parasitoids are attracting special interest because they have developed an impressive range of sophisticated strategies of host colonization which often eventually kill the parasitized hosts. Adult females lay their eggs in or on host bodies, where maternal and virulence factors create favorable conditions for the development of parasitoid progeny. Therefore, the study of physiological and molecular mechanisms underlying these host-parasitoid associations promises to yield candidate bioactive molecules that could be used as means to control pests attacking a wide variety of commercial crops.

1.1 Parasitoids

Parasitoids are entomophagus insects that parasitize other arthropods exploiting their host for both nourishment and reproduction, and at the same time damaging it. Their life style falls between parasitism and predation: they lay their eggs either at the surface or into an arthropod host, generally another insect, often, but not necessarily, during the larval or pupal stages, perform their own larval development at its expense, and end-up killing their host as predators.

Even if various organisms use the parasitoid life style, it is mainly studied in holometabolous insects. Although there are parasitoid insect species in six different orders (Diptera, Coleoptera, Lepidoptera, Trichoptera, Neuroptera and Strepsiptera), more than 80% of the described species are Hymenoptera (Quicke, 1997).

Parasitoids have developed a huge variety of strategies to colonize their hosts through specialized mechanisms generated by long adaptive processes occurred within host-parasitoid interactions (Vinson and Scott, 1974; Vinson and Iwantsch, 1980; Godfray, 1994; Quicke, 1997).

Based on their specific colonization features, parasitoids can be classified for example as solitary or gregarious depending on the number of eggs laid, as ectoparasitoids which feed outside the host body, and endoparasitoids, which feed inside the host body (Godfray, 1994); and as koinobionts and idiobionts depending on their behavior. Idiobiont females block host development by injecting specific secretions which are able to preserve host tissues and/or facilitate its digestion by their larvae. Koinobionts, instead, allow host growth until the maturation of their own progeny is complete. Koinobionts include the so called *conformers*, endoparasitoids that conform their own development to host physiology, and the *regulators*, endoparasitoids able to alter host physiology to create an environment suitable for successful egg development.

Generally, *regulators* parasitize early host stages and modulate host physiology, morphology and development, redirecting host metabolism to their own advantage. Therefore, a close anatomic-physiological interaction is established between the host and the parasitoid, which generally shows a significant degree of morphological simplification combined with a high degree of specialization (Pennacchio and Strand, 2006). The latter is converted in the association of the parasitoid species with only a given host species, or a wider but homogenous systematic group. This has led, in turn, to the evolution of fine regulatory mechanisms allowing the parasitoid to evade host immune defenses.

Host regulation is exerted by the action of both maternally-derived and embryonic factors. For example, there are special polyploid cells, the teratocytes, generated by the dissociated embryonic membrane when the egg hatches. These cells circulate freely within the host's haemolymph and they grow in size without undergoing cell division (Pennacchio and Strand, 2006). These cells influence host metabolic and endocrine balance, allowing parasitoid development.

Maternal factors of host regulation consist of venom and ovarian fluid proteins. They are injected into the host during oviposition, and play a key role in the induction of the major alterations observed in parasitized hosts. In certain wasp groups the ovarian fluids also contain a symbiotic virus of the family *Polydnaviridae*.

1.2 Polydnaviruses

Polydnaviruses (PDVs) are among the major host regulation factors used by parasitic wasps to subdue their hosts. They function as immunosuppressant and cause a number of developmental and reproductive alterations associated with disruption of the host's endocrine balance (Turnbull and Webb, 2002). These parasitic insects have a peculiar injection device, the ovipositor, which is used to deliver the egg along with viral particles into the host body (Figure 1) (Beckage and Gelman, 2004). Unlike most viruses, PDVs are not transmitted by infection, indeed no virus replication occurs in parasitized host tissues. PDVs are integrated as proviruses in the genome of parasitoid wasps and their transmission to offspring is strictly vertical, through the germline.

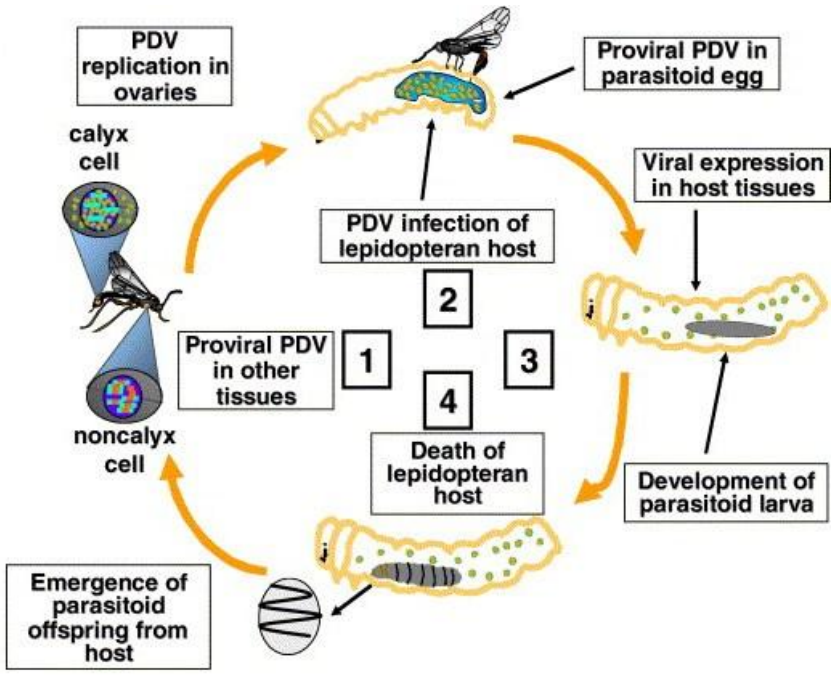

Figure 1. Life cycle integration of PDV and parasitoid wasps. 1: PDV genes are integrated into wasp chromosomes, but replicate only in female wasp calyx cells. 2: Female wasp injects eggs and PDV into host. 3: PDV is expressed in wasp host, suppressing its immune system and facilitating parasitoid development. 4: Parasitoid wasp larva kills its host during emergence (Webb et al., 2006).

The genome encapsidated in the PDV viral particles is made of multiple circular dsDNA segments, which have an aggregate size ranging between 190 and 600 kb (Webb and Strand, 2005).

PDVs can only replicate in pupal and adult stages in the epithelial cells of the calyx, a specific region of the ovary, where they accumulate to a high density and are injected at oviposition, along with the venom and the egg. Free viral particles infect the host tissues and express virulence factors that alter host physiology in ways essential for offspring survival (Strand, 2010).

The *Polydnaviridae* are a unique family of insect viruses with peculiar molecular features of their genomes and with obligate association with endoparasitoid wasps (Stoltz et al., 1984; Volkoff et al., 2002). They are composed of two genera with distinct evolutionary origins, bracoviruses and ichnoviruses, associated with braconid and ichneumonid wasps, respectively, (Turnbull and Webb, 2002). Bracovirus-bearing wasp species have a common ancestor. The classical hypothesis is that bracoviruses originate from an ancestor virus initially integrated into the genome of the ancestor wasp species that lived 73.7 ± 10 million years ago (Whitfield, 2002). The encapsidated genomes of all PDVs have clear eukaryotic architectural features characterized by low coding density and many intron-containing genes, which are often members of gene families (Espagne et al., 2004; Webb et al., 2006). Evolutionary convergence has favored the selection of gene families shared by both ichnoviruses and bracoviruses, among which, protein tyrosine phosphatases (PTP) and ankyrin motif proteins (ANK), widely distributed in many PDVs and expressed to different degrees in virtually all host tissues analyzed so far (Strand, 2012b). The wide distribution of these genes indicates that they play a key role in successful parasitism. However, the mechanistic aspects involved

have been only marginally characterized to date, largely in terms of immune suppression and developmental alterations (Strand, 2012a).

1.3 The host-parasitoid association *Heliothis virescens* - *Toxoneuron nigriceps*

The host-parasitoid complex *Heliothis virescens* (Fabricius) (Lepidoptera, Noctuidae) - *Toxoneuron nigriceps* (Viereck) (Hymenoptera, Braconidae) is one of the better characterized model systems so far (Beckage, 1993).

T. nigriceps, formerly in the genus Cardiochiles (Whitfield and Dangerfield, 1997), is an endophagous parasitoid of the tobacco budworm *H. virescens* larvae (Figure 2).

Figure 2. *Toxoneuron nigriceps* parasitizes a tobacco budworm larva, *Heliothis* virescens (Pennacchio et al., 2003).

T. nigriceps females can successfully parasitize host at any larval stage from first to early fifth instar, but parasitoid development is arrested in the first instar until the host reaches the last larval stadium, at which point the parasitoid molts to the second instar

(Pennacchio et al., 1993). Parasitized *H. virescens* last instar larvae fail to pupariate and, as it happens in other host-parasitoid associations, they show the suppression of the immune system and alterations in the endocrine balance (Pennacchio and Strand, 2006). The modified biochemical profile of haemolymph from parasitized *H. virescens* leads to an increased concentration of proteins, resulting in a better nutritional environment for the developing parasitoid larvae (Pennacchio et al., 2003).

The larval developmental arrest of the host is due to a peak of juvenile hormone (JH) (Li et al., 2003), associated with the suppression of 20-hydroxyecdysone (20E) production, and gradual accumulation of polar ecdysteroids (Pennacchio et al., 2001). These hormonal alterations are caused by maternal (calyx fluid and venom) and embryonic-derived (teratocytes) host regulatory factors of parasitic origin. The combined action of maternal secretions and *T. nigriceps*-associated bracovirus (*Tn*BV) inactivates the prothoracic gland in last instar host larvae, without altering the PTTH production (Tanaka and Vinson, 1991), while the teratocytes transform the 20E into inactive polar compounds (Pennacchio et al., 1994). It has been demonstrated that teratocytes also produce parasitism-specific proteins (PSP) that are released into the host haemolymph. PSP are involved in the inhibition of host immune reaction, in the facilitation of the parasitoid larva egression by aiding on the digestion of the host cuticle, since *T. nigriceps* larva lacks an elaborated mandibular apparatus, or in the accumulation of host nutrients to support parasitoid larval development (Consoli et al., 2007).

Furthermore, the hormonal disruption in *H. virescens* larvae after *T. nigriceps* parasitization prevents normal replacement of the midgut epithelium, which undergoes cell death during the fifth instar, making available additional nutritional resources for parasitoid larval development (Tettamanti et al., 2008). Host proteins represent a rich

source of aromatic amino acids that may be required at the end of parasitoid larval development.

1.4 The Braconidae polydnavirus associated with *T. nigriceps* (*Tn*BV)

*Tn*BV is a typical polydnavirus, showing a segmented genome, made of circular dsDNA molecules, which range in size from 2.5 kb to 23 kb (Varricchio et al., 1999). PDV genes can be classified into three classes according to their different spatial and temporal expression patterns. Class I genes are expressed in the wasp during virus replication, class II genes are expressed in the lepidopteran host after parasitization and class III genes are expressed in both hosts (Theilmann and Summers, 1988). Class I genes are thought to be associated with virus replication, class II genes with disruption of lepidopteran physiology and class III genes with unspecified functions that may be important in both hosts (Webb, 1998). Most of identified and characterized *Tn*BV genes belong to class II.

The first *Tn*BV gene isolated (*TnBV1*) is small in size and contains a single intron. *TnBV1* cDNA encodes for a putative protein of 124 amino acids with a molecular mass around 15 kDa. This protein shows no striking sequence similarity with other known proteins and it contains one potential N-linked glycosylation site, one potential phosphorylation site for cAMP and cGMP-dependent protein kinases, and two protein kinase C phosphorylation sites. The *TnBV1* gene produces a transcript of about 0.5 kb starting from 12 h after parasitoid oviposition, which abundance increases rapidly and peaks between 24 h and 48 h after parasitization (Varricchio et al., 1999). The *TnBV1* transcript is present, exclusively in parasitized host tissue, in both fat body and haemocytes, showing a much higher level of expression in haemocytes. The transient expression of this gene in different cell types, especially in haemocytes, suggests that it

may have a role in immune suppression. Also, detection of *TnBV1* mRNA in the host's prothoracic gland indicated a possible influence on endocrine and developmental disruption (Malva et al., 2004).

The second *Tn*BV gene (*TnBV2*) characterized (Falabella et al., 2003) contains two small exons and a small intron encoding for a putative protein composed of 153 amino acids, with a calculated molecular mass of 18 kDa. The gene produces a transcript of 0.6 kb in parasitized hosts, as early as 6 h after parasitoid oviposition, and its abundance increases rapidly and reaches the maximum level between 24 h and 48 h after parasitization. The same 0.6 kb transcript is present, 48 h after parasitoid oviposition, in various host tissues, such as fat body, haemocytes, prothoracic gland and the head/thorax region (Falabella et al., 2003). A conserved retroviral type aspartic protease domain (Rawlings and Barrett, 1995), from amino acid 42 to amino acid 119, with the characteristic Asp–Thr–Gly active site, is located in a conserved region in the *Tn*BV2 gene product (Malva et al., 2004).

The major gene family identified in the *Tn*BV genome codes for protein tyrosine phosphatases (PTPs) with 13 members expressed in host different tissues. The large number of genes in the bracovirus PTP families, the complex profile of their expression and their key role, along with tyrosine kinases, in the regulation of signal transduction pathways (Andersen et al., 2001), suggest that these proteins may induce the alteration of several physiological traits of parasitized hosts (Falabella et al., 2006).

Two cDNAs have been identified in this gene family: the first (*TnBVPTP5*) codes for a putative protein composed of 294 amino acids and the second (*TnBVPTP7*) codes for a putative protein composed of 293 amino acids, both with a calculated molecular mass of 34.7 kDa (Falabella et al., 2006). At 24 h post-parasitsm, *Tn*BVPTP5 and *Tn*BVPTP7 are expressed in haemocytes and in fat body from the thorax region of the host larvae

and only the *Tn*BVPTP7 is also observed in prothoracic gland. This suggests that PTPs expression may be tissue- and/or substrate-specific (Falabella et al., 2006). The presence of PTPs in the haemocytes of parasitized host larvae (Provost et al., 2004) suggests that these genes reinforce and maintain the haemocyte inactivation mechanisms triggered soon after parasitoid oviposition by the combined action of the venom and *Tn*BV expression (Ferrarese et al., 2005).

Another gene family found in the bracovirus associated with *T. nigriceps* includes members which code IκB-like proteins (ANK). These putative proteins, consisting mostly of ankyrin repeats, display significant sequence similarity (approximately 50%) with members of the IκB protein family, which act as inhibitors of NF-κB signaling pathways in insects and vertebrates (Silverman and Maniatis, 2001), but lack the regulatory domains controlling their signal-induced degradation (Falabella et al., 2007).

In *Drosophila*, the IκB protein Cactus regulates multiple cellular responses activated by the nuclear import of a set of NF-κB/Rel proteins, which control embryonic dorsoventral patterning (Bergmann et al., 1996) and antimicrobial response (De Gregorio et al., 2001; Hoffmann, 2003).

In parasitized *H. virescens* larvae the ANK proteins, along with ovarian proteins, venom components and other PDV products, bind irreversibly to NF-κB/Rel immunoreactive proteins which function is repressed by cytoplasmic sequestration. These larvae are unable to encapsulate foreign invaders because of the PDV-induced disruption of NF-κB signaling that possibly affects both the humoral and cellular immune responses (Falabella et al., 2007).

Three open reading frames were found by genome sequencing in *Tn*BV that were denoted *TnBVank1–3*. *TnBVank1* and *TnBVank3* were isolated from a library prepared with mRNAs extracted from haemocytes of parasitized *H. virescens* larvae, but not

TnBVank2. This result indicates that *TnBVank2* may correspond to a pseudogene or may be expressed and functional in a different host (Falabella et al., 2007).

1.5 *TnBVank1*

TnBVank1 is located on a 4.7 kb genome segment and codes for a putative protein composed of 155 amino acids with a calculated molecular mass of 17.1 kDa. The *Tn*BVANK1 protein predicted from its isolated cDNA is made up of an ankyrin domain comprising four repeats, which show similarity with repeats 3–6 of Cactus and IκBα (Figure 3) (Falabella et al., 2007). Interestingly, *Tn*BVANK1, like the other viral ANK proteins, does not contain the N-terminal IKK target motif that mediates the signal-induced degradation of Cactus or the C-terminal PEST domain, present in the Cactus/IκB proteins, which is involved in rapid protein turnover (Rogers et al., 1986).

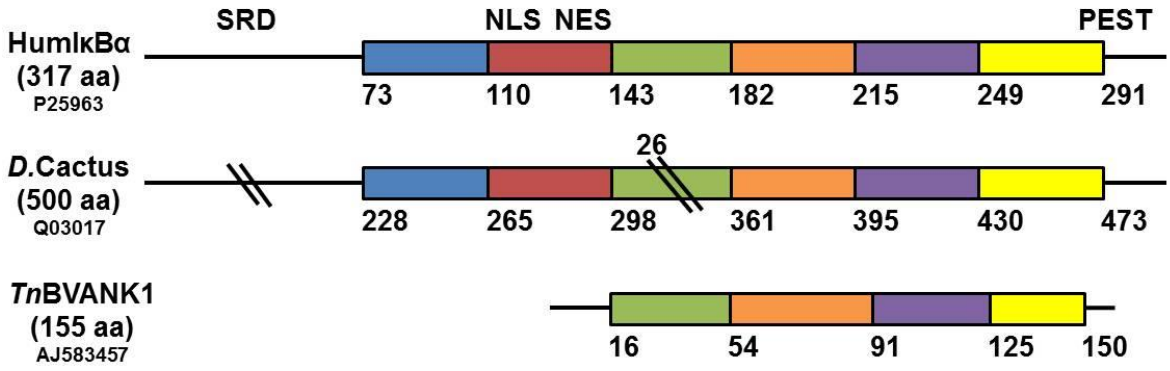

Figure 3. Schematic representation of the protein encoded by *TnBVank1* gene compared with the ankyrin repeats of human (Hum) IκBα and *Drosophila* (*D.*) Cactus. The GenBank accession numbers are indicated below the name of the proteins. The numbers under each protein scheme indicate the amino acid positions delimiting the different ankyrin repeats. HumIκBα regulatory regions: SRD, signal-receiving domain mediating phosphorylation and ubiquitination; PEST, region responsible for rapid protein turnover; NES, leucine-rich nuclear-export sequences, NLS, nuclear-localization signal. Modified from (Falabella et al., 2007).

In the haemocytes of *H. virescens* larvae after parasitization by *T. nigriceps*, *TnBVank1* was transcribed very early (3 h post-parasitization) and the level of its expression declined clearly by 48 h post-parasitization (Falabella et al., 2007).

1.6 *Drosophila melanogaster* as a model system

From the pioneering studies of T. H. Morgan and members of his laboratory in the early 1900s, *Drosophila melanogaster* has early become the most characterized model organism for genetic studies due to the relative simplicity of its genome, the shortness of its life cycle and the abundance of progeny.

With the development of molecular biology techniques and genome sequencing, the fruit fly has served as an excellent model system for studying the mechanisms regulating essential biological processes and has had a major role in unraveling the molecular mechanisms at the basis of almost all metazoan development and physiology. The availability of genome sequences, the ease of genetic manipulation, and the large collection of available mutants make *Drosophila* an attractive system that has enabled a better understanding of different diseases at the molecular level (Niwa and Niwa, 2011). More recently, studies on hormonal homeostasis and metabolism have also been performed in this excellent genetic model organism. Similar to vertebrates, insects require cholesterol as a precursor for steroid hormones and as a structural component of cell membranes (Niwa and Niwa, 2011). The regulation of ecdysteroidogenesis has been studied continuously for the past several decades and recent discoveries using *Drosophila* molecular genetics have advanced our knowledge. For example, studies with both invertebrates and vertebrates revealed an important conserved property in steroidogenesis, the involvement of cytochrome P450 enzymes (CYPs) (Beckstead and Thummel, 2006; Rewitz et al., 2006b). Thus, studying steroidogenesis in insects, and in

particular in the model organism *Drosophila melanogaster*, can not only help gain insights into the biosynthesis of steroid hormone but may also provide valuable information about the regulation of insect development.

1.7 Overview of *Drosophila* development

The *Drosophila* life cycle is summarized in Figure 4. At 25° C the development from egg to adult takes approximately 10 days and includes four distinct developmental phases: egg, larva, pupa and adult. Embryonic development lasts for about 24 h, after which a feeding larva hatches from the egg. The larvae undergo three successive stages, referred to as larval instars: L1, L2 and, L3, which last for about 24 h, 24 h, and 48 h, respectively. At the end of the third instar, larvae cease to feed and enter a wandering stage in search of a suitable site for pupariation. The pupal phase holds over the next four days and on the fifth day flies emerge from their pupal cases (Mulinari, 2008).

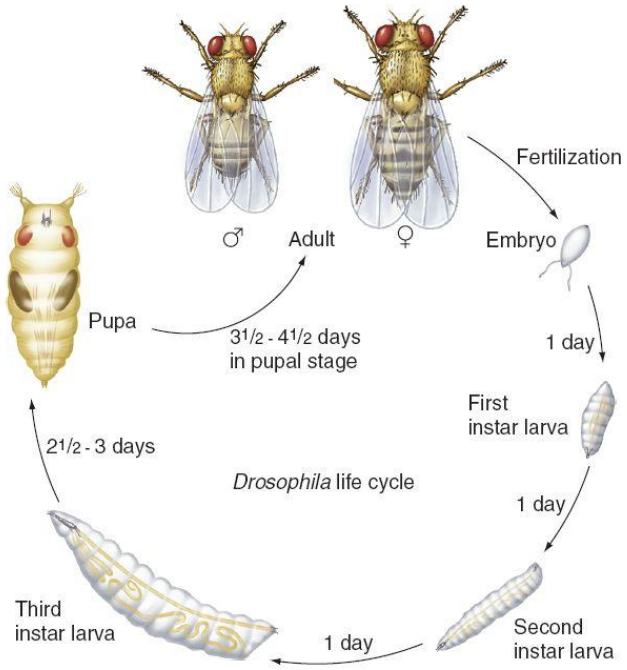

Figure 4. The life cycle of *Drosophila melanogaster*. At 25°C the complete life cycle lasts approximately for 10 days. Larvae molt through three larval instars before metamorphosing into their adult form (Hartwell et al., 2011).

The larva is characterized by two cellular types: larval cells, that are polyploid, and imaginal cells that are diploid. Imaginal cells segregate precociously from the surrounding larval cells, forming small cell groups at 9-10 h after egg deposition and are organized in two fundamental groups, imaginal discs and abdominal histoblasts. Imaginal discs begin an intense proliferative activity from the second larval instar until pupariation, while abdominal histoblasts proliferate later, during the pupal stage. At this moment the majority of larval cells are eliminated and substituted by imaginal cells that originate the integument and the adult appendages. Imaginal discs originate the structures of the head, thorax external appendages, genitalia and adult muscles. The histoblats originate the abdomen structures at the exception of the 8^{th} segment that derives from the genital imaginal disc (Fristrom and Fristrom, 1993). The primary mechanism by which the larva grows is molting. At each molt the entire cuticle of the insect, including its many specialized structures, as well as the mouth armature and the spiracles, is shed and rebuilt again. During each molt, therefore, many reconstruction processes occur leading to the formation of structures characteristic of the ensuing instar. The growth of the internal organs proceeds gradually and seems to be largely independent of the molting process, which mainly affects the body wall. Organs such as Malpighian tubes, muscles, fat body, intestine and ring gland grow by an increase in cell size; the number of cells in the organ remains constant. The imaginal discs, on the other hand, grow chiefly by cell multiplication and the size of the individual cells remains about the same (Deepa Parvathi et al., 2009).

A series of developmental steps by means of which the insect passes from the larval into the adult organism is called “metamorphosis”. The most drastic changes in this transformation process take place during the pupal stage. The larva everts its anterior spiracles and becomes motionless. Metamorphosis involves the destruction of certain

larval tissues and organs (histolysis) and the organization of adult structures from imaginal discs (Demerec and Kaufman, 1996). The duration and extent of these transformation processes vary greatly for the different organs involved. Larval organs which are completely histolyzed during metamorphosis are the salivary glands, the fat bodies, the prothoracic gland, the intestine and apparently the muscles. The extremities, eyes, mouthparts, antennae, and genital apparatus differentiate from their appropriate imaginal discs, which were already present in the larval stage and which undergo histogenesis during pupal development (Milislav, 1950). When metamorphosis is complete, the adult flies emerge from the pupal case.

1.8 The role of the steroid hormone ecdysone in *Drosophila melanogaster*

The transformation from larva to adult is one of the most fascinating processes of insect biology and is characterized by different developmental phenomena, including cellular proliferation, tissue remodeling, cell migration and programmed cell death. Cells undergo one or more of these processes in response to hormone secretion. In particular, in *Drosophila* most of developmental processes are governed primarily by ecdysone (E) and juvenile hormone (JH) whose balance likely affects the nature of developmental transitions. In particular, the JH has a classic “status quo” action in preventing the program-switching action of ecdysone during larval molts (Riddiford et al., 2010).

The molting process is initiated by the brain, where two pairs of neurosecretory cells release prothoracicotropic hormone (PTTH) in response to neural, hormonal or environmental signals. PTTH itself is synthesized as a pre-prohormone, processed intracellularly to its final size (109 amino acids) and released into the hemolymph as a

homodimeric molecule containing intra- and intermolecular disulfide bonds. This neuropeptide stimulates the prothoracic gland to produce ecdysone.

The PTTH transduction cascade has been well elucidated in lepidopteran model insects where the interaction of PTTH with its receptor (Torso in *Drosophila*) at the cell membrane surface of prothoracic gland cells involves phospholipase C (PLC), phosphatidylinositol-4,5-biphosphate (PIP2), inositol triphosphate (IP3) and diacylglycerol (DAG). PIP2 stimulates protein kinase C (PKC) while IP3 elicits the release of calcium from the endoplasmic reticulum into the cytosol where it can act to open both the store operative and L-type voltage gated channels so that even more Ca^{2+} can enter the cell. The increase of calcium is followed by an intracellular cAMP level rising mediated by Ca^{2+}-calmodulin dependent adenylyl cyclase activity and the protein kinase A (PKA), important cAMP-dependent kinase, is rapidly activated (Figure 5).

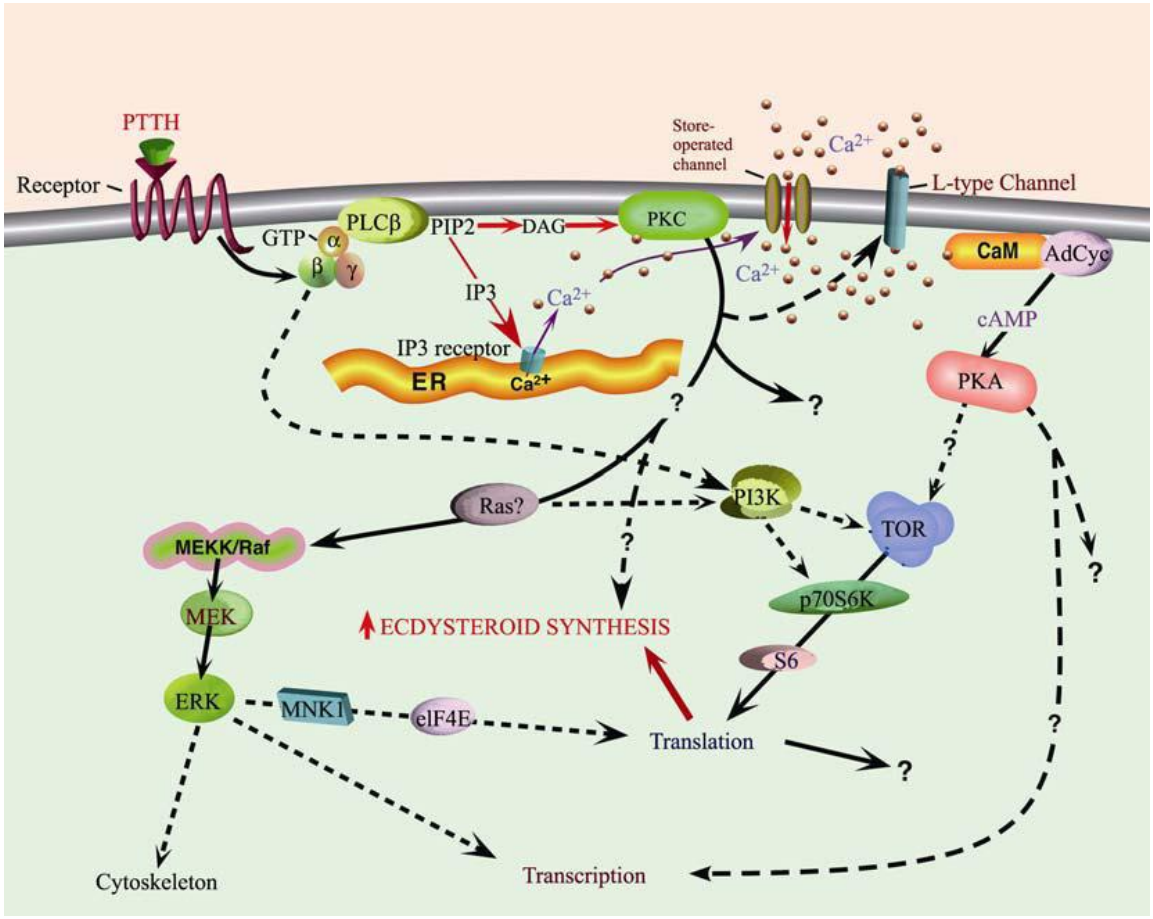

Figure 5. The PTTH signal transduction cascade in prothoracic gland cells. Solid lines indicate demonstrated or highly likely interactions; dashed lines indicate hypothetical relationships. PTTH, prothoracicotropic hormone; PLCβ, phospholipase C β; PIP2, phosphatidylinositol-4,5-biphosphate; DAG, diacylglycerol; IP3, inositol triphosphate; GTP, guanosine triphosphate; cAMP, cyclic adenosine monophosphate; CaM, calmodulin; AdCyc, adenylyl cyclase; ER, endoplasmic reticulum; PKA, protein kinase A; PI3K, phosphoinositide 3hydroxy-dependent kinase; TOR, target of rapamycin; MEKK, MEK kinase; MEK, MAP/ERK kinase; ERK, extracellular signal-regulated kinase; S6, ribosomal protein S6; p70S6K, 70 kDa S6 kinase; MNK 1, MAP kinase-interacting kinase; Ras, a small GTP binding protein; Raf, a serine-threonine kinase; elF-4E, eukaryotic translation initiation factor 4E (Huang et al., 2008).

Of great importance is the phosphorylation in five sites of ribosomal protein S6 which can result in the selective translation of specific mRNAs required for ecdysone biogenesis.

PTTH also activates the MAPK pathway resulting in a rapid increase of ERK phosphorylation, indicating that ecdysteroidogenesis in the prothoracic gland requires the presence of a small basal population of di-phosphorylated (active) ERK molecules (Gilbert, 2004).

During larval stages, ecdysone is produced and released from the prothoracic gland, while in the adult after histolisys of the PG, itis produced in the fat body and in the ovary.

Once released into the hemolymph, ecdysone is modified in peripheral tissues to become the active molting hormone 20-hydroxyecdysone (20E).

Each molt is initiated by one pulse of 20E (Figure 6). For a larval molt, the first pulse produces a small rise in the 20E concentration in the larval hemolymph and elicits a change in cellular commitment. A second, large pulse of 20E initiates the differentiation events associated with molting. The 20E produced by these pulses commits and stimulates the epidermal cells to synthesize enzymes that digest and recycle the components of the cuticle.

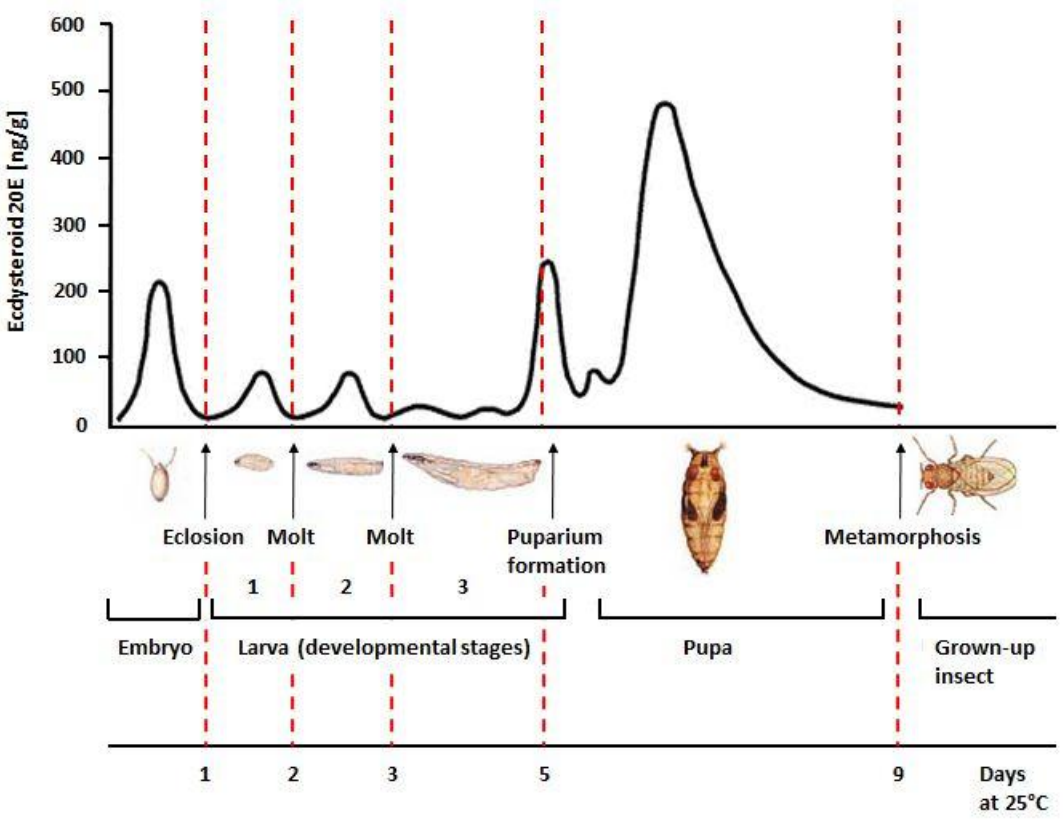

Figure 6. The life cycle of *Drosophila melanogaster* at 25°C in the context of changing ecdysteroid hormone titer. The fruit fly develops through three larval stages before it reaches puparium formation. The larval stages are separated by molts, which are controlled by pulses of ecdysone. Other major developmental events, such as hatching and the transition from larva to pupa, are also controlled by this hormone.

Juvenile hormone is secreted by the corpora allata, one of the two parts of the ring gland. The secretory cells of the corpora allata are active during larval molts and inactive during the metamorphic molt. As long as JH is present, the 20E-stimulated molts result in a new larval instar. In the last larval instar, however, the medial nerve from the brain to the corpora allata inhibits the gland from producing JH, and there is a simultaneous increase in the body's ability to degrade existing JH (Safranek and Williams, 1989). Both these mechanisms cause JH levels to drop below a critical threshold value. This triggers the release of PTTH from the brain (Nijhout and

Williams, 1974) while the resulting 20E, in the absence of high levels of JH, commits cells to pupal development.

After the second ecdysone pulse, new pupa-specific gene products are synthesized (Riddiford, 1982) and the subsequent molt shifts the organism from larva to pupa. It appears, then, that the first ecdysone pulse during the last larval instar triggers the processes that inactivate the larva-specific genes and prepare the pupa-specific genes to be transcribed. The second ecdysone pulse transcribes the pupa-specific genes and initiates the molt (Nijhout, 1994). At the imaginal molt, when ecdysone acts in the absence of juvenile hormone, the imaginal discs differentiate, and the molt gives rise to the adult. Larval tissues such as the gut, salivary glands, and larval-specific muscles undergo programmed cell death and subsequent histolysis. The imaginal discs undergo physical restructuring and differentiation to form rudimentary adult appendages such as wings, legs, eyes and antennae (Jiang et al., 1997).

Hence, ecdysone tightly coordinates the array of physiological changes that characterize each stage of the life cycle. Interestingly, while all tissues are exposed to the hormone, different tissue types have unique responses to the signal. This is ensured by the different spatial and temporal expression profile and unique biochemical properties of its nuclear receptors and by the ability of these receptors to interact with many cofactors.

The ecdysone signal is transduced to target genes in the genome via the ecdysone receptor complex. This complex is made up of a heterodimer of the Ultraspiracle protein (USP) (Oro et al., 1990; Shea et al., 1990; Henrich et al., 1994) and the Ecdysone Receptor (EcR) proteins (Koelle et al., 1991; Koelle, 1992; Yao et al., 1992; Talbot et al., 1993; Thomas et al., 1993; Yao et al., 1993). The EcR/USP complex binds ecdysone and affects transcription of ecdysone target genes. This molecular interaction

is the means by which ecdysone regulates the genes responsible for the plethora of physiological changes that are characteristic of the developmental progression through the life cycle. These early genes encode transcription factors that coordinate the induction of large sets of secondary-response late genes, leading to the appropriate stage and tissue-specific biological responses (Figure 7) (Ashburner et al., 1974).

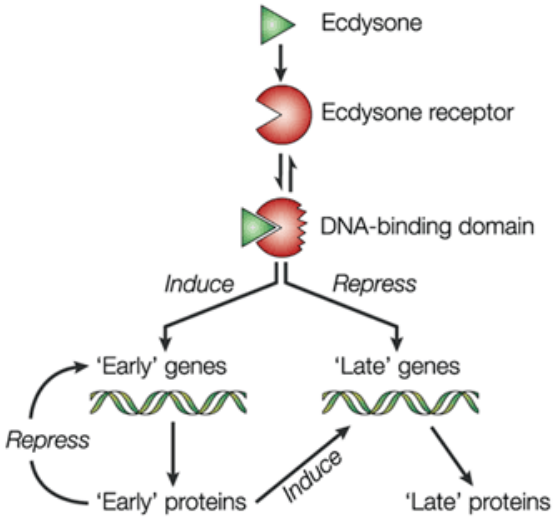

Figure 7. The Ashburner model. Ecdysone binding to its receptor initially activates the expression of genes in the early puff regions, but represses the expression of those in the late puffs. As the proteins encoded by the early puff genes become abundant, they repress their own promoters while activating the expression of late puff genes (Tata, 2002).

Ecdysone regulates a wide range of developmental and physiological responses in *Drosophila*, including reproduction, oogenesis, embryogenesis, post-embryonic development other than metamorphosis. Ecdysone also triggers neuronal remodeling in the central nervous system (Schubiger et al., 1998).

Moreover, it has been demonstrated that ecdysone controls larval growth rate and final adult size and this function is mediated by an antagonistic interaction with insulin signaling (Colombani et al., 2005).

1.9 The prothoracic gland: the site of ecdysteroidogenesis

The *Drosophila* larval ring gland lies above the brain hemispheres with its dorsal portion tilted anteriorly. Its lateral extremities encircle the aorta like a ring, hence the name. The ring gland consists mainly of the prothoracic gland which comprises the anterior and lateral portions of the two limbs of the ring gland, the corpora allata, source of juvenile hormone, which is located in the anterior medial area, and the corpora cardiaca, a neurohemal organ, which occupies the posterior ends of the two limbs (Figure 8) (Dai and Gilbert, 1991).

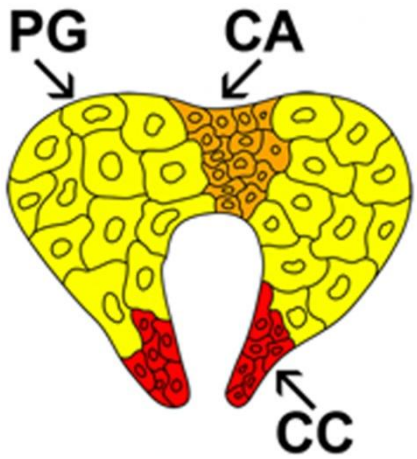

Figure 8. Cartoon of the *Drosophila* ring gland. The ring gland is composed of the prothoracic gland (PG; yellow), the corpora allata (CA; orange) and the corpora cardiaca (CC; red).

It is the prothoracic gland portion of the ring gland that is responsible for the synthesis of ecdysteroids that, in turn, elicit the sequence of events termed molting. This gland usually begins to degenerate during pharate adult life (Wigglesworth, 1955; Herman and Gilbert, 1966) since the molt from pupa to adult is normally the last molt in the life of an insect. At the early wandering third instar, ultrastructural observation reveal some distinct features of an active prothoracic gland cell including abundant tubular smooth

endoplasmic reticulum, numerous and various shaped mitochondria and large and deep intercellular channels (Dai and Gilbert, 1991).

The *Drosophila* ring gland does not persist in the adult fly; in fact it undergoes drastic changes during larva-pupa and pupa-adult transitions. Particularly, the prothoracic gland degeneration is a gradual process initiated after puparium formation. Individual prothoracic gland cell of the same gland also show differential sensitivity during the process, so that the ring gland retains a reduced, but significant, ability to synthesize ecdysteroids during the period of gland demise. However, by 30-40 h after puparium formation, the majority of gland cells are undergoing cell death, characterized by the presence of numerous giant autophagic vacuoles in the cytoplasm and fragmentation of the cytoplasm (Dai and Gilbert, 1991).

1.10 Ecdysone biosynthesis

Among all gene categories required for ecdysteroidogenesis, the enzymes needed for converting cholesterol to 20E are best known, including a group of seven genes named "Halloween": *spook* (*spo*), *spookier (spok) shroud (sro)*, *phantom* (*phm*), *disembodied* (*dib*), *shadow* (*sad*) and *shade* (*shd*) (Jurgens et al., 1984; Nusslein-Volhard et al., 1984; Wieschaus et al., 1984; Ono et al., 2006; Niwa et al., 2010). These genes have likely been highly conserved since the presence of these genes has been confirmed in other insect species (Niwa et al., 2004; Warren et al., 2004; Warren et al., 2006) and encode cytochrome P450 enzymes that are believed to act sequentially in the biosynthesis of ecdysone (Figure 9).

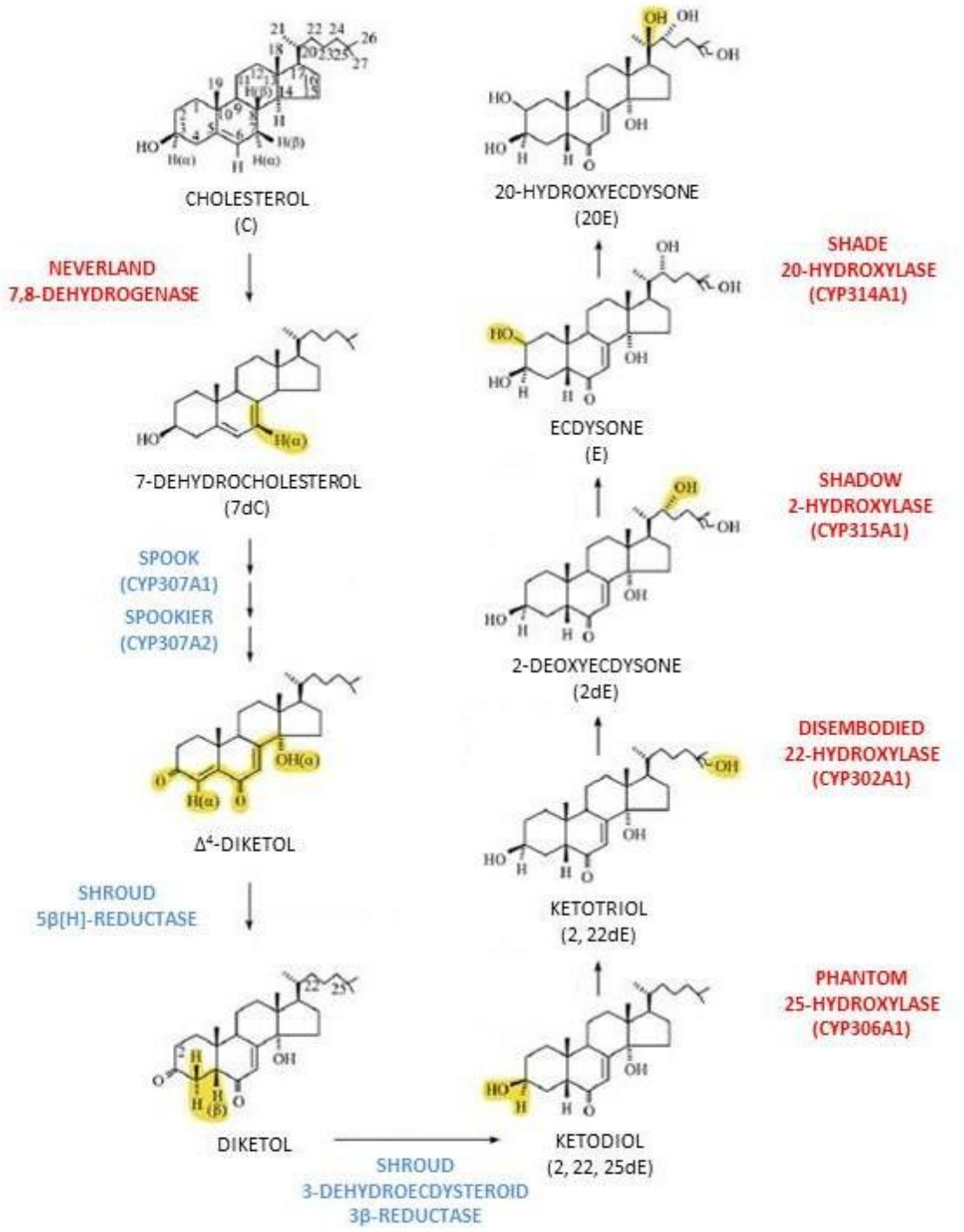

Figure 9. Scheme of the biosynthesis of 20E in *Drosophila*. The 7, 8-dehydrogenase may be encoded by the Rieske non-heme oxygenase gene *neverland*. *spook* and *spookier* encode for a P450 enzyme that may operate in the Black Box along with the product encoded by *shroud*. Modified from (Huang et al., 2008).

In *Drosophila*, synthesis of ecdysone during larval stages takes place primarily within the prothoracic gland cells, while the conversion of ecdysone to 20E occurs in other tissues including the midgut and fat body (Gilbert, 2004). In the adult female, 20E is required for proper oogenesis and follicle cells appear to be an additional major site of ecdysone production. Consistent with these tissues being the major sources of ecdysone and 20E, the *Drosophila phm*, *dib* and *sad* genes, are all expressed in the prothoracic gland cells of the ring gland beginning midway through embryogenesis and show periodic expression within this tissue during larval stages (Chavez et al., 2000; Warren et al., 2002; Niwa et al., 2004; Warren et al., 2004; Warren et al., 2006). During the third instar, expression of these genes correlates well with the hemolymph ecdysteroid titer (Parvy et al., 2005; Warren et al., 2006). In adult female flies, all three genes show pronounced expression in the follicle cells of the ovary beginning at approximately stage 8 of oogenesis. In contrast, the *Drosophila shd* gene is not expressed in the prothoracic gland cells, but instead is found in peripheral target tissues such as the epidermis, midgut, Malpighian tubules and fat body, where Shd mediates conversion of ecdysone into the active hormone 20E (Petryk et al., 2003; Rewitz et al., 2006a). As with the other three enzymes, however, *shd* is also expressed in the follicle cells of the ovary, consistent with a 20E requirement for normal oogenesis (Buszczak et al., 1999; Carney and Bender, 2000; Terashima et al., 2005).

The Halloween gene *spo* is expressed in both the follicle cells of the ovary and in the early embryo prior to the differentiation of the ring gland but is not expressed at detectable levels in the prothoracic gland cells of the ring gland throughout the remainder of embryonic and larval development. This surprising difference in the temporal expression of *spo* compared to that of other Halloween genes suggested that *Drosophila* must have a gene that codes for an enzyme that should substitute for the Spo

protein during larval stages. This gene turns out to be *spookier* (*spok*). Spok is about 57% identical to the *Drosophila* Spo protein and displays the highest degree of identity between all *Drosophila* P450 proteins. As such, Spo and Spok are paralogs and so likely code for P450 enzymes that catalyze the same reaction. *spok* is expressed in the prothoracic gland cells of the ring gland (with *phm*, *dib* and *sad*) from embryonic stage 16 through to the end of larval development and continuing through to the end of pupal-adult development, but not in the adult ovary, exactly complements the expression of *spo*. Just like *phm*, *dib* and *sad*, during larval development, *spok* expression peaks in the ring gland at the end of the each instar, falls at the beginning of the next, to rise again with the rising ecdysteroid titer (Ono et al., 2006).

Unlike vertebrate steroidogenesis, where all the metabolites between cholesterol and the various active steroid hormones have been isolated and identified, no intermediate between the initial hydrogenation product of cholesterol (7-dehydrocholesterol) and the first recognizable ecdysteroid-like product (ketodiol) has been observed in *Drosophila*. These reactions are still a "black box" as defined by Dennis Horn (Gilbert, 2011). *spo* and *spok*, which encode CYP307A1 and CYP307A2 respectively, may operate in the black box converting 7-dehydrocholesterol to Δ^4-diketol and then Shroud reduces Δ^4-diketol to ketodiol. The following biosynthetic reactions are fully understood. In the prothoracic gland cells there are Phm (CYP306A1; 25-hydroxylase) which converts ketodiol to ketotriol, Dib (CYP302A1; 22-hydroxylase) that converts ketotriol to 2-deoxyecdysone and Sad (CYP315A1; 2-hydroxylase) which converts 2-deoxyecdysone to ecdysone. The final reaction occurs in the target tissues where Shd (CYP314A1; 20-hydroxylase) transforms ecdysone in 20E (Figure 9).

Consistent with their sub-cellular localization and enzymatic function (Kappler et al., 1988), both Phm and Spo/Spok are in the endoplasmic reticulum according to their

characteristic N-terminal string of hydrophobic residues, while Dib, Sad and Shd localize at the mitochondria.

Recently, another gene has been characterized whose expression is also up-regulated in the prothoracic gland during the last instar of *Drosophila* development: *neverland* (*nvd*) which encodes a Rieske non-heme iron oxygenase. Like most of the Halloween genes, it is expressed specifically in both the embryonic and larval prothoracic gland and in the nurse cells of the developing adult ovary. Here too, its expression varies in step with both the haemolymph ecdysteroid titer and prothoracic gland activity (Yoshiyama et al., 2006). As Rieske-oxygenases have been shown to catalyze a multitude of reactions, including desaturation reactions, it is possible that Nvd catalyzes the long-sought cholesterol to 7-dehydrocholesterol reaction in *Drosophila* (Yanagawa et al., 2011).

Over the last years, many other genes were identified and characterized, like *without children (woc), molting defective (mld)* and *ecdysoneless (ecd)* (Gaziova et al., 2004; Neubueser et al., 2005). Since these genes do not encode enzymatic products, it has been proposed that they may have a role in regulating ecdysone biosynthesis and in the transfer of the biosynthetic intermediate between cellular organelles.

1.11 Cholesterol trafficking in steroidogenic cells

Since cholesterol is the substrate for steroidogenesis, its uptake, transport and trafficking must be crucial for ecdysone biosynthesis.

There are two general sources of cellular cholesterol: dietary uptake and *de novo* synthesis. Cells maintain proper cholesterol homeostasis through a negative feedback: once dietary derived cholesterol level is high, *de novo* synthesis is inhibited and vice versa. However, in order to regulate *de novo* synthesis, dietary derived cholesterol must

go through multiple steps (intestinal uptake, intercellular transport and intracellular trafficking) before reaching the endoplasmic reticulum (Niwa and Niwa, 2011).

It has been known that insects are not able to synthesize sterols from simple precursors and thus depend solely on dietary sterol uptake for ecdysteroid biosynthesis and other cellular needs (Clark and Block, 1959). Insects take up phytosterols (such as campesterol and β-sitosterol) through the intestinal absorption. Then the intestinal derived sterol is transported peripherally *via* haemolymph. As in the case of mammalian cells, insect cells take up exogenous cholesterol through the classic receptor-mediated low density lipoprotein (LDL) endocytic pathway. LDL binds to its receptor, LDLR, which is then internalized into the endosome. LDL is then released, while LDLR recycles back to the plasma membrane. Once in the endosomal compartment, esterified cholesterol in the LDL is hydrolyzed by lipase to free cholesterol which then leaves the endosomal compartment to move to other membrane compartments including the endoplasmic reticulum, plasma membrane and mitochondria for various cellular usages (Figure 10) (Rodenburg and Van der Horst, 2005).

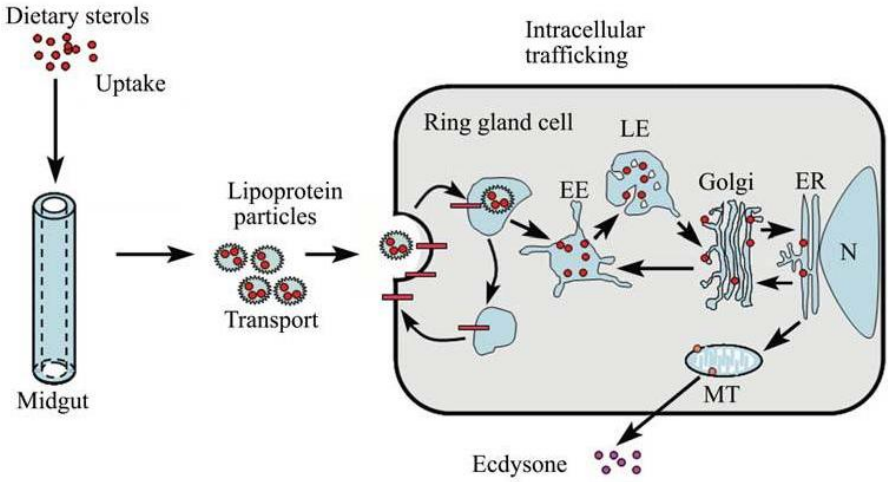

Figure 10. Regulating sterol availability for ecdysteroidogenesis. Dietary sterols are transported in the midgut as lipoprotein particles to the ring gland cells. The lipoprotein particles move into the cell through receptor-mediated endocytosis, then to the endosomal system where sterols are released and transported subsequently to Golgi, ER and mitochondria for ecdysone biosynthesis. EE: early endosome; LE: late endosome; ER: endoplasmic reticulum; N: Nucleus; MT: mitochondria. Modified from (Huang et al., 2008).

2- Research Aims

PDVs are unique viral obligate symbionts of parasitic wasps injected into the host at oviposition along with the egg, venom and ovarian secretions. PDVs infect the host tissues and express virulence factors that alter host physiology in ways essential to offspring survival. These virulence factors suppress the immune response in parasitized lepidopteran larvae and impair development and/or reproduction. To date, most studies have focused on the molecular mechanisms underpinning immunosuppression, whereas how viral genes disrupt the endocrine balance remains largely uninvestigated.

During my PhD research program I have analyzed a member (*TnBVank1*) of the *ankyrin* gene family of the bracovirus associated with *Toxoneuron nigriceps*, a larval parasitoid of the noctuid moth *Heliothis virescens*. The aim of my studies was to gain insight into the molecular mechanisms through which *Tn*BVANK1 acts as a virulence factor disrupting host endocrine system.

To this purpose, I analyzed the effects of *TnBVank1* during *Drosophila* development. *Drosophila* provides an excellent model system to investigate fundamental topics linked to endocrine system because of the relative simplicity of its signaling pathways. Moreover, the well-established genetic and genomic tools define the fruit fly as an ideal model system for studying the molecular mechanisms of essential biological processes.

I focused my studies on directing the expression of *TnBVank1* in the prothoracic gland by using the Gal4/UAS binary system. In particular, I analyzed the involvement of this viral ankyrin protein in the cholesterol endosomal trafficking, the first step of ecdysone hormone synthesis.

3-Materials and Methods

3.1 Fly food

The *Drosophila melanogaster* strains used were grown on a corn meal based food supplemented with glucose, yeast, agar and water. The food is prepared by melting 10 gr of agar and 50 gr of glucose in 1600 ml water. Then 150 gr of corn meal are added and food is cooked for 15 minutes mixing well. Afterward 50 gr of yeast are added and food is cooked for 10 minutes more, again on medium and mixing well. While food is cooking, 4 gr of Nipagine, an antimicotic, are dissolved in 16 ml of EtOH 98% and added. The food is left to dry for at least 2 hours.

3.2 Fly strains

The following stocks are used:

- y^{1},w^{67c23} as a wild-type stock;
- *UASp-TnBVank1/UASp-TnBVank1;UASp-TnBVank1/UASp-TnBVank1;+/+* generated in our lab (Duchi et al., 2010). In the text the transgene will be referred as *UASp-TnBVank1*;
- 1734: w^{*}*;+/+;P{GawB}*h^{1J3} (Brand and Perrimon, 1993), (Bloomington *Drosophila* Stock Center). In the text the transgene will be referred as *hairy-Gal4*;
- 1878: w^{*}*;P{GawB}T80/CyO;+/+* (Wilder and Perrimon, 1995), (Bloomington *Drosophila* Stock Center). In the table will be referred as *T80-Gal4*;
- 5073: w^{*}*;+/+;P{UAS-p35.H}BH2* (Zhou et al., 1997), (Bloomington *Drosophila* Stock Center). In the text will be referred as *UAS-p35*;
- 5535: w^{*}*;P{GAL4-ey.H}4-8/CyO;+/+* (Carrera et al., 1998), (Bloomington *Drosophila* Stock Center). In the table will be referred as *Eyeless-Gal4*;

- 6357: *y^1w^{1118};+/+;P{Lsp2-GAL4.H}3* (Roignant et al., 2003), (Bloomington *Drosophila* Stock Center). In the text and in the table will be referred as *Lsp2-Gal4*;
- 6479: *y^1w^*;P{GawB}sca^{109-68}/CyO;+/+* (Manning and Doe, 1999), (Bloomington *Drosophila* Stock Center). In the table will be referred as *Scabrous-Gal4*;
- 6990: *w^{1118};+/+;P{GawB}C855a* (Hrdlicka et al., 2002), (Bloomington *Drosophila* Stock Center). In the table will be referred as *c885a-Gal4*;
- 7019: *w*;P{w^{+mC}=tubP-GAL80^{ts}}20;TM2/TM6B,Tb^1* (Davis et al., 2003), (Bloomington *Drosophila* Stock Center). In the text the transgene will be referred as *tub-Gal80^{ts};*
- 7374: *y^1w^*;P{UASp-GFPS65C-αTub84B}14-6-II;+/+* (Grieder et al., 2000), (Bloomington *Drosophila* Stock Center). In the text will be referred as *UASp-α-tubulin-GFP*;
- 8700: *w^*;+/+;P{He-GAL4.Z}85,P{UAS-GFP.nls}8* (Zettervall et al., 2004), (Bloomington *Drosophila* Stock Center). In the table will be referred as *Hemese-Gal4*;
- 8760: *w^*;+/+;P{GAL4-elav.L}3* (Luo et al., 1994), (Bloomington *Drosophila* Stock Center). In the table will be referred as *Elav-Gal4*;
- 30140: *w^{1118};P{Hml-GAL4.Î”}2,P{UAS-2xEGFP}AH2;+/+* (Sinenko and Mathey-Prevot, 2004), (Bloomington *Drosophila* Stock Center). In the table will be referred as *Hemolectin-Gal4*;
- 32040: *P{Appl-GAL4.G1a}1*, *y^1w^*;+/+;+/+* (Torroja et al., 1999), (Bloomington *Drosophila* Stock Center). In the table will be referred as *Appl-Gal4*;

- 32119: *w***;+/+;P{GawB}337Y* (Manseau et al., 1997), (Bloomington *Drosophila* Stock Center). In the table will be referred as *337Y-Gal4*;
- v32047: *w*^{1118}*;P{GD7853}v32047;+/+* (Dietzl et al., 2007), (Vienna Drosophila RNAi Center). In the text will be referred as *UAS-ALIX-RNAi*;
- *yw;+/+;phantom-Gal4,UAS-mCD8GFP/TM6B*, kindly provided by C. Mirth (Mirth et al., 2005). In the text will be referred as *phantom-Gal4*;
- *w*;+/+;P0206-Gal4,UAS-mCD8GFP*, a gift from C. Mirth (Mirth et al., 2005). In the text will be referred as *P0206-Gal4*;
- *yw;august21-Gal4/CyO;+/+* was generated in our lab from the stock *yw;august21-Gal4/CyO;phantom-Gal4/phantom-Gal4* kindly provided by M. Jindra. In the text will be referred as *august21-Gal4*.

3.3 Genetic crosses

Females *UASp-TnBVank1* were crossed to males of the different *Gal4* lines. As control, females *y*^{1}*,w*^{67c23} were crossed to males of the same *Gal4* lines.

For microtubules analysis, females *UASp-TnBVank1* were crossed to males *UASp-α-tubulin-GFP;phantom-Gal4*.

To coexpress p35 and *Tn*BVANK1 in PG cells females *UASp-TnBVank1;UASp-TnBVank1;UAS-p35* were crossed to males *phantom-Gal4,UAS-mCD8GFP/TM6B*.

All the previous crosses are performed at 25°C.

For Gal80^{ts} experiment, females *UASp-TnBVank1* were crossed to males *tub-Gal80*^{ts}*;phantom-Gal4,UAS-mCD8GFP/TM6B* at 21°C and then the resulting larvae were shifted to 31°C at 96 h, 72 h and 48 h after egg deposition (AED).

3.4 Larval length measurements

Five *UASp-TnBVank1/+;UASp-TnBVank1/+;hairy-Gal4/+* larvae at different days AED and five control larvae were ice-anesthetized and photographed using a Nikon Eclipse 90i microscope. Images were taken at 4X magnification and the larval length was measured with NIS-Elements Advanced Research 3.10 software.

3.5 20-hydroxyecdysone (20E) titration

This analysis was performed by Professor Sheng Li's group of the Institute of Plant Physiology & Ecology (Shanghai).

Five larvae at different developmental stages were collected and washed with PBS buffer and immediately frozen by liquid nitrogen. Samples were added 200 μl of methanol, homogenized and transferred into 1.5 ml plastic tubes. After 10 minutes centrifugation (12,000 rpm at 4°C) the supernatant was collected into a new tube, the precipitate was re-extracted with 200 μl of methanol and the supernatant was added to the previous one. After 30 minutes on ice, the samples were centrifuged following the same conditions. Samples were dried to remove methanol and then dissolved in the borate buffer. The standard curve was generated according to the standard process of the RIA protocol (Warren et al., 2006) and then the 20E titer in samples was calculated.

3.6 Rescue experiments

UASp-TnBVank1/+;UASp-TnBVank1/+;phantom-Gal4,UAS-mCD8GFP/+ larvae and controls were collected at 106 hours AED and placed in three groups of ten individuals at 25°C in new tubes supplemented with 20E (Sigma) dissolved in ethanol at 1 mg/ml. Control larvae were fed only with ethanol.

3.7 Prothoracic gland and cellular size measurements

For measurements of PG area and its cellular size, confocal images of 50 PGs taken at 40X magnification were quantified with ImageJ software.

3.8 Immunofluorescence Microscopy

Larvae were dissected at room temperature in phosphate buffer saline (1xPBS) pH 7.5 and fixed in 4% formaldehyde in 1xPBS pH 7.5 for 20 minutes at room temperature. After three washes 5 minutes each in 1xPBS pH 7.5, larvae were permeabilized in 1xPBT (1xPBS pH 7.5 + 0.3% Triton X-100) for 1 hour, washed three times 5 minutes each in 1xPBT and 10 minutes in 1xPBT + 2% BSA solution. After that, the larvae were incubated, overnight at 4°C, with primary antibodies diluted in 1xPBT + 2% BSA. Next day larvae were washed three times 10 minutes each in 1xPBT, 10 minutes in 1xPBT + 1% BSA solution and incubated at room temperature on a rotating wheel with secondary antibodies diluted in 1xPBT + 1%BSA. After three washes 5 minutes in 1xPBT, the ring glands were dissected and mounted on microscopy slides in Fluoromount G (Electron Microscopy Sciences), an anti-quenching slide mounting medium. Subsequently samples were analyzed by conventional epifluorescence with a Nikon Eclipse 90i microscope or with TCS SL Leica confocal system. Images were processed using Adobe Photoshop CS4.

TRITC-Phalloidin staining was carried out, after incubation with secondary antibodies, by washing larvae three times 5 minutes each with 1xPBS pH 7.5 and then by incubating larvae for 20 minutes at room temperature with TRITC-Phalloidin (40 μg/ml in 1xPBS pH 7.5; Sigma). After three washes 5 minutes each in 1xPBS pH 7.5, the ring glands were dissected and mounted as indicated above.

For Propidium Iodide nuclear counterstaining, the larvae were treated with RNase A (400 μg/ml in 1xPBT; Sigma) overnight at 4°C. After three washes 10 minutes each in 1xPBT, the larvae were labeled for 2 hours with Propidium Iodide (10 μg/ml in 1xPBT; Molecular Probes) then the ring glands were dissected and mounted in Fluoromount G.

3.9 Antibodies

The following primary antibodies were used in this study:

- polyclonal rabbit anti-Disembodied, Dib, kindly provided by M. O'Connor (Parvy et al., 2005), was raised against the peptide KTLLINKPDAPVLIDLRLRREC of the *Drosophila* Disembodied protein and was used at 1:200;
- polyclonal rabbit anti-Without children, Woc, a gift from M. Gatti (Raffa et al., 2005), recognizes a specific domain of the *Drosophila* Without children protein (aa 230-626) and was used at 1:500 dilution;
- polyclonal rabbit anti-*Tn*BVANK1 (Duchi et al., 2010) is directed against two *Tn*BVANK1 peptides, one located at the N-terminal domain (LLGERNELGNNFFHE) and the other at the C-terminal domain (NDKKMMEILKKNGAK), was used at 1:200 dilution;
- polyclonal rabbit anti-Cleaved Caspase-3 (9661, Cell Signaling Technology, (Fernandes-Alnemri et al., 1994)) detects endogenous levels of a large fragment (17/19 kDa) of activated caspase-3 resulting from cleavage adjacent to Asp175 and was used at 1:50 dilution;
- sheep anti-Digoxigenin-fluorescein (1207741, Roche) is directed against the whole Digoxigenin protein and conjugated with 5(6)-carboxy-fluorescein-N-hydroxy-succinimide ester (FLUOS) and was used at 1:100 dilution;

- monoclonal mouse P1H4 anti-Dynein heavy chain (McGrail and Hays, 1997) recognizes a region of the cytoplasmic dynein heavy chain protein (aa 128-422) and was used at 1:200 dilution;
- monoclonal mouse anti-Rab5 (610281, BD Biosciences) recognizes human Rab5 (aa 1-215) and was used at 1:25 dilution;
- polyclonal rabbit anti-Rab7, kindly provided by A. Nakamura (Tanaka and Nakamura, 2008), recognizes a region of Rab7 protein (aa 184-200) and was used at 1:2000 dilution;
- polyclonal rabbit anti-Rab11, kindly provided by A. Nakamura (Tanaka and Nakamura, 2008), recognizes a region of Rab11 protein (aa 177-191) and was used at 1:5000 dilution;
- polyclonal guinea pig anti-Hrs, a gift from T. Lloyd (Lloyd et al., 2002), recognizes the amino-terminal half (aa1-376) of the Hrs protein and was used at 1:1000 dilution;
- monoclonal mouse anti-ALIX, kindly provided by T. Aigaki (Tsuda et al., 2006), was raised against the full length of ALIX protein and was used at 1:100 dilution.

Secondary antibodies:

- rabbit antibodies were detected with Cy3-conjugated sheep anti-rabbit used 1:1000 (Sigma), Cy3-conjugated goat anti-rabbit used 1:1000 (Jackson), DyLight 649-conjugated goat anti-rabbit used 1:500 (Jackson) and BODIPY-conjugated goat anti-rabbit used 1:2000 (Sigma);

- mouse antibodies were detected with Cy3-conjugated goat anti-mouse used 1:1000 (Jackson) and DyLight 649-conjugated goat anti-mouse used 1:500 (Jackson);
- guinea pig antibodies were detected with DyLight 649-conjugated goat anti-guinea pig used 1:500 (Jackson).

3.10 Terminal deoxynucleotidyl transferase-mediated dUTP Nick End Labeling (TUNEL) Analysis

Five days AED larvae were dissected at room temperature in 1xPBS pH 7.5, fixed in 4% formaldehyde in 1xPBS pH 7.5 for 20 minutes at room temperature. After three washes 5 minutes each in 1xPBS pH 7.5, larvae were dissected and permeabilized for 1 hour with a solution of 1xPBS pH 7.5 + 0.3% Triton X-100 (1xPBT) at room temperature. After three washes 5 minutes each with 1xPBT, larvae were incubated in 250 μl of TUNEL solution (5X Reaction Buffer, 25mM $CaCl_2$, 1mM d-UTP-digoxigenin, 25U/μl TdT) for 90 minutes at 37°C in dark condition. Afterward, larvae were accurately washed several times with 1xPBT and then for 10 minutes in 1xPBT + 2% BSA. Next, larvae were incubated with Cy3-conjugated-digoxigenin antibody for 2 hour at room temperature on a rotating wheel. After incubation, larvae were washed many times with 1xPBT, the ring glands were dissected and mounted in Fluoromount G.

3.11 Filipin and Oil Red O stainings

Larvae were dissected at room temperature in 1xPBS pH 7.5, fixed in 4% formaldehyde in 1xPBS pH 7.5 for 20 minutes and washed three times in 1xPBS pH 7.5 for 5 minutes each. Samples were stained with 50 μg/ml of Filipin (Sigma) for 1 hour or

incubated in an Oil Red O (Sigma) solution at 0.06% for 30 minutes. After incubation larvae were washed twice with 1xPBS pH 7.5 for 5 minutes each, the ring glands were dissected and mounted in Fluoromount-G. Samples were analyzed by conventional epifluorescence with a Nikon Eclipse 90i microscope or with a Nikon Eclipse 90i confocal microscope. Images were processed using Adobe Photoshop CS4.

3.12 Colocalization analysis

Thresholds of confocal images were set in Adobe Photoshop CS4 to exclude background staining. 509 Hrs positive vesicles were analyzed per *Tn*BVANK1 and Hrs staining. 443 *Tn*BVANK1 positive vesicles were analyzed per *Tn*BVANK1 and ALIX staining. 118 Hrs positive vesicles were analyzed per ALIX and Hrs staining.
Images were processed with the CDA plugin of ImageJ to obtain Pearson's coefficient (from +1=complete correlation, to -1=anti-correlation with 0=no correlation) (Zinchuk and Zinchuk, 2008).

3.13 Statistical analysis

Statistical comparison of mean values was performed by unpaired t-test, using GraphPad Prism 4 software.

4-Results

4.1 The expression of *TnBVank1* arrests development during larval stage three

In order to explore the function of the *TnBVank1* gene, I induced its expression during *Drosophila* development through the Gal4/UAS binary system (Brand and Perrimon, 1993). This system is based on two genetic elements kept in different lines: the yeast transcriptional activator Gal4 downstream of a given promoter (*driver*) and the Gal4-dependent UAS cis-regulatory sites upstream of the target gene (*responder*). When responder and driver lines are brought together by crossing, the resulting progeny express the responder in the transcriptional pattern of the driver.

I used a transgenic *Drosophila* stock carrying two copies of the *TnBVank1* gene under the control of *UASp* sequences, which allow the expression either in the somatic cells or in the female germline (Figure 11) (Duchi et al., 2010).

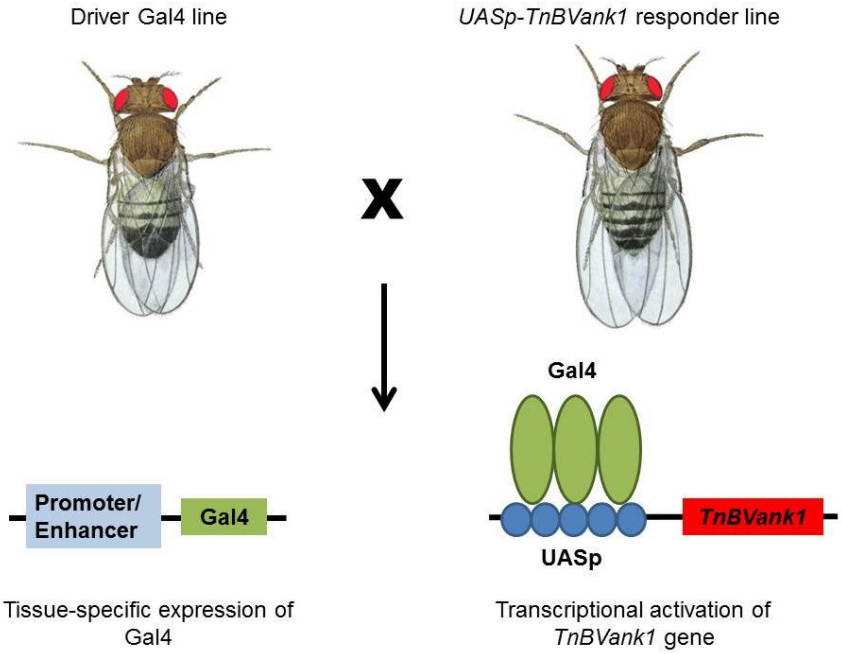

Figure 11. The *TnBVank1* expression is directed using the Gal4/UAS system. Crossing flies of the driver line with the stock carrying the *TnBVank1* gene under the control of *UASp* sequences, the resultant progeny expresses the *TnBVank1* transgene in specific tissues.

The expression of the *TnBVank1* transgene was induced using different *Gal4* drivers. I expressed this transgene during embryonic and larval development using the *hairy-Gal4* driver (*h-Gal4*) (Brand and Perrimon, 1993). This line expresses the UAS-linked genes during the embryonic development and in different larval tissues as brain, ring gland, salivary gland, imaginal discs and midgut. All the *h-Gal4>TnBVank1* larvae completed the embryonic and larval development but, interestingly, failed to pupariate and died after an extended third instar, which lasted up to three weeks (Figure 12A). At four days after egg deposition (AED), when the last larval stage starts, these larvae did not significantly differ in size from the control *yw;h-Gal4* ones (n=5; t=0.8557; NS) (Figure 12B). Interestingly, while control larvae regularly pupariated on day six AED (Figure 12A), the larvae expressing *TnBVank1* continued to feed and significantly increased in size during their prolonged larval life, reaching the maximal length at eighteen days (Figure 12A, C; n=5; t=6.765; $p<0.0001$).

The observed developmental arrest suggested me that *Tn*BVANK1 could have reasonably affected the hormonal endocrine system. Particularly, since *h-Gal4* is expressed in various larval tissues among which the ring gland, the expression of *TnBVank1* gene in this organ could cause the block during development.

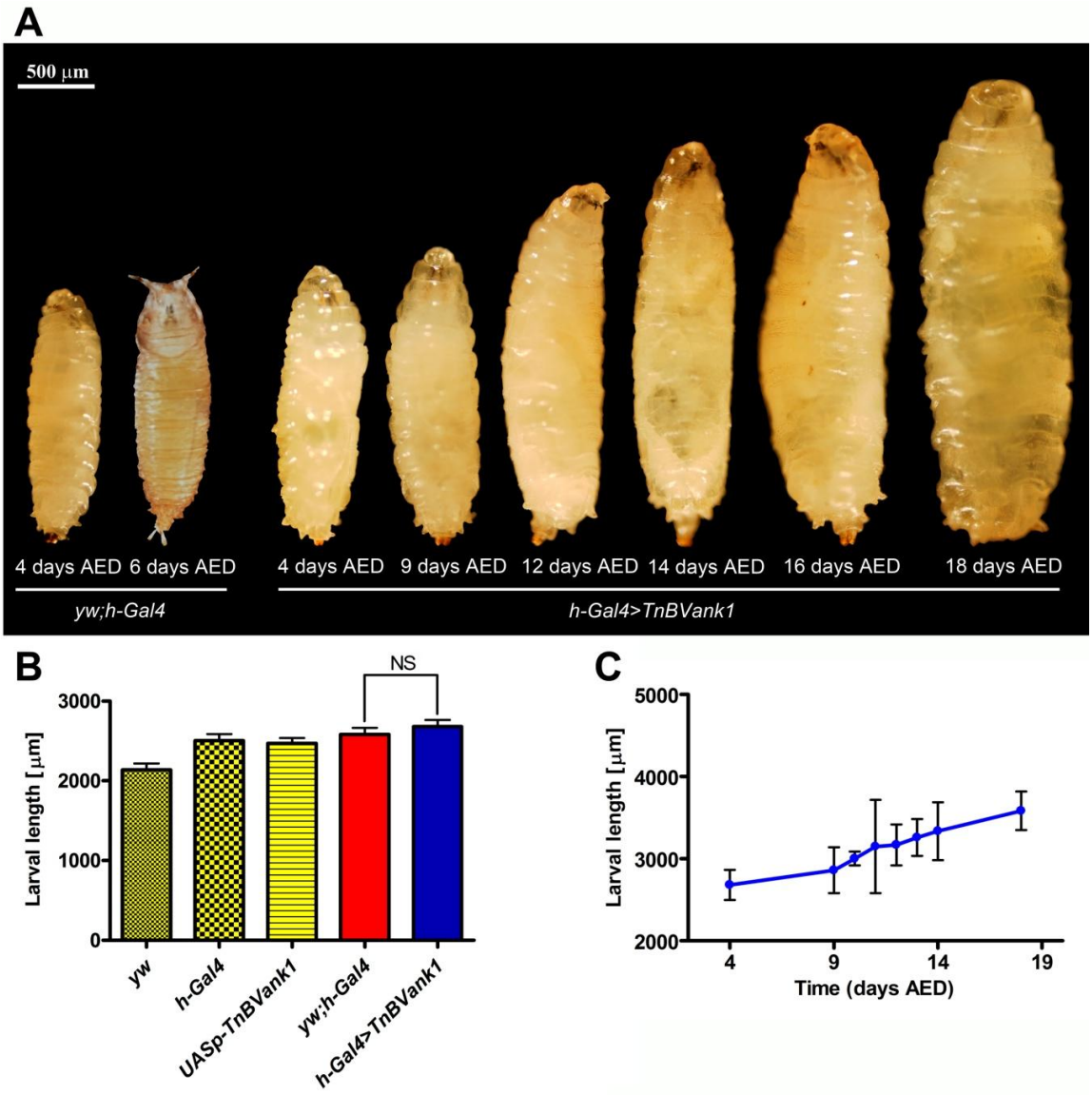

Figure 12. Larvae expressing *TnBVank1* fail to pupariate and continue to grow. (A) Light micrographs of *yw;h-Gal4* larva and pupa (control) and *h-Gal4>TnBVank1* larvae at different days AED. (B) The larval length of five larvae of different genotypes is measured at 96 h AED. Graph represents mean ± standard deviation (SD). There is no significant (NS) length difference between *h-Gal4>TnBVank1* (blue; 2680±83 µm) and *yw;h-Gal4* larvae (red; 2580±82 µm). As additional controls (patterned yellow), the larval length of *yw* and *h-Gal4* and *UASp-TnBVank1* stocks is measured. (C) Five *h-Gal4>TnBVank1* larvae are monitored during their extended third instar and their larval length is analyzed at different days AED. Values are the mean ± SD of three independent experiments. The mean values of *h-Gal4>TnBVank1* larval length at four and eighteen days AED are shown above the bars.

4.2 *TnBVank1* expression in the prothoracic gland cells blocks the larva-to-pupa transition

As described in detail in paragraph 1.9, the *Drosophila* ring gland is the major site of production and release of developmental hormones. It is composed of the prothoracic gland (PG), which synthesizes the ecdysone; the corpora allata (CA) that produce the juvenile hormone, and the corpora cardiaca (CC), which play a key role in the regulation of metabolic homeostasis (Figure 8) (Dai and Gilbert, 1991). To verify if the expression of *TnBVank1* in the ring gland were able to reproduce the effect observed when the transgene was expressed using the *h-Gal4*, I targeted its expression using different ring gland-specific *Gal4* drivers (Figure 13). When the *TnBVank1* gene was expressed in both CA and PG cells using the *P0206-Gal4* driver, the larval development arrested during the third instar showing the same phenotype obtained with *h-Gal4*. Conversely, when the *august21-Gal4* (*aug21-Gal4*) driver specifically targeted the expression of *TnBVank1* in the CA, no effects on development were observed and regular progeny were obtained. Finally, I specifically induced the expression of *TnBVank1* gene in the PG using the *phantom-Gal4* (*phm-Gal4*) driver, which is strongly expressed in this gland. All the larvae failed to pupariate and presented an extended life as shown using the *P0206-Gal4* driver. Therefore, the block of larval-pupal transition is due to the activity of *Tn*BVANK1 in the prothoracic gland cells.

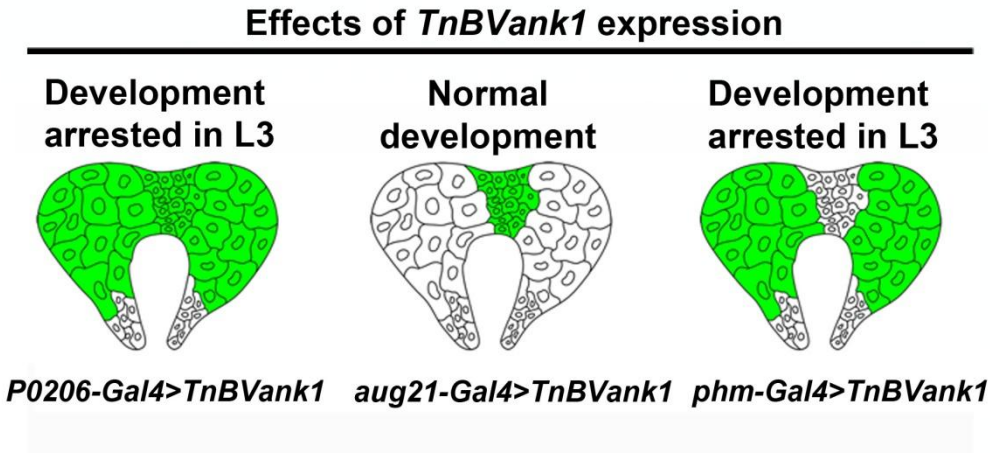

Figure 13. Effects of *TnBVank1* expression in the ring gland. The expression of the *TnBVank1* gene is driven in the different ring gland compartments, highlighted in green, by three *Gal4* drivers. *P0206-Gal4*, expressed in PG and CA, causes the developmental arrest at the last larval stage; *aug21-Gal4* (CA) does not induce any developmental defects; *phm-Gal4* (PG) blocks the transition from larval to pupal stage.

Recently, it has been demonstrated that in insects tissue damage is frequently associated with a systemic injury response, resulting in a delay of development as prolonged larval or pupal stages (Hackney et al., 2012). To verify that this was not the case with the expression of *TnBVank1* in specific tissues, I expressed the transgene in several other tissues using different *Gal4* drivers. Monitoring the timing of development and the adult phenotype, no effects were observed in all cases analyzed (Table 1).

Collectively, these data suggest that the expression of *Tn*BVANK1 has the potential to interfere with the steroid biosynthesis, as further indicated by the targeted expression of this viral ANK protein in the PG, which is characterized by developmental arrest of last instar larvae.

Gal4 driver (Bloomington stocks)	Tissue specificity	Effects on developmental timing	% of normal adults
Eyeless (#5535)	eye disc	None	100 (n=95)
Scabrous (#6479)	eye disc, bristles, proneural clusters, sensory organ precursor cells	None	100 (n=89)
Appl (#32040)	larval nervous system	None	100 (n=66)
Hemolectin (#30140)	lymph glands, circulating hemocytes	None	100 (n=58)
Elav (#8760)	nervous sysytem	None	100 (n=88)
Lsp2 (#6357)	third instar fat body	None	100 (n=80)
Hemese (#8700)	hemocytes and salivary glands	None	100 (n=83)
337Y (#32119)	all late embrionic tissues	None	100 (n=112)
T80 (#1878)	ubiquitous in third instar imaginal discs	None	100 (n=81)
c885a (#6990)	larval optic lobes, wing discs, fat body, leg and eye disc peripodial membranes	None	100 (n=65)

Table 1. Effects of *TnBVank1* expression in specific tissues on developmental timing. All the *Gal4* drivers used are identified by the Bloomington stock center number. For each cross, the percentage (%) of normal adults is calculated by dividing the number of normal adults by the total number of animals of the same genotype.

4.3 *phm-Gal4>TnBVank1* larvae contain low levels of 20-hydroxyecdysone

The developmental arrest induced by *Tn*BVANK1 during the third instar could be due to an insufficient level of 20E to trigger the puparium formation. In order to verify this hypothesis the whole body 20E titer in *phm-Gal4>Tn*BV*ank1* and in control larvae (Figure 14A) was measured by a collaboration with Professor Sheng Li's group of the Institute of Plant Physiology & Ecology (Shanghai) who performed this analysis. At 25°C wild type third instar larvae enter the wandering stage at 110 h AED and then, after the surge of a 20E peak, become white pre-pupae at 120 h AED (Warren et al., 2006). The 20E level measured in *phm-Gal4>TnBVank1* larvae is extremely reduced and significantly lower than that measured both in *UASp-TnBVank1* larvae (n=5;

t=10.12; p<0.0001) and in *phm-Gal4/TM6B* larvae (n=5; t=8.196; p<0.0001) at 120 h AED. Moreover, it keeps low during their abnormal extended larval life.

To further demonstrate that the block of transition from larval to pupal stages showed by the *phm-Gal4>TnBVank1* larvae was actually due to a low level of 20E, I carried out an ecdysteroid-feeding rescue experiment. At 25°C, third instar *phm-Gal4>TnBVank1* larvae were fed with yeast paste containing 20E dissolved in ethanol at 106 h AED, just before the onset of the ecdysteroid peak occurring in the wild-type. As expected, at 120 h AED, 70% of *yw;phm-Gal4* control larvae started to pupariate and within the following 20 h all of them reached the pupal stage (n=30). Pupariation of *phm-Gal4>TnBVank1* larvae fed with 20E followed an almost identical pattern, with 100% pupariation (n=30) attained only 1-day later, but failed to progress to the pharate stage (Figure 14B). Instead, *phm-Gal4>TnBVank1* larvae treated only with yeast and ethanol persisted as third instar individuals (n=30). This result confirmed that the developmental arrest of *phm-Gal4>TnBVank1* larvae was due to a reduced level of 20E. However, the rescued pupae failed to develop into adult flies. This may be due to the fact that the large peak of 20E required to trigger metamorphosis was not generated by *phm-Gal4>TnBVank1* pupae and cannot obviously be supplied with food at this developmental stage.

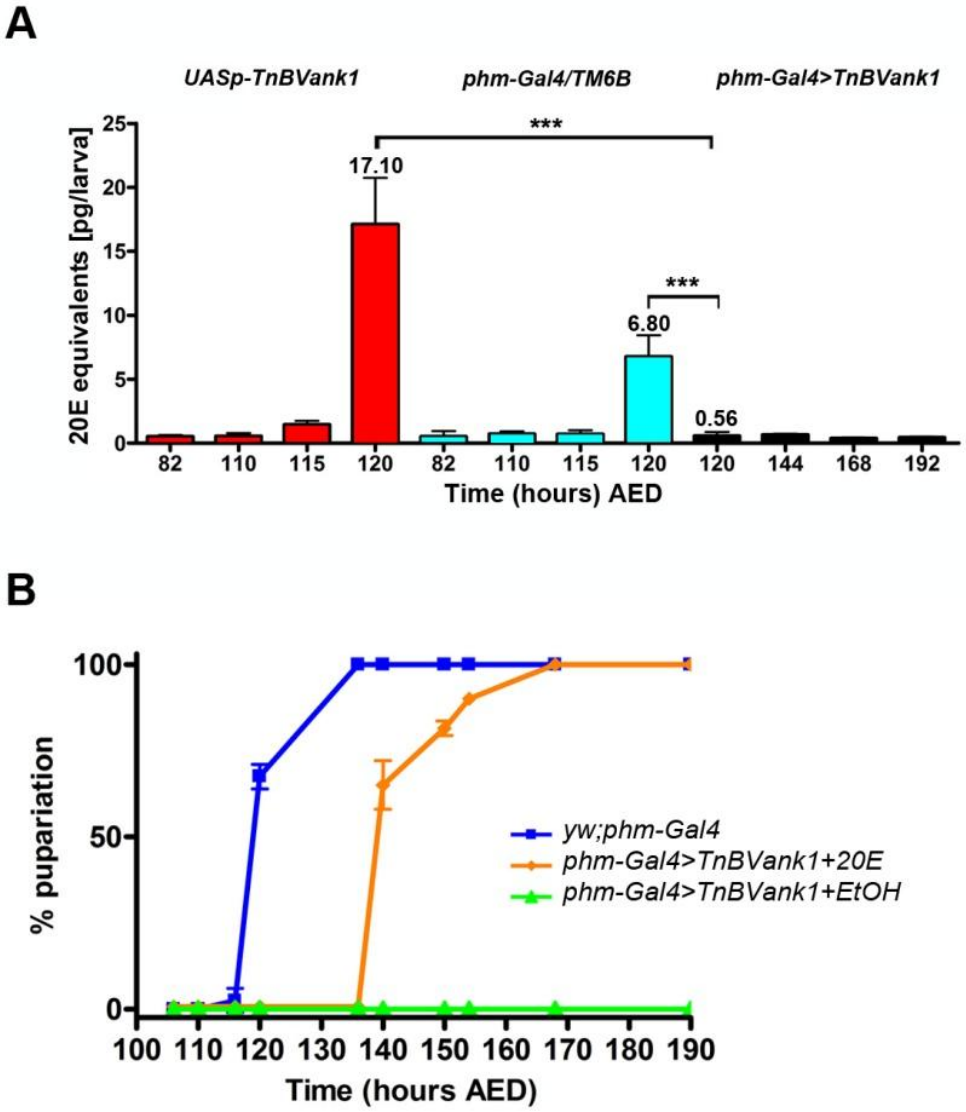

Figure 14. In *phm-Gal4>TnBVank1* there are low levels of 20E. (A) Total 20E titer in *UASp-TnBVank1* (red bars), *phm-Gal4/TM6B* (cyan bars) and *phm-Gal4>TnBVank1* (black bars) larvae at different developmental stages. In the control stocks *UASp-TnBVank1* and *phm-Gal4/TM6B*, the 20E peak which induces the pupariation is present at the white prepupal stage (120 h AED). Instead, this peak is absent in *phm-Gal4>TnBVank1* larvae and the total 20E titer remains low during the extended larval life. Error bars represent SD; ***=p < 0.0001 *versus* controls (*UASp-TnBVank1* and *phm-Gal4/TM6B*). The mean values of total 20E at 120 h AED of different genotype larvae are shown above the bars. (B) Feeding *phm-Gal4>TnBVank1* larvae with medium supplemented with 20E induces the pupariation (orange), while *phm-Gal4>TnBVank1* larvae fed with medium containing ethanol (EtOH) do not reach the pupal stage (green). The *yw;phm-Gal4* larvae serve as background control (blue).

Recently, it has been reported that in the late third instar the genes involved in ecdysone biosynthesis in PG are up-regulated to support high ecdysone production (Moeller et al., 2013). To evaluate if the up-regulation of these gene were present in *phm-Gal4>TnBVank1* PG, I analyzed the expression and localization of Disembodied (Dib), the 22-hydroxylase which converts ketotriol to 2-deoxyecdysone. I dissected the PGs of *yw;phm-Gal4* and *phm-Gal4>TnBVank1* larvae at 120 h AED, during the ecdysone peak for pupariation, and I performed an immunostaining with anti-Dib antibody (Parvy et al., 2005). Interestingly, Dib was strongly reduced in *phm-Gal4>TnBVank1* cells compared to controls (Figure 15A, B). Another gene essential for the ecdysone biosynthesis is *neverland* which encodes for the cholesterol 7,8-dehydrogenase. Its transcription is controlled by the transcription factor Without children (Woc) (Warren et al., 2001). In PGs dissected from *yw;phm-Gal4* and *phm-Gal4>TnBVank1* larvae at 120 h AED I analyzed the expression of Woc by immunostaining (Raffa et al., 2005). This transcription factor was largely localized in the nucleus in control PG cells (Figure 15C), whereas it was present at reduced levels and was also localized in the cytoplasm in *phm-Gal4>TnBVank1* PG cells (Figure 15D). Thus, in *phm-Gal4>TnBVank1* PG at 120 h AED Dib and Woc were not up-regulated and these data consolidate the low levels of 20E in *phm-Gal4>TnBVank1* larvae.

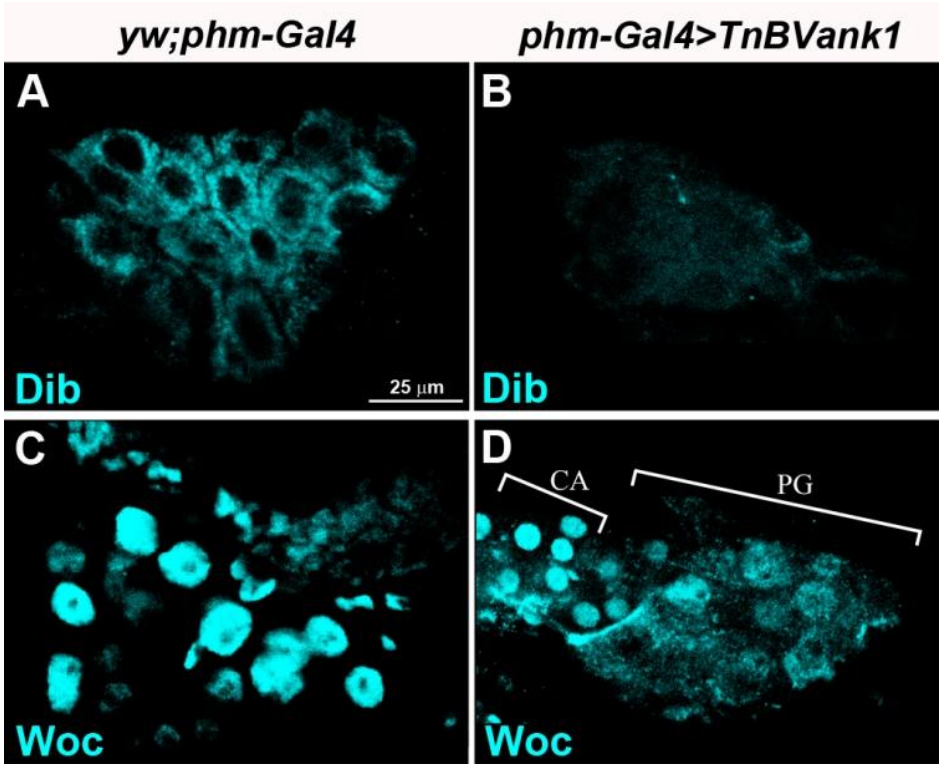

Figure 15. The expression of Dib and Woc is reduced in PG of *phm-Gal4>TnBVank1* larvae. Immunostaining with anti-Dib in *yw;phm-Gal4* (A) and *phm-Gal4>TnBVank1* (B) PG reveals that the expression of Dib is strongly reduced in *phm-Gal4>TnBVank1* larvae. (C) The transcription factor Woc is normally localized in the nucleus, as shown in *yw;phm-Gal4* PG. (D) Instead, in *phm-Gal4>TnBVank1* PG Woc is present also in cytoplasm and its expression level is reduced, while in CA it is strictly nuclear. All confocal images are at the same magnification and the reference scale bar is shown in A.

4.4 The expression of *TnBVank1* affects the PG morphology

In order to investigate the expression and the distribution of *Tn*BVANK1 in PG cells I performed an immunostaining using a polyclonal antibody raised against two synthetic peptides of *Tn*BVANK1 (Duchi et al., 2010). To visualize the PG I used the *phm-Gal4,UAS-mCD8GFP* driver line which expresses the membrane-bound GFP only in the PG cells. As shown in Figure 16, the *Tn*BVANK1 protein was strongly detected only in the cytoplasm of PG cells, confined to stroke-shaped particles.

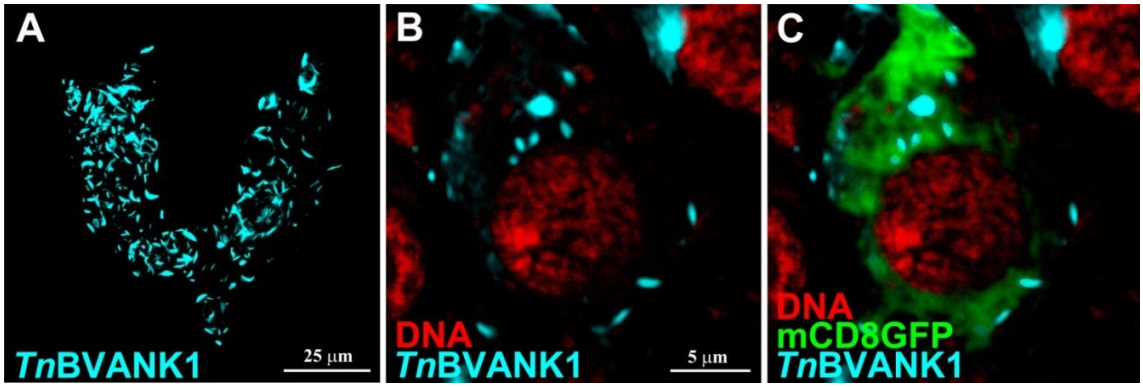

Figure 16. The distribution of *Tn*BVANK1 in the PG cells. The immunolocalization of *Tn*BVANK1 (cyan) in PG cells (marked with mCD8GFP), shows its presence in stroke-shaped particles distributed only in the cytoplasm. In B and C nuclei are stained with Propidium Iodide (red). Confocal images in B and C are at the same magnification and the reference scale bar is shown in B.

Moreover, analyzing these glands I observed that PGs from control larvae (Figure 17A) were significantly larger (n=50; t=50.41; $p<0.0001$) (Figure 17C) than *phm-Gal4>TnBVank1* PGs (Figure 17B). Measurements of the PG cell area did not show a significant reduction in *phm-Gal4>TnBVank1* cells compared to control cells (Figure 17D). Therefore, the observed size difference of PG can be attributed to a reduction of cell number that may be caused by the *Tn*BVANK1-induced apoptosis in some PG cells.

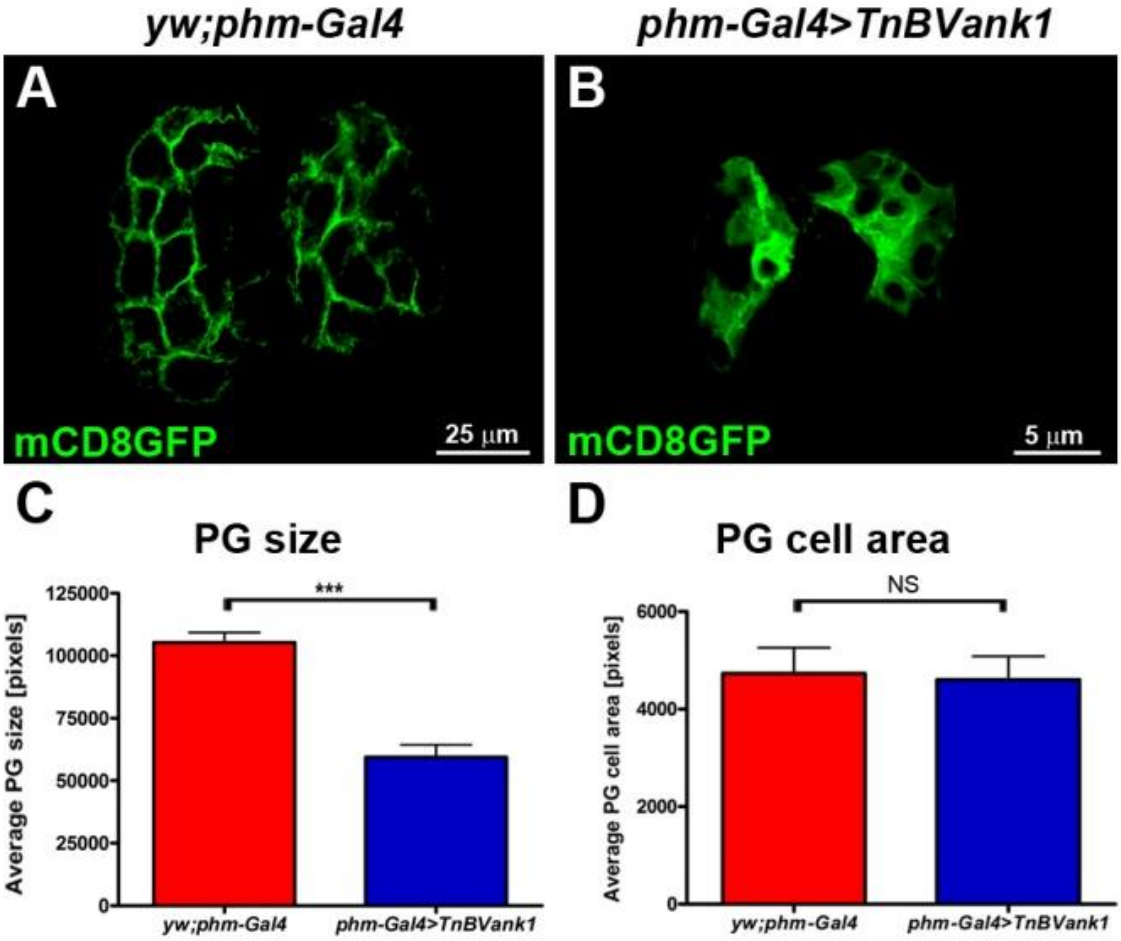

Figure 17. *phm-Gal4>TnBVank1* PG are smaller than *yw;phm-Gal4* PG. Confocal images of five days AED PG, marked with mCD8GFP of *yw;phm-Gal4* (A) and *phm-Gal4>TnBVank1* (B) larvae. (C) By measuring the PG size, *phm-Gal4>TnBVank1* larvae have significantly smaller PGs than control. The graph represents the mean ± SD; 50 PGs were analyzed; ***=p<0.0001. (D) No differences in PG cell area were observed (50 PGs analyzed, NS: non-significant).

In order to assay if apoptosis occurs in *phm-Gal4>TnBVank1* PG, I performed an immunostaining on PGs dissected at 120 h AED using Cleaved Caspase-3 antibody (Florentin and Arama, 2012) and TUNEL labeling assay (Gavrieli et al., 1992).

The Caspase-3 activity (Figure 18B, B'; n=60) and the TUNEL positive staining (Figure 18D, D'; n=60) found in some cells of the *phm-Gal4>TnBVank1* PGs, and not detected

in control PGs (Figure 18A, C), suggested that the occurrence of cell death during development can partly account for this difference. Thereby, the size reduction of *phm-Gal4>TnBVank1* could be related to the developmental arrest induced by *Tn*BVANK1.

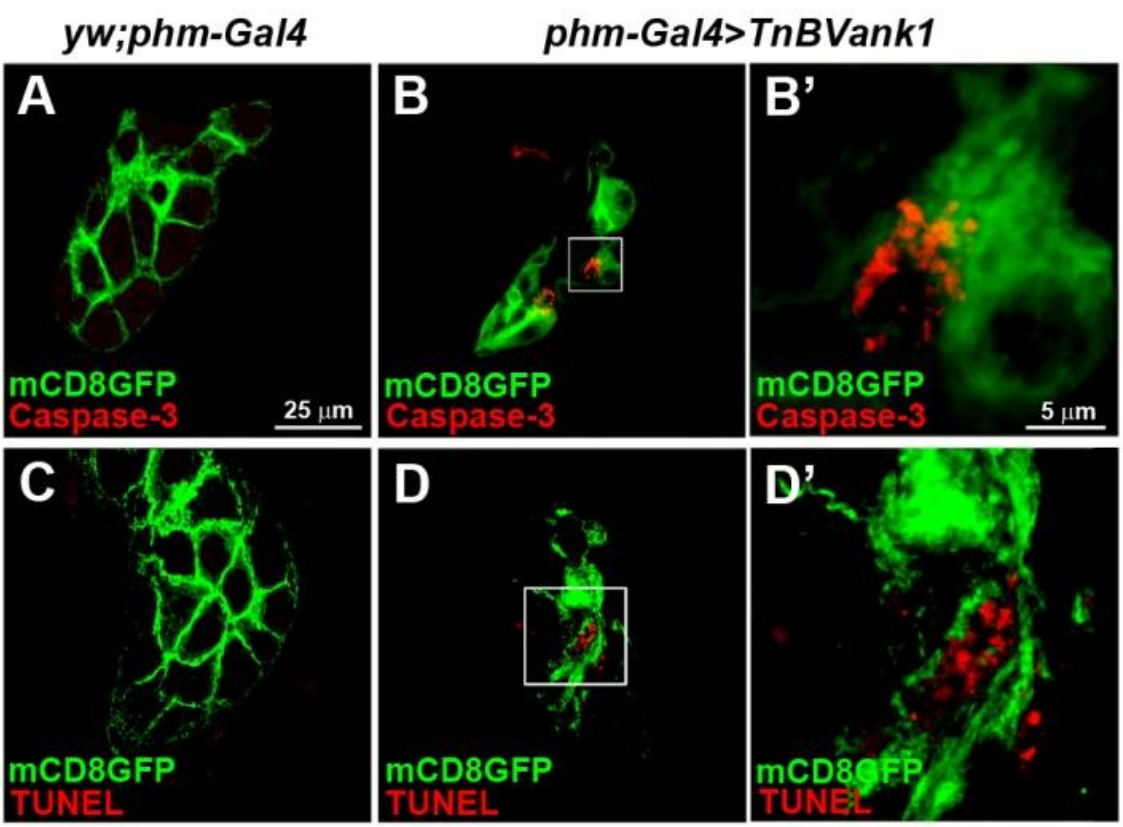

Figure 18. Apoptosis in *phm-Gal4>TnBVank1* PG. Confocal images of immunostaining with anti-Cleaved Caspase-3 (A-B', red) and TUNEL (C-D', red) in PG cells marked with mCD8GFP. In the control *yw;phm-Gal4* no caspase (A) or TUNEL (C) signals are detected, while in *phm-Gal4>TnBVank1* PG few cells undergo apoptosis (B, B', D, D'). PGs in panels A, B, C, D are at the same magnification and the scale bar is shown in A. Boxed regions are magnified in B' and D' and the reference scale bar is shown in B'.

However, the possibility that *Tn*BVANK1 can also disrupt the PG steroidogenic activity cannot be ruled out. Therefore, to assess the relative contribution of these two effects, which could be not mutually exclusive, I expressed the transgene *TnBVank1* in PG cells

at different time points during larval life, using a temperature-sensitive form of the Gal4 repressor Gal80, Gal80^{ts} (McGuire et al., 2003). Gal80 represses activation of Gal4 by binding specifically to its activation domain, and its temperature-sensitive mutant Gal80^{ts} is active at 21°C but does not repress Gal4 at 31°C (Figure 19). This system allowed me to regulate the *phm-Gal4* activity throughout development.

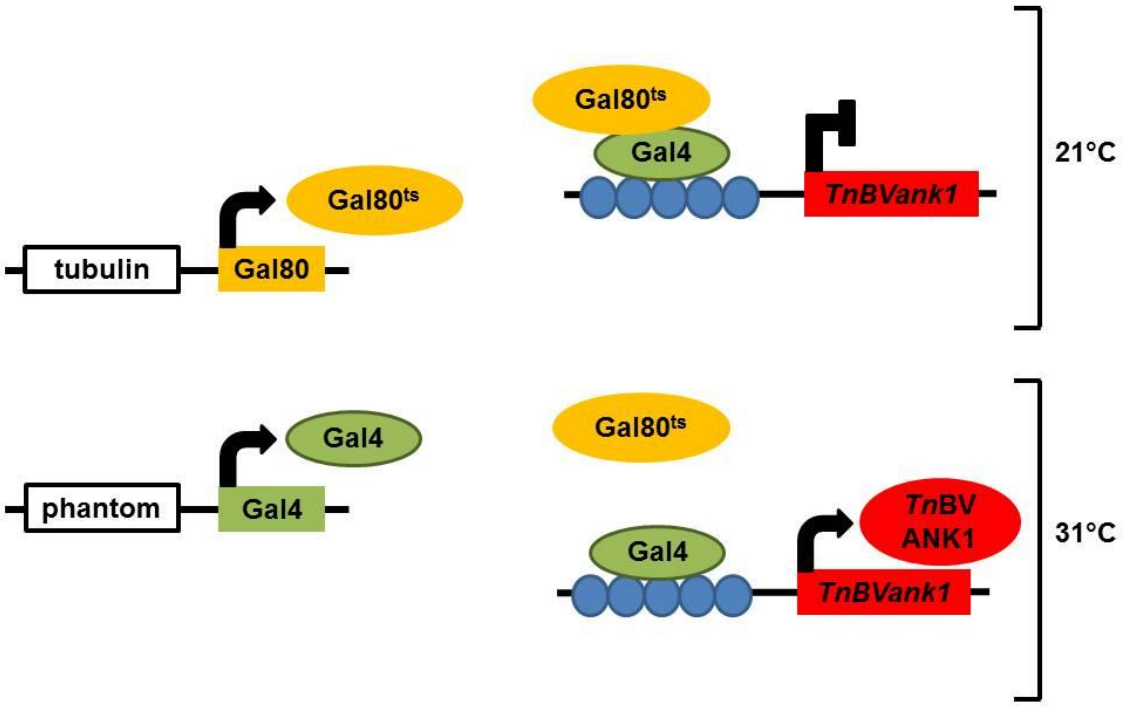

Figure 19. Schematic representation of the UAS/Gal4 and Gal80^{ts} system used to regulate the expression of *TnBVank1* in the PG. The temperature-sensitive Gal80 protein (Gal80^{ts}), expressed ubiquitously from the tubulin promoter, represses the transcriptional activity of Gal4 at 21°C and thus prevents the expression of the *UAS-TnBVank1* transgene in the PG cells. At 31°C, Gal80^{ts} becomes inactive and allows Gal4 to drive the expression of the *UAS-TnBVank1* transgene in the PG.

UASp-TnBVank1;UASp-TnBVank1/tub-Gal80^{ts};phm-Gal4/+ larvae and *yw;tub-Gal80^{ts}/+;phm-Gal4/+* control larvae were initially raised at 21°C, and then shifted to the restrictive temperature (31°C) at specific time points (96 h, 72 h and 48 h AED) to

promote Gal4 activity. The temperature shift did not affect the proper development of the control larvae, which pupariated normally. Conversely, the larvae expressing *TnBVank1* failed to pupariate, increased their size and survived for an extended period. For each time point I also analyzed the PG size at 120 h AED (Figure 20). When the *TnBVank1* expression was triggered at 96 h or 72 h, the PG size was not significantly different from the control (respectively n=10; t=0.07636; NS and n=10; t=1.336; NS). Instead, the earlier induction of the transgene expression, at 48 h AED, strongly affected the PG size, which appeared significantly reduced (n=10; t=11.68; p<0.0001).

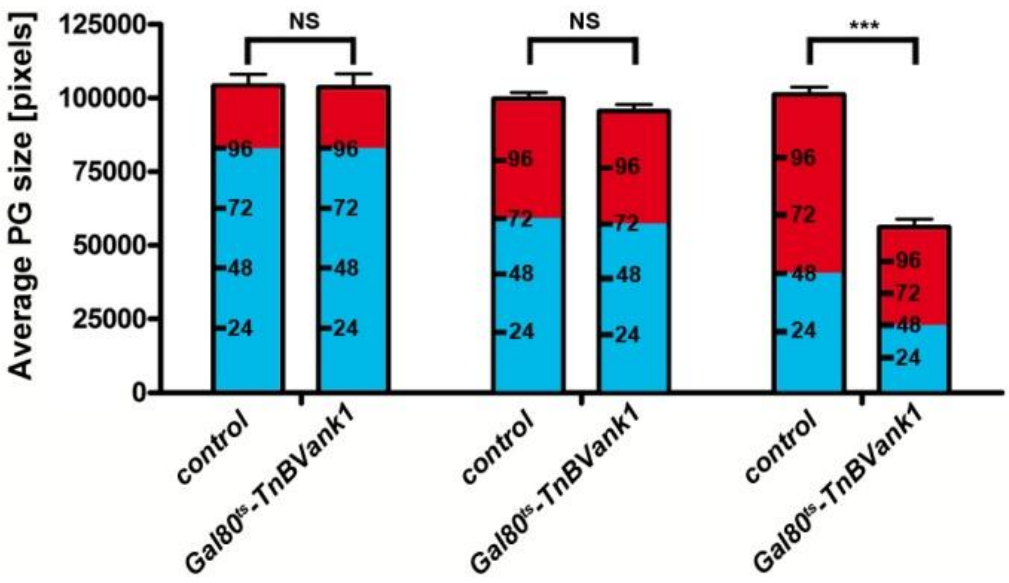

Figure 20. The reduction of PG size is due to an early induction of *TnBVank1* expression. *yw;tub-Gal80^{ts}/+;phm-Gal4/+* larvae (control) and *UASp-TnBVank1;UASp-TnBVank1/tub-Gal80^{ts};phm-Gal4/+* (*Gal80^{ts}-TnBVank1)* larvae are raised at 21°C (cyan) for different time intervals, then shifted at 31°C (red) and their PG dissected at 120 h AED. PG size from *Gal80^{ts}-TnBVank1* larvae incubated at 21°C until 96 h AED or until 72 h AED shows no significant (NS) differences from that of control larvae. PG size is strongly reduced in *Gal80^{ts}-TnBVank1* larvae incubated at 21°C until 48 h AED compared to PG from control larvae (***=p<0.0001). Graph represents mean ± SD; 10 PGs were analyzed for each experiment.

In addition, I examined whether ectopic expression of the anti-apoptotic protein p35 (Hay et al., 1994) should rescue the phenotype produced by the expression of *TnBVank1* in the PG. Co-expression of *UAS-p35* and *UASp-TnBVank1* in the same PG cells through the *phm-Gal4* driver did not rescue the developmental arrest phenotype (n=58). Collectively, these data indicate that the developmental arrest induced by *Tn*BVANK1 does not depend on the reduced PG size caused by apoptosis, but on its capacity to disrupt the PG steroidogenic function when expressed before the production of the 20E peak.

4.5 The expression of *TnBVank1* in the PG impairs the cytoskeletal network

The *phm-Gal4>TnBVank1* PG cells revealed a cytoplasmic rather than the expected membrane distribution of mCD8GFP, as showed in Figure 17B (Lee and Luo, 1999). The observed mislocalization of mCD8GFP and the altered morphology of *phm-Gal4>TnBVank1* PG prompted me to analyze the cytoskeletal network in these cells. I dissected PGs from *phm-Gal4>TnBVank1* and *yw;phm-Gal4* larvae at 120 h AED and I evaluated the organization of the cytoskeleton in PG cells by analyzing F-actin and α-tubulin distribution. The organization of F-actin was evaluated by phalloidin staining (Sigma) (Figure 21A, A', D, D'). The cortical actin did not appear regularly distributed in *phm-Gal4>TnBVank1* PG cells, in which thick masses of actin filaments were detected (Figure 21D, D'). The microtubule network was investigated by analyzing the distribution of an α-tubulinGFP fusion protein, which was co-expressed with *TnBVank1* in the PG. In the control, the PG cells expressed only α-tubulinGFP protein (Figure 21B, B'). The microtubule cytoskeleton of the *phm-Gal4>TnBVank1* PG cells appeared strongly affected, as shown by the formation of thick bundles of microtubules (Figure 21E, E'). The dynamic function of the microtubule network was then analyzed by

assessing the distribution of the minus-end-directed microtubule motor Dynein**,** using an anti-Dynein heavy chain antibody (McGrail and Hays, 1997). Compared to the *yw;phm-Gal4* cells (Figure 21C, C'), the *phm-Gal4>TnBVank1* PG cells displayed a reduced cortical distribution of Dynein, along with some large Dynein dots (Figure 21F, F'). These data indicate that the whole cytoskeletal network is markedly altered in the PG cells expressing *Tn*BVANK1.

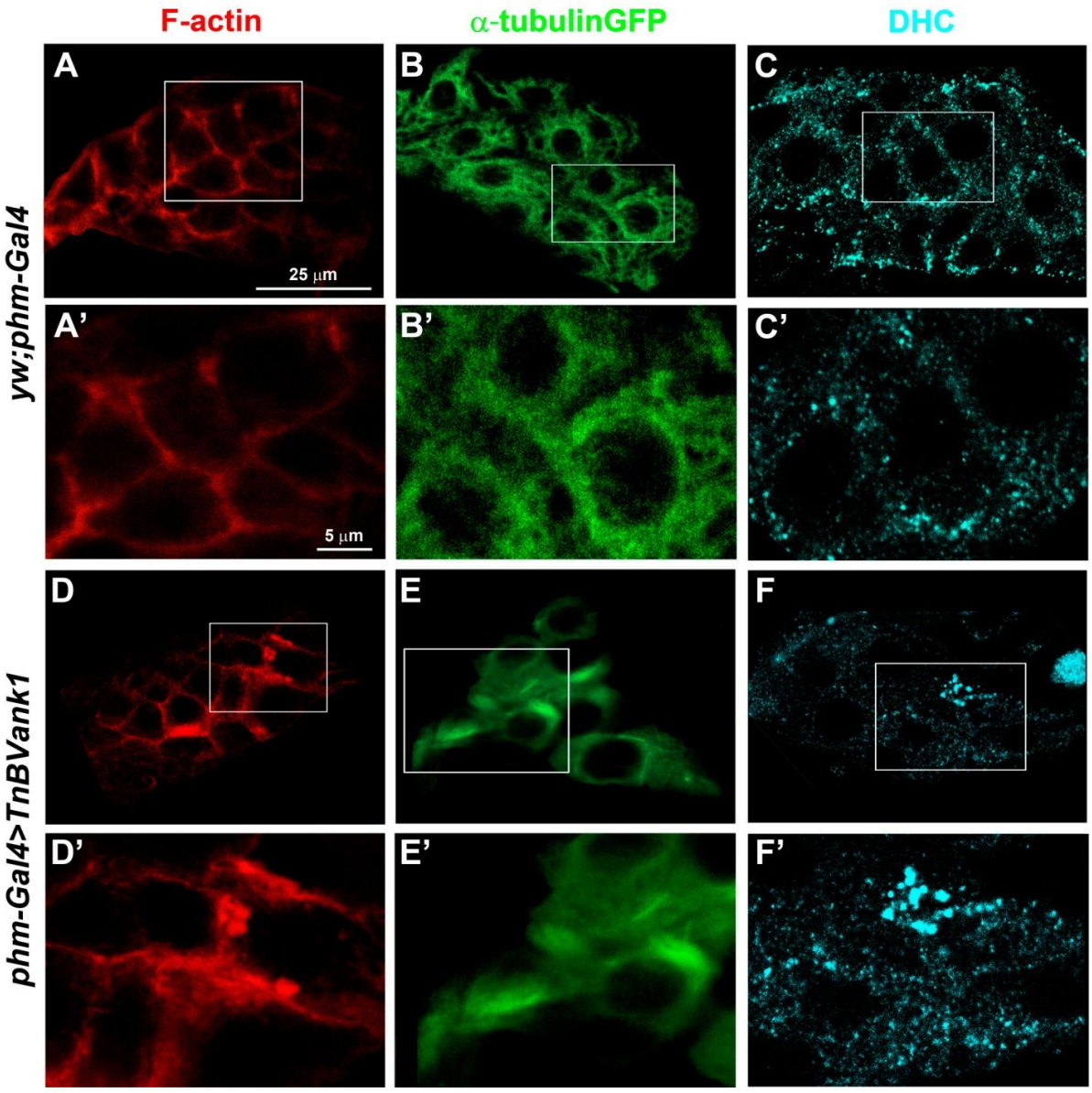

Figure 21. *phm-Gal4>TnBVank1* PG cells show an altered cytoskeleton. Phalloidin staining in control (A, A') and in *phm-Gal4>TnBVank1* (D, D') PG cells. F-actin shows an altered distribution, characterized by thick masses of filaments in *phm-Gal4>TnBVank1* PG cells. (B-E') α-tubulinGFP fusion protein was expressed in *yw;phm-Gal4* and *phm-Gal4>TnBVank1* PG to investigate the microtubule network. Compared to control (B, B'), in *phm-Gal4>TnBVank1* the microtubule cytoskeleton is strongly affected and forms bundles (E, E'). (C-F') Immunostaining with anti-Dynein heavy chain shows that, compared to control (C, C'), in *phm-Gal4>TnBVank1* PG cells the cortical localization of this protein is reduced and characterized by an evident dotted distribution (F, F'). Confocal images in panels A, B, C, D, E, F are at the same magnification and the scale bar is shown in A. Boxed regions are magnified in A', B', C', D', E', F' and the reference scale bar is shown in A'.

Moreover, I analyzed the cytoskeletal structure in other tissues where the transgene *TnBVank1* was expressed. Using the driver line *lsp2-Gal4*, which directs the expression of UAS-linked genes in the fat bodies, I evaluated the F-actin distribution. No differences in phalloidin staining were observed between *yw;lsp2-Gal4*;*UAS-mCD8GFP* control and *lsp2-Gal4>TnBVank1* fat bodies (Figure 22C, D). As shown in Figure 22A, B the cell membrane architecture appeared regular in *yw;lsp2-Gal4*;*UAS-mCD8GFP* and *lsp2-Gal4>TnBVank1* fat bodies.

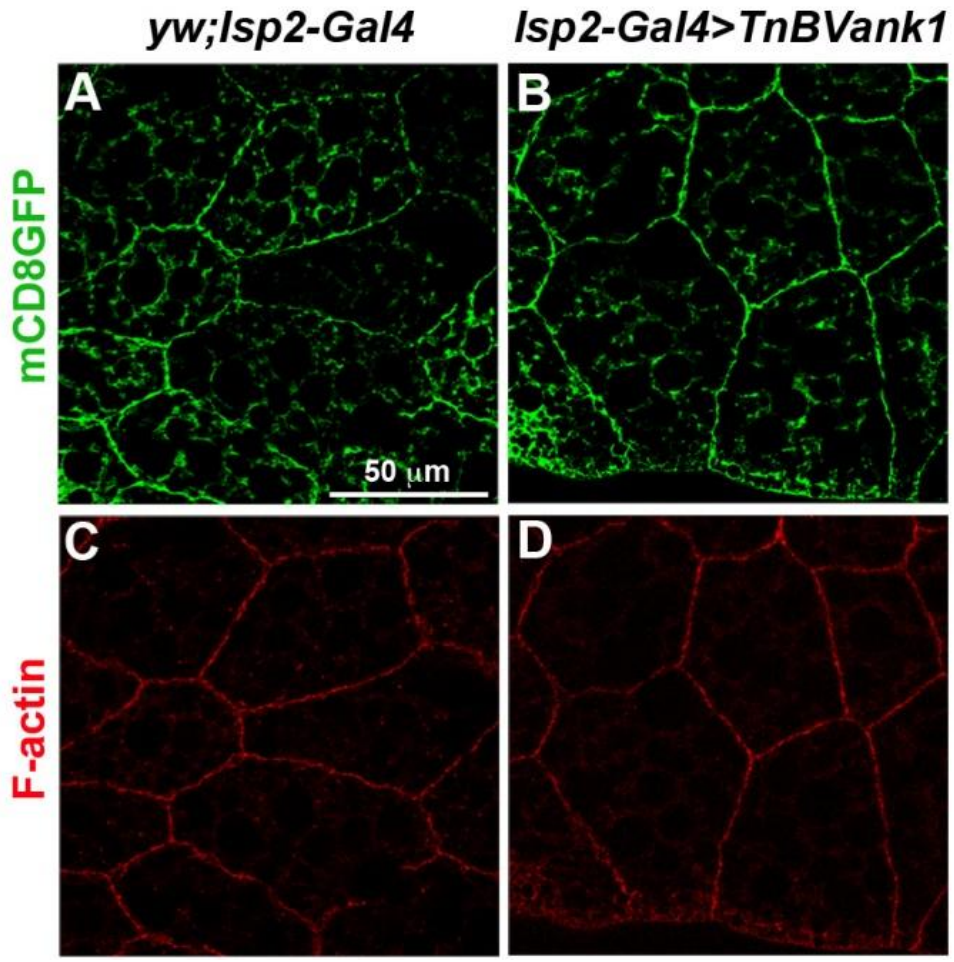

Figure 22. Expression of *TnBVank1* in fat bodies does not affect cell morphology. Confocal images of Phalloidin staining in fat bodies from the control *yw;lsp2-Gal4;UAS-mCD8GFP* (A, C) and from fat bodies expressing *TnBVank1 lsp2-Gal4,UAS-mCD8GFP/TnBVank1* (B, D). Fat bodies are at the same magnification in all panels and the scale bar is indicated in A.

The expression of *TnBVank1* in different tissues, using a wide range of tissue-specific *Gal4* drivers, did not alter the developmental timing and the adult formation, as discussed in paragraph 4.2 (Table 1). Hence these results suggest that the cytoskeletal structure is not affected in all tissues.

4.6 *Tn*BVANK1 expression causes increased accumulation of lipids in PG cells

The cytoskeleton and its associated motor proteins play an important role in protein sorting and endocytic pathways (Huotari and Helenius, 2011). Therefore the observed negative impact of *Tn*BVANK1 on PG cells could reduce the level of ecdysteroid biosynthesis by disrupting the uptake, transport and trafficking of sterols, essential steps for ecdysteroid biosynthesis (Huang et al., 2008). To evaluate if the cytoskeletal alterations detected in PG cells may impair the endocytic pathway, I analyzed lipid vesicular internalization and trafficking in the *phm-Gal4>TnBVank1* PG cells with a staining procedure using Oil Red O (Sigma). This fat-soluble diazol dye, with a maximum absorption at 518 nm, stains neutral lipids and cholesteryl esters but not biological membranes (Annika et al., 2013). Conversely to controls (Figure 23A), *phm-Gal4>TnBVank1* PG cells showed an increased accumulation of lipid droplets (Figure 23C, C') in all PGs analyzed (n=60). These droplets most likely include sterol precursors required for ecdysteroid production. To better characterize this observation, I used Filipin (Sigma) staining which specifically reveals non-esterified sterols (Friend and Bearer, 1981). I observed that, compared to controls (Figure 23B), all *phm-Gal4>TnBVank1* PGs analyzed (n=60) displayed a marked cholesterol accumulation in discrete vesicular drops (Figure 23D, D'). These data suggest that *Tn*BVANK1 does not affect lipid uptake, but the endocytic pathway is impaired.

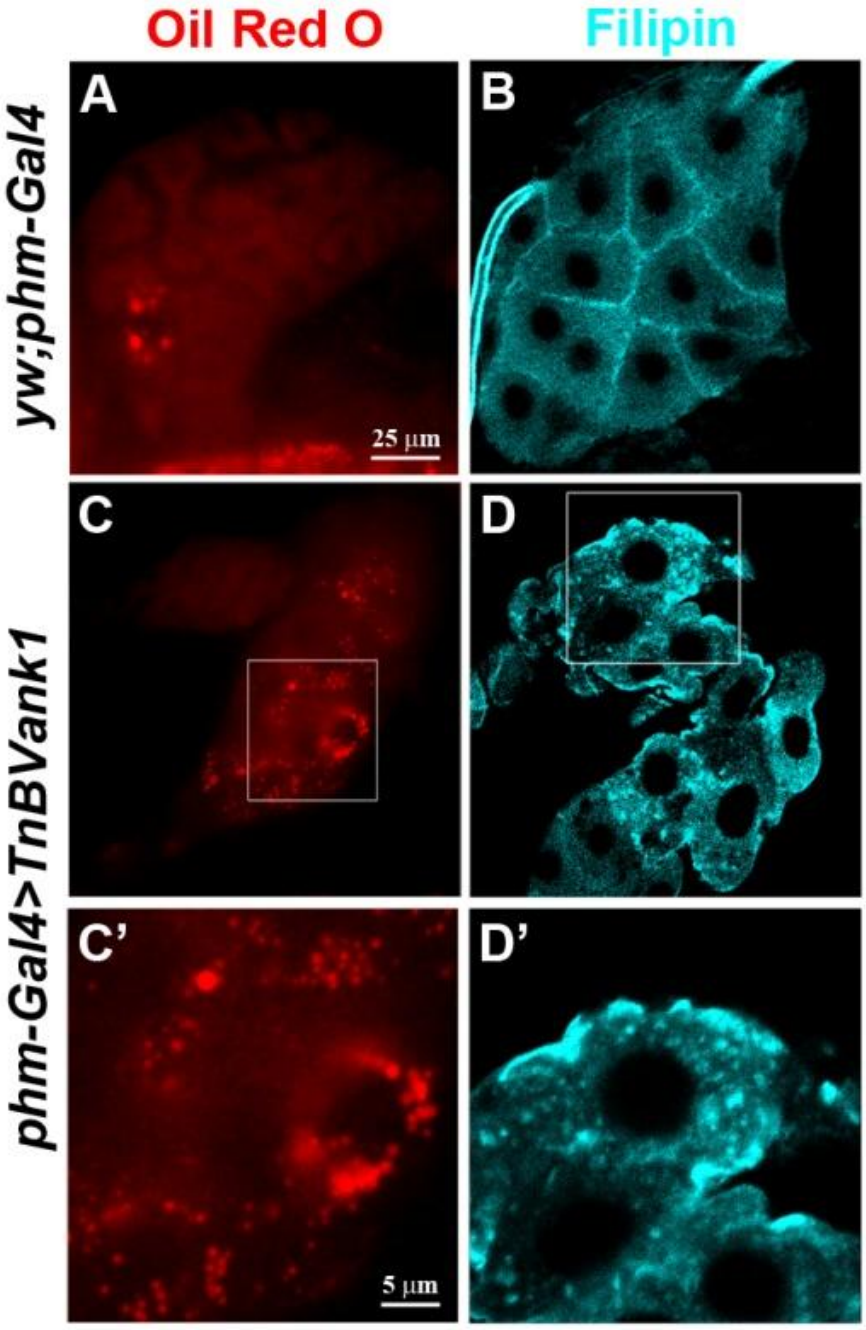

Figure 23. *phm-Gal4>TnBVank1* PG cells show lipids accumulation. (A) In control *yw;phm-Gal4* there are few lipid droplets stained with Oil Red O, while in *phm-Gal4>TnBVank1* PG cells several lipid droplets are detected (C, C'). (D, D') In *phm-Gal4>TnBVank1* there is also a sterol accumulation, shown by Filipin staining, which is absent in control PG (B). Panels A, B, C, D are at the same magnification and the reference scale bar is shown in A. Boxed regions are magnified in C', D' and the reference scale bar is shown in C'.

4.7 The organization of the cholesterol trafficking pathway in PG cells

As discussed in detail in paragraph 1.11, cholesterol, which cannot be synthesized by insects (Gilbert and Warren, 2005), enters in the steroidogenic cells through a receptor-mediated low-density lipoprotein (LDL) endocytic pathway (Rodenburg and Van der Horst, 2005), which targets cholesterol to the endosomes. Transport to the lysosome is characterized by the maturation of the vacuolar regions of early endosomes into late endosomes, which are able to fuse directly with the lysosome (Figure 24).

The three major compartments of the endocytic pathway are characterized by specific Rab GTPase proteins that can be used as tags for the different endosomes (Zerial and McBride, 2001). Early endosomes are enriched in Rab5; Rab11 marks the recycling endosomes and late endosomes are associated with Rab7. During the early-to-late endosome transition, multivesicular endosomes form on early endosomal membranes and mediate transport to late endosomes. They have thus been referred to as endosomal carrier vesicles (ECVs) or multivesicular bodies (MVBs) according to their function or appearance, respectively (Dikic, 2006). The Hepatocyte growth factor-regulated tyrosine substrate (Hrs) can be used as a tag for MVBs. In fact this protein regulates inward budding of endosome membrane and MVBs/late endosome formation (Lloyd et al., 2002).

In late endosomes and lysosomes, acid lipase hydrolyses cholesteryl esters and the resulting free cholesterol partition into neighboring membranes. Cholesterol is then transformed into 7-dehydrocholesterol in endoplasmic reticulum and transported to other subcellular compartments through further metabolic steps of the ecdysteroidogenic pathway (Gilbert and Warren, 2005).

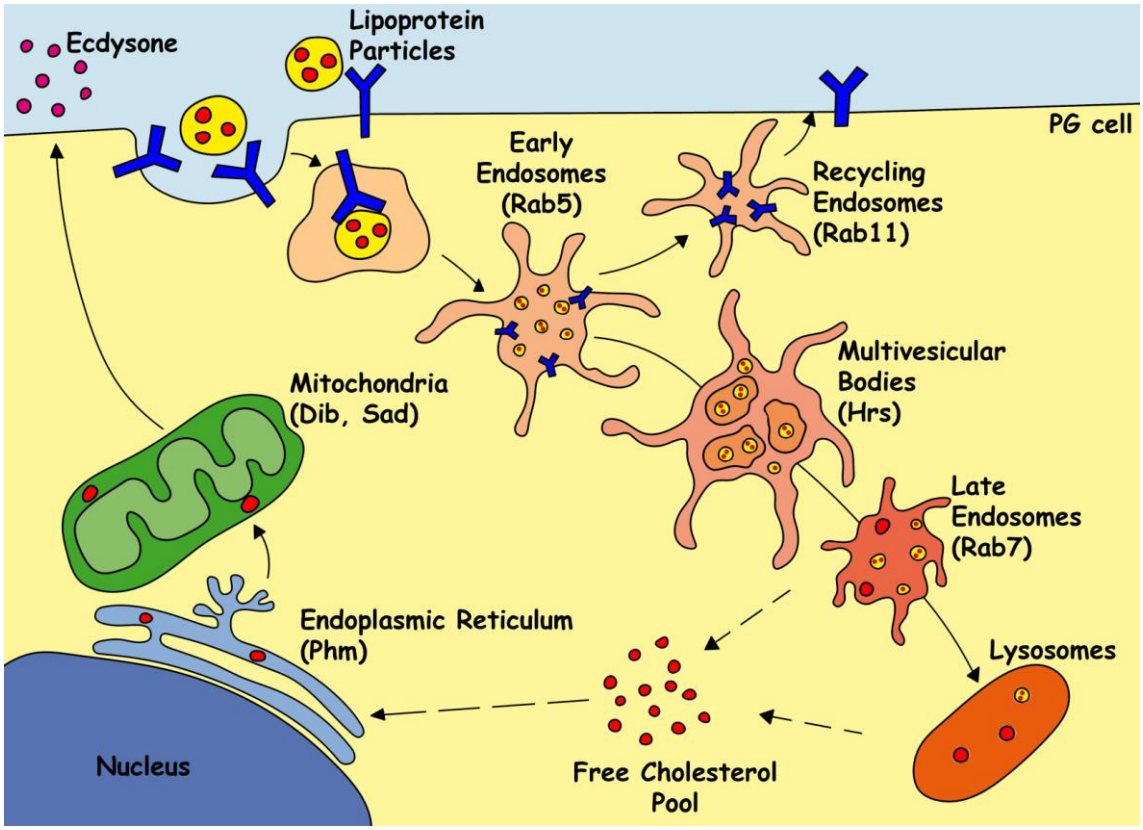

Figure 24. Involvement of cholesterol trafficking in insect ecdysteroidogenesis. Cholesterol enters PG cells through LDL endocytic pathway and is then internalized by the endosomes. Early Endosomes are marked by Rab5, Multivesicular bodies by Hrs, Recycling Endosomes by Rab11 and Late Endosomes by Rab7. The esterified cholesterol is hydrolyzed by lipase to free cholesterol which then leaves the endosomal compartment to move to other membrane compartments including the endoplasmic reticulum and mitochondria. The enzymes are referred to by their names as encoded from Halloween genes in *Drosophila*: Phm, phantom; Dib, disembodied; Sad, shadow.

4.8 The endocytic pathway is altered in PG cells expressing *TnBVank1*

In order to investigate the endocytic pathway in PG cells I analyzed the distribution of the endosomes. I dissected 60 PGs from *yw;phm-Gal4* and *phm-Gal4>TnBVank1* larvae at 120 h AED and I used antibodies directed against the Rab proteins to identify the endosomes (Tanaka and Nakamura, 2008).

Immunostaining with anti-Rab5 antibody (Biosciences) showed that the distribution of early endosomes in *TnBVank1* larvae (Figure 25B) appeared to be comparable to control PG cells (Figure 25A). Similarly, no differences in recycling endosomes, stained by anti-Rab11 antibody (Tanaka and Nakamura, 2008), were observed in *yw;phm-Gal4* (Figure 25C) and *phm-Gal4>TnBVank1* (Figure 25D) PGs. Differently, few endosomal vesicles were detected by anti-Rab7 antibody (Tanaka and Nakamura, 2008) in the presence of *Tn*BVANK1 (Figure 25F) compared to control (Figure 25E). This suggests that the expression of *TnBVank1* in PG cells alters the early-to-late endosome transition.

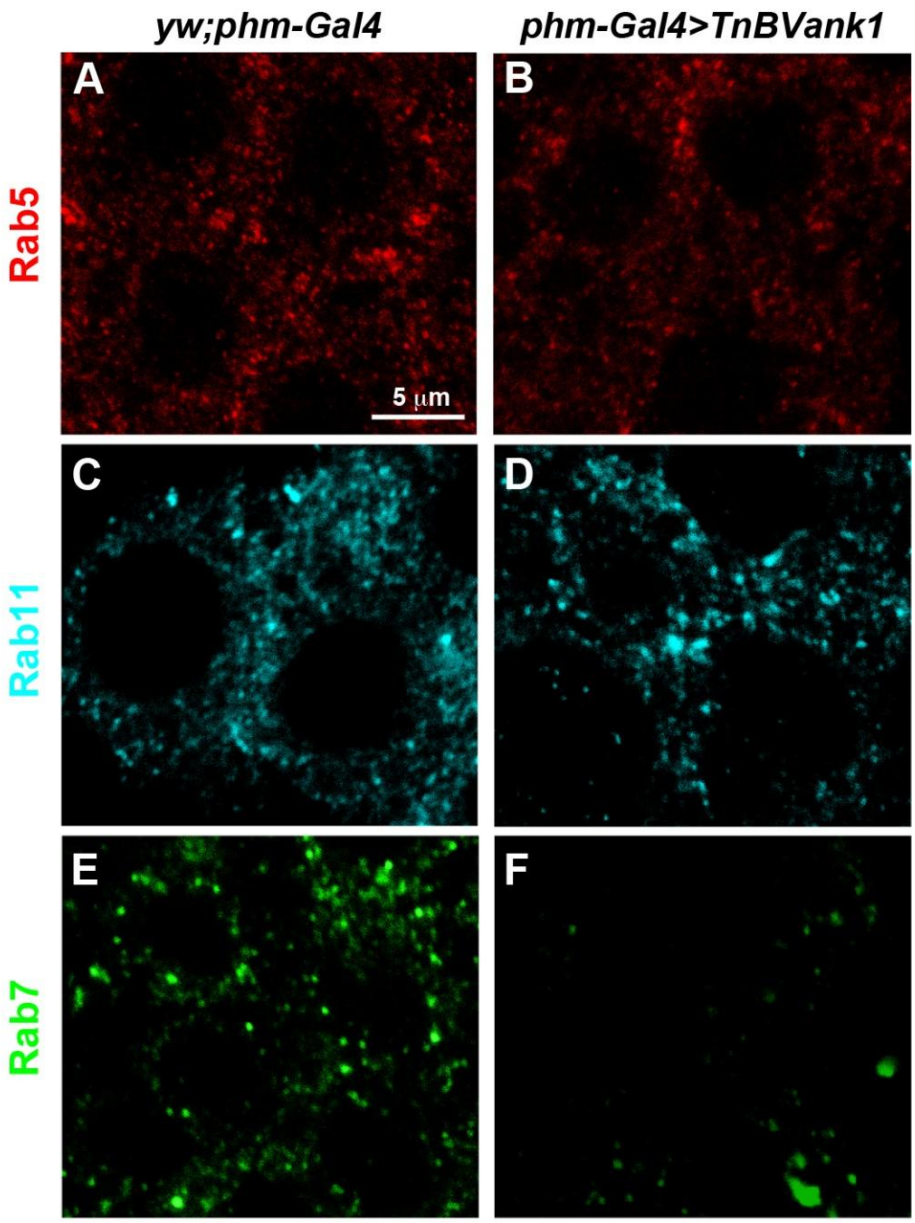

Figure 25. *Tn*BVANK1 disrupts the endocytic pathway in PG cells. Confocal images of five days AED PG stained for Rab5 (A, B), Rab11 (C, D) and Rab7 (E, F) in *yw;phm-Gal4* (left column) and *phm-Gal4>TnBVank1* (right column) larvae. The distribution of endosomes marked with Rab5 (A, B) and Rab11 (C, D) is not affected by *TnBVank1* expression, while a strong reduction in number was observed for late endosomes marked with Rab7 (E, F). All panels are at the same magnification and reference scale bar is shown in A.

4.9 *Tn*BVANK1 is localized in multivesicular bodies

Since the expression of *TnBVank1* in PG cells showed an altered maturation of the early endosomes into late endosomes, I analyzed the distribution of multivesicular bodies carrying the Hepatocyte growth factor-regulated tyrosine substrate (Hrs). Immunostaining with anti-Hrs antibody (Lloyd et al., 2002) in *yw;phm-Gal4* PGs showed a wide cytoplasmic distribution of round shape vesicles containing this protein (Figure 26A, A'). Interestingly, in the *phm-Gal4>TnBVank1* PG cells quite a few Hrs marked vesicles exhibited a stroke-shaped form (Figure 26B, B'), similar to the form observed for the *Tn*BVANK1 signal (Figure 26C, C'). I performed an immunostaining with anti-*Tn*BVANK1 and anti-Hrs antibodies in *phm-Gal4>TnBVank1* PGs and I found that most of the immunodetection signals of *Tn*BVANK1 colocalized with the Hrs-marked vesicles (Figure 26D, D'). To quantify the level of colocalization in these PG cells, I calculated the Pearson's correlation coefficient using the CDA plugin of ImageJ. This coefficient, being one of standard measures in pattern recognition, was first employed to estimate colocalization and is used for describing the correlation of the intensity distributions between channels (Zinchuk and Zinchuk, 2008). The *Tn*BVANK1-Hrs Pearson's coefficient was 0.96 ± 0.06. Since the Pearson's coefficient values range from -1.0 (complete separation of two structures) to +1.0 (complete colocalization of two signals) (Zinchuk and Zinchuk, 2008), the colocalization of *Tn*BVANK1 and Hrs marked MVBs appears complete. In contrast, the Hrs-marked vesicles showing a normal round shape did not colocalize with *Tn*BVANK1. This finding suggests an interaction of *Tn*BVANK1 with endosome associated proteins, which may partly account for the observed alterations of the endocytic trafficking routes.

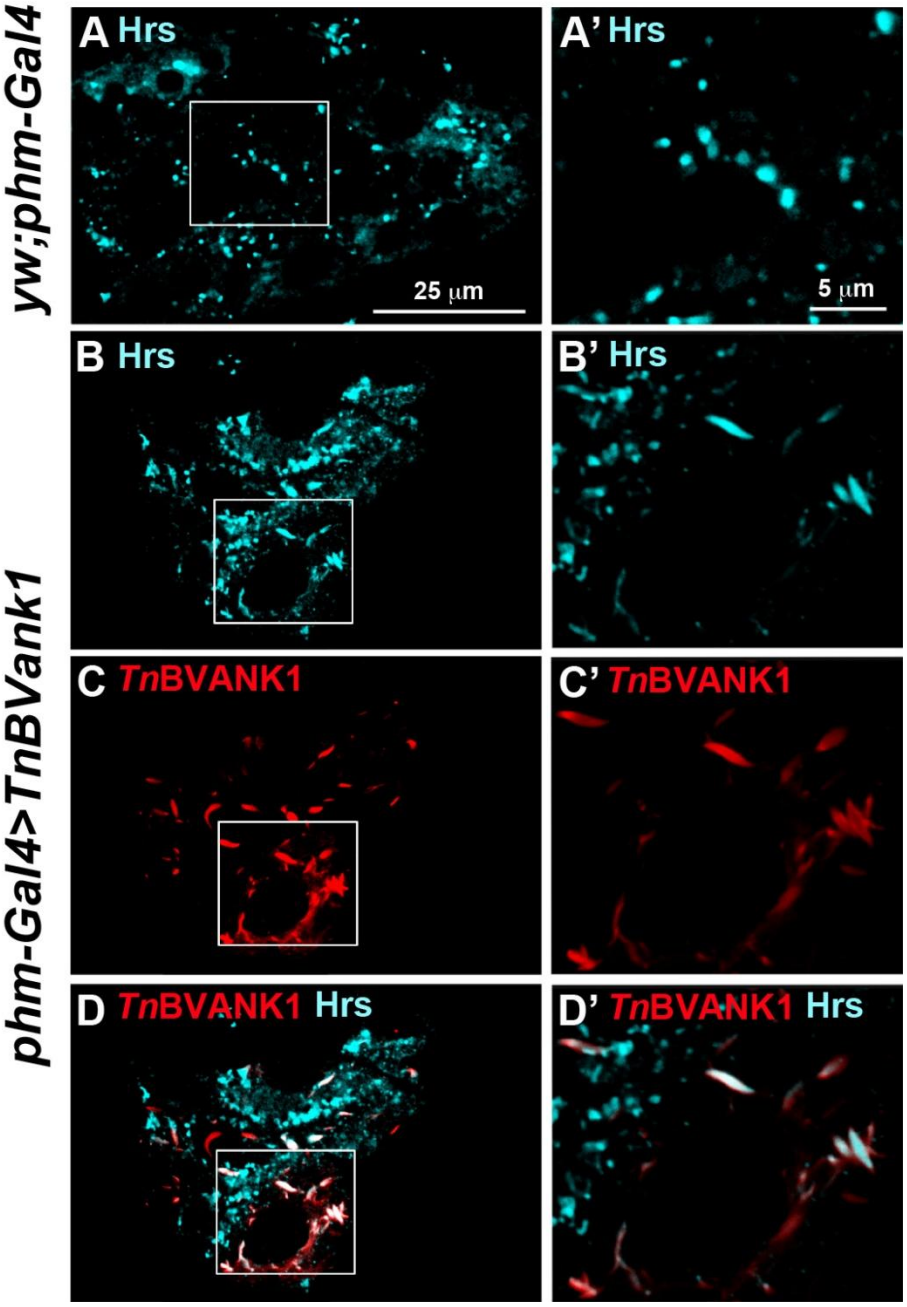

Figure 26. *Tn*BVANK1 protein colocalizes with Hrs-positive vesicles. Confocal images of PG from *yw;phm-Gal4* (A, A') and *phm-Gal4>TnBVank1* (B-D') larvae stained for Hrs (cyan) and *Tn*BVANK1 (red). A number of vesicles marked by Hrs in *phm-Gal4>TnBVank1* cells (B, B') have a shape different from that present in controls (A, A'). These modified vesicles show a strong colocalization with *Tn*BVANK1 signal (C-D'), demonstrating that *Tn*BVANK1 protein is associated with Hrs-marked vesicles. PGs in panels A, B, C, D are at the same magnification and the reference scale bar is shown in A. Boxed regions are magnified in A', B', C', D' and their reference scale bar is shown in A'.

4.10 The role of ALIX in the endosomal trafficking

MVBs formation is controlled by a set of proteins, the endosomal sorting complex required for transport, ESCRT-0 to III, which sequentially associates with the cytosolic surface of endosomes (Williams and Urbe, 2007). A partner of the ESCRT proteins is ALIX (formerly Apoptosis-Linked gene 2-Interacting protein X), previously characterized as an interactor of ALG-2 (Missotten et al., 1999).

Recently it has been reported that ALIX plays a role in the biogenesis of intralumenal vesicles (ILVs). The lysobisphosphatidic acid (LBPA)-mediated recruitment of ALIX onto the endosome limiting membrane leads to the partial insertion of a hydrophobic loop present within an exposed site of ALIX Bro1 domain into the membrane cytoplasmic leaflet. This in turn causes local perturbations of the bilayer organization, followed by ALIX dimerization, ESCRT-III-binding and assembly. The same mechanism controls ILV back-fusion with the limiting membrane, either indirectly by controlling intralumenal membrane homeostasis, or more directly by providing a privileged site for back-fusion events within the endosome lumen (Bissig and Gruenberg, 2014).

Proteins and lipids that transit trough endosomes, including LDL-derived cholesterol, utilize this ILV back-fusion as an escape route from lysosomes (Falguieres et al., 2008; Falguieres et al., 2012). Cholesterol is abundant in ILVs (Mobius et al., 2003) and, since the mechanism of its export from endosomes to other subcellular destinations is still a matter of debate (Ikonen, 2008; Maxfield and van Meer, 2010), several lines of evidence indicate that the LBPA and its partner protein ALIX play a direct role in cholesterol export (Bissig and Gruenberg, 2013).

4.11 In PG cells *Tn*BVANK1 colocalizes with ALIX positive endosomes

Using an antibody directed against ALIX (Tsuda et al., 2006), I analyzed the distribution of this protein in *yw;phm-Gal4* and *phm-Gal4>TnBVank1* PGs. According to its multifunctional activity (Odorizzi, 2006), ALIX was found widely distributed in the cytoplasm of control PG cells (Figure 27A), and, as expected, marked some Hrs-positive vesicles (Figure 27B). In the *phm-Gal4>TnBVank1* PG cells the anti-ALIX antibody detected stroke-shaped structures similar to *Tn*BVANK1 signal (Figure 27C, E). The immunostaining analysis performed with anti-ALIX and anti-*Tn*BVANK1 antibodies revealed in the *phm-Gal4>TnBVank1* PG cells a strong colocalization of the two signals (Pearson's coefficient: 0.99 ± 0.07; Figure 27D).

In addition, several of these ALIX positive stroke-shaped structures colocalized with Hrs marked endosomes (Pearson's coefficient: 0.95 ± 0.16), indicating that these are modified endocytic vesicles (Figure 27F).

This strong interaction of *Tn*BVANK1 with ALIX-containing vesicles and the altered cholesterol distribution observed in PG are concurrent evidence that the cholesterol route is altered. Therefore, the interaction between *Tn*BVANK1 and endosomes specifically affects the endosomal trafficking of sterols, likely limiting their supply to subcellular compartments where ecdysteroid biosynthesis takes place (Gilbert and Warren, 2005).

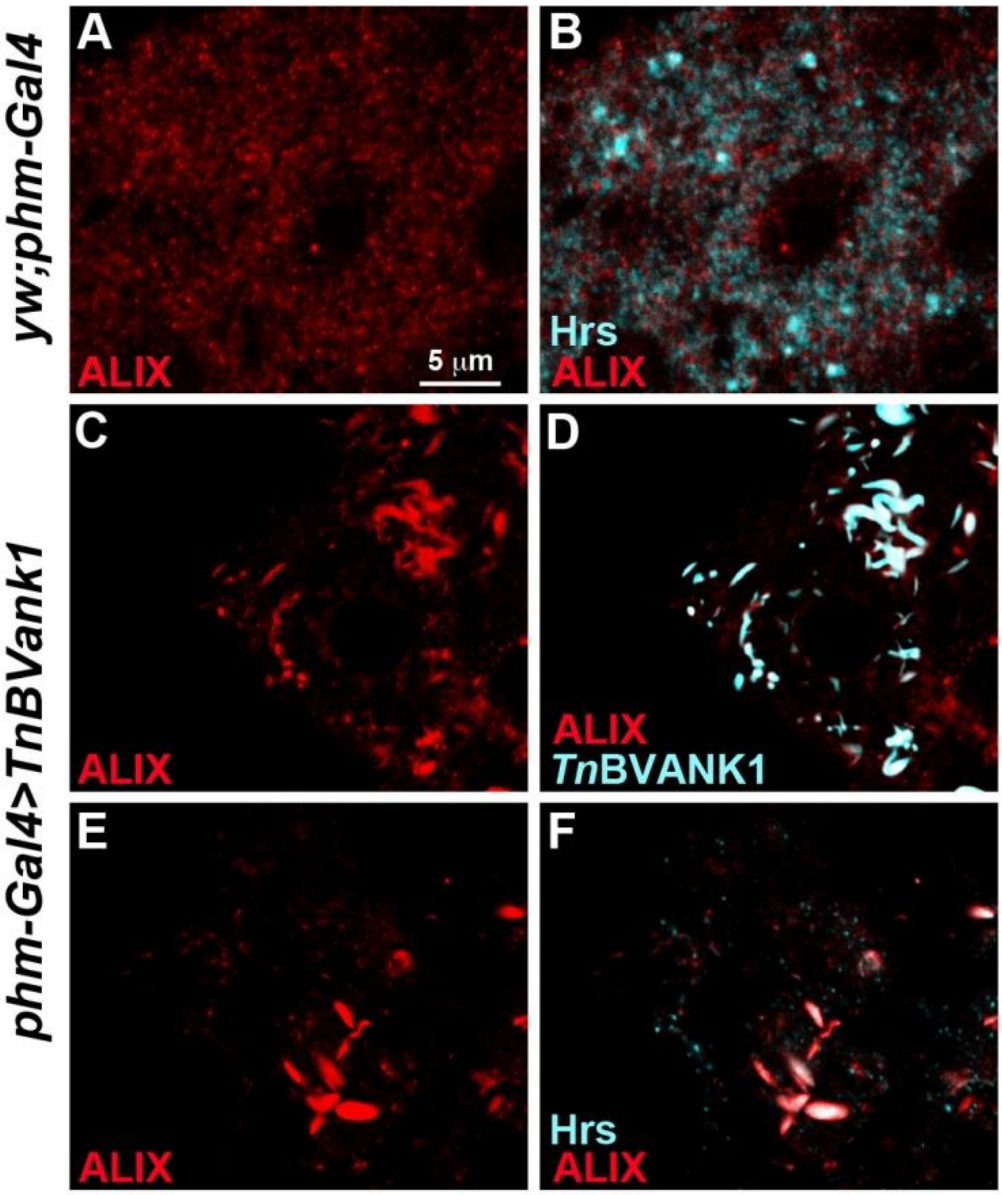

Figure 27. *Tn*BVANK1 protein colocalizes with ALIX marked endosomes. Confocal images of PG of *yw;phm-Gal4* (A, B) and *phm-Gal4>TnBVank1* (C-F) larvae stained for ALIX (red) and *Tn*BVANK1 (cyan) or Hrs (cyan). In the control PG cells ALIX (red) and Hrs (cyan) are widely distributed in the cytoplasm and their signals partially overlap (B). In *phm-Gal4>TnBVank1* PG cells (C-F) most of ALIX-marked vesicles have a different shape compared to that of the controls (A, B). Immunostaining with anti-ALIX and anti-*Tn*BVANK1 (cyan) shows a strong colocalization between *Tn*BVANK1 signal and the ALIX stroke-shaped vesicles (D). In *phm-Gal4>TnBVank1* PG cells, most of the ALIX (red) and Hrs (cyan) modified vesicles colocalize (F). PGs are at the same magnification and the reference scale bar is shown in A.

4.12 ALIX knockdown in the PG cells impairs larval development and lipid endosomal trafficking

To investigate ALIX involvement in the PG endocytic pathway, I knocked down *ALIX* gene function by overexpressing a specific RNA interference transgene. I took advantage of the *UAS-ALIX-RNAi* transgene containing inverted repeats of 328 bp designed to target a region of *ALIX* mRNA (Dietzl et al., 2007).

I specifically induced the expression of *ALIX-RNAi* in the PG using the *phm-Gal4* driver. All the *phm-Gal4>ALIX-RNAi* larvae completed the embryonic and larval development, but, interestingly, they showed an extended third larval instar. In fact, they reached the pupal stage four days after the *yw;phm-Gal4* control larvae.

Since a prolonged larval life has also been observed when *TnBVank1* was expressed in the PG, I performed an Oil Red O staining to evaluate the potential alteration of endocytosis due to *ALIX* silencing. In ALIX knockdown PG the lipid vesicular trafficking is impaired (Figure 28B) compared to *yw;phm-Gal4* control PG (Figure 28A), as showed in *phm-Gal4>TnBVank1* (Figure 23C, C').

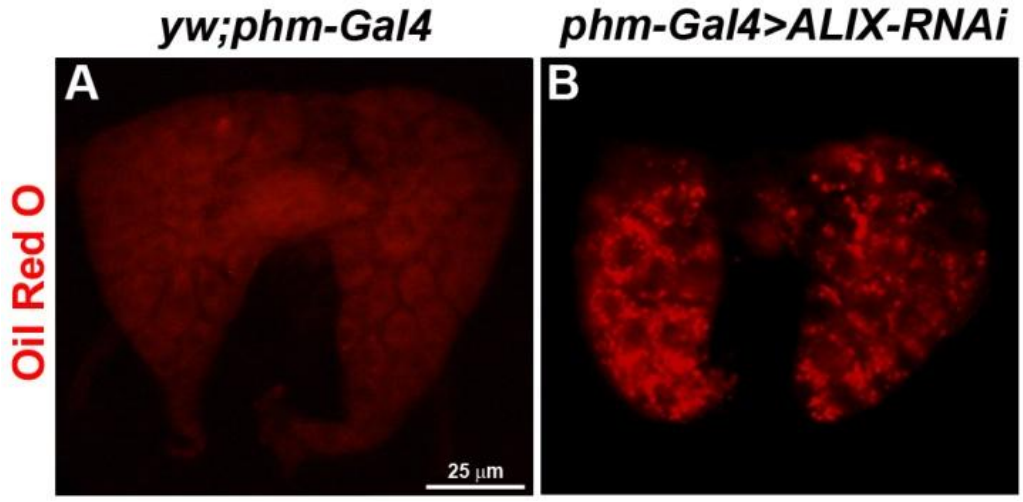

Figure 28. *ALIX* silencing in PG cells alters the lipid vesicular trafficking. (A) In control *yw;phm-Gal4* there are few lipid droplets stained with Oil Red O, while in *phm-Gal4>ALIX-RNAi* PG all cells show the increased accumulation of lipid droplets (B). Panels are at the same magnification and the reference scale bar is shown in A.

Therefore, this result suggests that *Tn*BVANK1 may hamper ALIX function in the cholesterol endocytic pathway.

5-Discussion

The associations between parasitic wasps and PDVs represent unique examples of virus domestication by a cellular organism, the parasitic wasp, to manipulate the physiology of another organism, the lepidopteran host (Bezier et al., 2009).

PDV infection contributes to a number of developmental and reproductive alterations associated with immunosuppression and disruption of host endocrine balance (Webb et al., 2000; Webb and Strand, 2005; Pennacchio and Strand, 2006). Relatively more studies have addressed the host immunosuppression mechanisms, focusing on virulence factors of the *ankyrin* gene family, largely shared among different taxa (Strand, 2012a). The proteins encoded by PDV *ankyrin* genes show significant sequence similarity with members of the IκB protein family involved in the control of NF-κB signaling pathways in insects and vertebrates (Silverman and Maniatis, 2001). Since they lack the N- and C-terminal domains controlling their signal-induced and basal degradation, they are able to bind NF-κB and prevent its entry into the nucleus to activate the transcription of genes under κB promoters (Thoetkiattikul et al., 2005; Falabella et al., 2007; Bitra et al., 2012).

The *ankyrin* gene family is one of the most widely distributed in PDVs and contains members which are rather conserved across viral isolates associated with different wasp species (Kroemer and Webb, 2005; Thoetkiattikul et al., 2005; Falabella et al., 2007; Shi et al., 2008; Strand, 2012b). These genes likely originated from horizontal gene transfer from eukaryotes, possibly the wasp itself, the host or another organism. Consistent with this possibility, the nudiviruses, ancestors of bracoviruses (Bezier et al., 2009), do not encode any gene showing similarity with *ankyrin* family members. Their multiple acquisition and stabilization in different evolutionary lineages are clearly indicative of the key role they play in successful parasitism. This also suggests that *ankyrin* genes may be involved in multiple tasks during host parasitization, by

influencing different physiological pathways. While an immunosuppressive function has been demonstrated for the PDV *ankyrin* gene family (Thoetkiattikul et al., 2005; Falabella et al., 2007; Bitra et al., 2012; Gueguen et al., 2013), if and how these viral genes impact endocrine pathways or other targets has not yet been addressed.

Here, I provided experimental data that corroborate this hypothesis for *TnBVank1*, a gene of the bracovirus associated with the wasp *Toxoneuron nigriceps* (*Tn*BV), which parasitizes the larval stages of the tobacco budworm, *Heliothis virescens*.

To better carry out my functional analyses I decided to use a well-established model organism, which offers me a variety of experimental tools that would not be available in *H. virescens*. Considering that many basic processes are evolutionarily conserved among the insects, *Drosophila melanogaster* appeared to be the best choice, not only because a plenty of molecular genetics techniques have been developed in this insect, but also because much information is available on *Drosophila* endocrine system.

I showed that *Tn*BVANK1 protein acts as a virulence factor in the prothoracic gland disrupting ecdysone biosynthesis and thus blocking the pupa formation.

Of note, the developmental arrest at L3 induced by *TnBVank1* gene expression in the PG perfectly mimics the developmental alteration of parasitized tobacco budworm larvae. In fact, *H. virescens* last instar larvae parasitized by endophagous braconid *T. nigriceps* fail to attain the pupal stage, due to a parasitoid-induced alteration of the endocrine system (Pennacchio et al., 1993; Pennacchio et al., 1997).

In *phm-Gal4>TnBVank1* larvae the 20E peak, which directs the entering in the wandering stage, is absent and the level of 20E remains extremely reduced during the extended larval life. Moreover, the larvae expressing *TnBVank1* in the PG, fed with 20E just before the onset of the ecdysteroid peak, are able to reach the pupal stage. In light of these data, it is reasonable to hypothesize that the developmental arrest may be due to

low levels of 20E. In agreement with this consideration, the expression of genes involved in ecdysone biosynthesis does not increase in the late third instar, as it occurs in wild-type larvae (Moeller et al., 2013). These results confirm that the developmental block induced by *Tn*BVANK1 during the third larval instar is caused by a reduced level of 20E in the whole body of *phm-Gal4>TnBVank1* larvae.

Similarly, it has been reported that the failure to pupariate of parasitized *H. virescens* last instar larvae is caused by the reduced amount of 20E produced by the depressed biosynthetic activity of PG (Pennacchio et al., 1993).

Furthermore, the analysis of PG expressing the transgene *TnBVank1* revealed that PGs from control larvae are significantly larger than *phm-Gal4>TnBVank1* PGs, but the cell area does not show a significant reduction between *phm-Gal4>TnBVank1* and control PG cells.

The reduced gland size observed in parasitized larvae and the low basal production of ecdysteroids (Pennacchio et al., 1997; Pennacchio et al., 1998) are fully compatible with a general reduction of the biosynthetic activity likely induced by *Tn*BV *ank* genes. However, in naturally parasitized larvae these symptoms are also associated with a disruption of PTTH signaling, which requires active *Tn*BV infection of PG, where different viral genes are expressed (Pennacchio et al., 2001; Falabella et al., 2006).

Immunostaining analyses with phalloidin, α-tubulinGFP and Dynein heavy chain antibody show that *Tn*BVANK1 disrupts the cytoskeletal structure of PG cells. Since the expression of *TnBVank1* in different tissues does not alter the developmental timing and adult formation, as demonstrated by using a wide range of tissue-specific *Gal4* drivers, the disruption of the cytoskeleton appears to be a PG-specific alteration.

Indeed, in a previous work it has been reported that the targeted expression of this *ank* gene in *Drosophila* germ cells alters microtubule network function in the oocyte, as

shown by the mislocalization of several maternal clues, without affecting the cytoskeletal structure (Duchi et al., 2010). Therefore, I cannot exclude that the specific effect of *Tn*BVANK1 on the cytoskeleton of PG cells may have a negative impact on ecdysteroidogenesis. However, the disruption of the cytoskeletal structure of these cells may rather be a downstream consequence of the impaired steroidogenic activity.

The ecdysone biosynthesis in the PG cells is preceded by the internalization of sterols precursors. *Tn*BVANK1 does not affect lipid uptake, however the endocytic pathway is impaired. In fact, stainings with Oil Red O and Filipin in the *phm-Gal4>TnBVank1* PG cells show high accumulation of lipid and sterol-rich vesicles.

The altered cell physiology and consequent accumulation of lipids and sterols may have wide-ranging and more generalized effects on cell architecture/dynamics and survival. In fact, the prolonged expression of *TnBVank1* through *phm-Gal4* during larval development induces apoptosis of a few cells, which could account for the observed reduction of the PG size.

In the same way, in *H. virescens* larvae, 120 h after parasitoid oviposition, cells start to undergo apoptosis (Pennacchio et al., 1997).

My immunostaining analysis performed with the Rab antibodies reveals that *TnBVank1* expression in PG cells causes an evident alteration of the endocytic pathway, which culminates in a reduction of Rab7-marked endosomes. Particularly, the endosomal system seems to be paused at the maturation of the early endosomes into late endosomes.

During the early-to-late endosome transition, MVBs form on early endosomal membranes and mediate transport to late endosomes. The strong colocalization of the *Tn*BVANK1 and Hrs immuno-detected signals suggests that this viral ankyrin protein is associated with MVBs.

In addition, the finding that *Tn*BVANK1 interacts with ALIX positive vesicles, altering their shape, strongly corroborates that in these cells the sterol trafficking is affected. Using an RNA interference approach, ALIX knockdown in the PG prolongs the last larval instar and interferes with sterol trafficking, as indicated by the accumulation of lipids stained by Oil Red O. Since the results obtained by silencing *ALIX* mimic those observed when *TnBVank1* is expressed in the PG, it is reasonable to hypothesize that *Tn*BVANK1 thwart the correct functioning of ALIX in the cholesterol trafficking endocytic pathway.

Recently, several lines of evidence indicate that in mammalian cells the lipid LBPA and its partner ALIX play a role in controlling the cholesterol export from endosomes (Bissig and Gruenberg, 2013). When ALIX interacts with LBPA via a mobile hydrophobic loop and promotes the ESCRT-III filaments nucleation, it induces perturbations of the endosomal limiting membrane. In particular, changes in membrane symmetry and curvature help clear the intralumenal face of the bilayer of its glycocalyx-like cover. In this way, the corresponding region of the membrane is prone to serve as the ILV docking site. The cholesterol stored into the ILVs can then leave the endosomal compartment to move to other membrane compartments, including the endoplasmic reticulum and the mitochondria, for ecdysone biosynthesis steps (Bissig and Gruenberg, 2014). Evidences from my *in vivo* studies suggest that ALIX could regulate the vesicular trafficking with the same mechanism also in *Drosophila*.

A possible model explaining the *Tn*BVANK1 function states that its expression in PG cells blocks the cholesterol export from endosomes. In agreement with the results reported here, I suppose that *Tn*BVANK1 may prevent the correct interaction between ALIX and its partners LBPA and ESCRT-III on the cytoplasmic leaflet of the endosomes. ILVs cannot do back-fusion with the limiting membrane and thus the

cholesterol is trapped into the MVBs (Figure 29). Finally, this block leads to insufficient sterol supplies to reach the ecdysone level necessary to complete development.

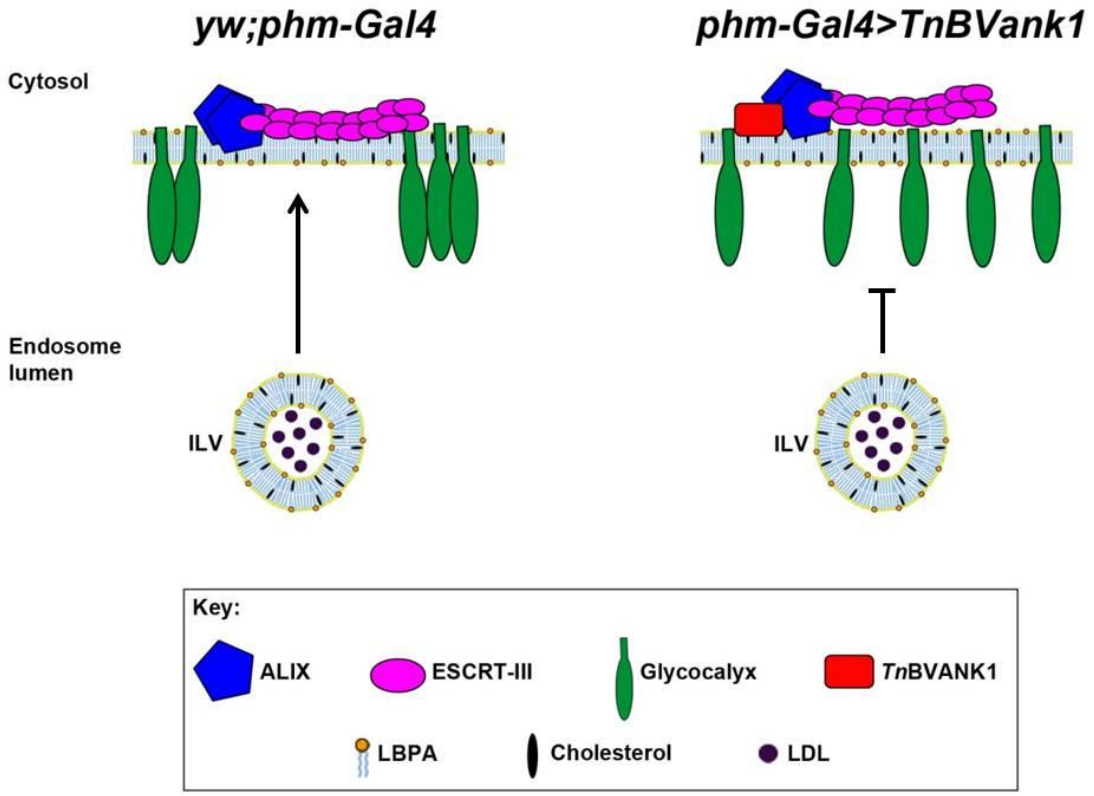

Figure 29. Proposed model of *Tn*BVANK1 action in MVBs of PG cells. In *phm-Gal4>TnBVank1 Tn*BVANK1 may avoid the interaction between ALIX, LBPA and ESCRT-III on the cytoplasmic leaflet of the MVBs. ILVs cannot do back-fusion with the limiting membrane and thus the LDL-derived cholesterol is trapped into the MVBs. Modified from (Bissig and Gruenberg, 2014).

The high similarity of the recorded phenotypes represents a solid background from which to start the design of specific experiments on the natural host. Indeed, the results reported here set the stage for specific *in vivo* studies, that will help address the respective roles of different PG-directed *Tn*BV genes in the suppression of ecdysteroidogenesis in parasitized host larvae.

6-References

Andersen, J. N., Mortensen, O. H., Peters, G. H., Drake, P. G., Iversen, L. F., Olsen, O. H., Jansen, P. G., Andersen, H. S., Tonks, N. K. and Moller, N. P. (2001). Structural and evolutionary relationships among protein tyrosine phosphatase domains. *Molecular and cellular biology* **21**, 7117-7136.

Annika, M., Carolina, E. H., Lars, M., Ulf, E. and Annelie, F. (2013). Imaging of neutral lipids by oil red O for analyzing the metabolic status in health and disease. *Nature Protocols* **8**, 1149-1154.

Ashburner, M., Chihara, C., Meltzer, P. and Richards, G. (1974). Temporal control of puffing activity in polytene chromosomes. *Cold Spring Harbor symposia on quantitative biology* **38**, 655-662.

Beckage, N. E. (1993). Endocrine and neuroendocrine host-parasite relationships. *Receptor* **3**, 233-245.

Beckage, N. E. and Gelman, D. B. (2004). Wasp parasitoid disruption of host development: implications for new biologically based strategies for insect control. *Annu Rev Entomol* **49**, 299-330.

Beckstead, R. B. and Thummel, C. S. (2006). Indicted: worms caught using steroids. *Cell* **124**, 1137-1140.

Bergmann, A., Stein, D., Geisler, R., Hagenmaier, S., Schmid, B., Fernandez, N., Schnell, B. and Nusslein-Volhard, C. (1996). A gradient of cytoplasmic Cactus degradation establishes the nuclear localization gradient of the dorsal morphogen in *Drosophila*. *Mechanisms of development* **60**, 109-123.

Bezier, A., Annaheim, M., Herbiniere, J., Wetterwald, C., Gyapay, G., Bernard-Samain, S., Wincker, P., Roditi, I., Heller, M., Belghazi, M. et al. (2009). Polydnaviruses of braconid wasps derive from an ancestral nudivirus. *Science* **323**, 926-930.

Bissig, C. and Gruenberg, J. (2013). Lipid sorting and multivesicular endosome biogenesis. *Cold Spring Harbor perspectives in biology* **5**, a016816.

Bissig, C. and Gruenberg, J. (2014). ALIX and the multivesicular endosome: ALIX in Wonderland. *Trends in cell biology* **24**, 19-25.

Bitra, K., Suderman, R. J. and Strand, M. R. (2012). Polydnavirus Ank proteins bind NF-kappaB homodimers and inhibit processing of Relish. *PLoS pathogens* **8**, e1002722.

Brand, A. H. and Perrimon, N. (1993). Targeted gene expression as a means of altering cell fates and generating dominant phenotypes. *Development* **118**, 401-415.

Buszczak, M., Freeman, M. R., Carlson, J. R., Bender, M., Cooley, L. and Segraves, W. A. (1999). Ecdysone response genes govern egg chamber development during mid-oogenesis in *Drosophila*. *Development* **126**, 4581-4589.

Carney, G. E. and Bender, M. (2000). The *Drosophila* ecdysone receptor (*EcR*) gene is required maternally for normal oogenesis. *Genetics* **154**, 1203-1211.

Carrera, P., Abrell, S., Kerber, B., Walldorf, U., Preiss, A., Hoch, M. and Jackle, H. (1998). A modifier screen in the eye reveals control genes for Kruppel activity in the *Drosophila* embryo. *Proceedings of the National Academy of Sciences of the United States of America* **95**, 10779-10784.

Chavez, V. M., Marques, G., Delbecque, J. P., Kobayashi, K., Hollingsworth, M., Burr, J., Natzle, J. E. and O'Connor, M. B. (2000). The *Drosophila disembodied* gene controls late embryonic morphogenesis and codes for a cytochrome P450 enzyme that regulates embryonic ecdysone levels. *Development* **127**, 4115-4126.

Clark, A. J. and Block, K. (1959). The absence of sterol synthesis in insects. *The Journal of biological chemistry* **234**, 2578-2582.

Colombani, J., Bianchini, L., Layalle, S., Pondeville, E., Dauphin-Villemant, C., Antoniewski, C., Carre, C., Noselli, S. and Leopold, P. (2005). Antagonistic actions of ecdysone and insulins determine final size in *Drosophila*. *Science* **310**, 667-670.

Consoli, F. L., Lewis, D., Keeley, L. and Vinson, S. B. (2007). Characterization of a cDNA encoding a putative chitinase from teratocytes of the endoparasitoid *Toxoneuron nigriceps*. *Entomologia Experimentalis et Applicata* **122**, 271-278.

Dai, J. D. and Gilbert, L. I. (1991). Metamorphosis of the corpus allatum and degeneration of the prothoracic glands during the larval-pupal-adult transformation of *Drosophila melanogaster*: a cytophysiological analysis of the ring gland. *Developmental biology* **144**, 309-326.

Davis, R. J., Tavsanli, B. C., Dittrich, C., Walldorf, U. and Mardon, G. (2003). *Drosophila* retinal homeobox (drx) is not required for establishment of the visual system, but is required for brain and clypeus development. *Developmental biology* **259**, 272-287.

De Gregorio, E., Spellman, P. T., Rubin, G. M. and Lemaitre, B. (2001). Genome-wide analysis of the *Drosophila* immune response by using oligonucleotide microarrays. *Proceedings of the National Academy of Sciences of the United States of America* **98**, 12590-12595.

Deepa Parvathi, V., Akshaya Amritha, S. and Solomon, F. D. (2009). Wonder animal model for genetic studies - *Drosophila Melanogaster* - its life cycle and breeding methods - a review. *Sri Ramachandra Journal of Medicine* **2**, 33-38.

Demerec, M. and Kaufman, P. (1996). *Drosophila* Guide: Introduction to the genetics and cytology of *Drosophila melanogaster*. Cold Spring Harbor Laboratory. 4-8.

Dietzl, G., Chen, D., Schnorrer, F., Su, K. C., Barinova, Y., Fellner, M., Gasser, B., Kinsey, K., Oppel, S., Scheiblauer, S. et al. (2007). A genome-wide transgenic RNAi library for conditional gene inactivation in Drosophila. *Nature* **448**, 151-156.

Dikic, I. (2006). Endosomes. *Landes Bioscience and Springer Science+Business Media*, 15.

Duchi, S., Cavaliere, V., Fagnocchi, L., Grimaldi, M. R., Falabella, P., Graziani, F., Gigliotti, S., Pennacchio, F. and Gargiulo, G. (2010). The impact on microtubule network of a bracovirus IkappaB-like protein. *Cellular and molecular life sciences : CMLS* **67**, 1699-1712.

Espagne, E., Dupuy, C., Huguet, E., Cattolico, L., Provost, B., Martins, N., Poirie, M., Periquet, G. and Drezen, J. M. (2004). Genome sequence of a polydnavirus: insights into symbiotic virus evolution. *Science* **306**, 286-289.

Falabella, P., Caccialupi, P., Varricchio, P., Malva, C. and Pennacchio, F. (2006). Protein tyrosine phosphatases of *Toxoneuron nigriceps* bracovirus as potential disrupters of host prothoracic gland function. *Arch Insect Biochem Physiol* **61**, 157-169.

Falabella, P., Varricchio, P., Gigliotti, S., Tranfaglia, A., Pennacchio, F. and Malva, C. (2003). *Toxoneuron nigriceps* polydnavirus encodes a putative aspartyl protease highly expressed in parasitized host larvae. *Insect molecular biology* **12**, 9-17.

Falabella, P., Varricchio, P., Provost, B., Espagne, E., Ferrarese, R., Grimaldi, A., de Eguileor, M., Fimiani, G., Ursini, M. V., Malva, C. et al. (2007). Characterization of the IkappaB-like gene family in polydnaviruses associated with wasps belonging to different Braconid subfamilies. *The Journal of general virology* **88**, 92-104.

Falguieres, T., Castle, D. and Gruenberg, J. (2012). Regulation of the MVB pathway by SCAMP3. *Traffic* **13**, 131-142.

Falguieres, T., Luyet, P. P., Bissig, C., Scott, C. C., Velluz, M. C. and Gruenberg, J. (2008). In vitro budding of intralumenal vesicles into late endosomes is regulated by Alix and Tsg101. *Molecular biology of the cell* **19**, 4942-4955.

Fernandes-Alnemri, T., Litwack, G. and Alnemri, E. S. (1994). CPP32, a novel human apoptotic protein with homology to *Caenorhabditis elegans* cell death protein Ced-3 and mammalian interleukin-1 beta-converting enzyme. *The Journal of biological chemistry* **269**, 30761-30764.

Ferrarese, R., Brivio, M., Congiu, T., Falabella, P., Grimaldi, A., Mastore, M., Perletti, G., F., P., Sciacca, L., Tettamanti, G. et al. (2005). Early suppression of immune response in *Heliothis virescens* larvae by the endophagous parasitoid *Toxoneuron nigriceps*. *Inv. Surv. J.* **2**, 60-68.

Florentin, A. and Arama, E. (2012). Caspase levels and execution efficiencies determine the apoptotic potential of the cell. *The Journal of cell biology* **196**, 513-527.

Friend, D. S. and Bearer, E. L. (1981). beta-Hydroxysterol distribution as determined by freeze-fracture cytochemistry. *The Histochemical journal* **13**, 535-546.

Fristrom, D. K. and Fristrom, J. W. (1993). The metamorphic development of the adult epidermis. In " The development of *Drosophila melanogaster*", vol. 2, pp. 843-898.

Gavrieli, Y., Sherman, Y. and Ben-Sasson, S. A. (1992). Identification of programmed cell death in situ via specific labeling of nuclear DNA fragmentation. *The Journal of cell biology* **119**, 493-501.

Gaziova, I., Bonnette, P. C., Henrich, V. C. and Jindra, M. (2004). Cell-autonomous roles of the *ecdysoneless* gene in *Drosophila* development and oogenesis. *Development* **131**, 2715-2725.

Gilbert, L. I. (2004). Halloween genes encode P450 enzymes that mediate steroid hormone biosynthesis in *Drosophila melanogaster*. *Molecular and cellular endocrinology* **215**, 1-10.

Gilbert, L. I. (2011). Insect endocrinology. Academic Press. 126.

Gilbert, L. I. and Warren, J. T. (2005). A molecular genetic approach to the biosynthesis of the insect steroid molting hormone. *Vitamins and hormones* **73**, 31-57.

Godfray, H. C. (1994). Parasitoids: behavioral and evolutionary ecology. *Princeton University Press. Princeton*.

Grieder, N. C., de Cuevas, M. and Spradling, A. C. (2000). The fusome organizes the microtubule network during oocyte differentiation in *Drosophila*. *Development* **127**, 4253-4264.

Gueguen, G., Kalamarz, M. E., Ramroop, J., Uribe, J. and Govind, S. (2013). Polydnaviral ankyrin proteins aid parasitic wasp survival by coordinate and selective inhibition of hematopoietic and immune NF-kappa B signaling in insect hosts. *PLoS pathogens* **9**, e1003580.

Hackney, J. F., Zolali-Meybodi, O. and Cherbas, P. (2012). Tissue damage disrupts developmental progression and ecdysteroid biosynthesis in *Drosophila*. *PloS one* **7**, e49105.

Hartwell, L., Hood, L., Goldberg, M., Reynolds, A. and Silver, L. (2011). Genetics: from genes to genomes. McGraw-Hill Higher education.

Hay, B. A., Wolff, T. and Rubin, G. M. (1994). Expression of baculovirus P35 prevents cell death in *Drosophila*. *Development* **120**, 2121-2129.

Henrich, V. C., Szekely, A. A., Kim, S. J., Brown, N. E., Antoniewski, C., Hayden, M. A., Lepesant, J. A. and Gilbert, L. I. (1994). Expression and function of the *ultraspiracle* (*usp*) gene during development of *Drosophila melanogaster*. *Developmental biology* **165**, 38-52.

Herman, W. S. and Gilbert, L. I. (1966). The neuroendocrine system of Hyalaphora cecropia (L) (Lepidoptera: Saturniidae). I. The anatomy and histology of the ecdysial gland. *General and comparative endocrinology* **7**, 275-291.

Hoffmann, J. A. (2003). The immune response of *Drosophila*. *Nature* **426**, 33-38.

Hrdlicka, L., Gibson, M., Kiger, A., Micchelli, C., Schober, M., Schock, F. and Perrimon, N. (2002). Analysis of twenty-four Gal4 lines in *Drosophila melanogaster*. *genesis* **34**, 51-57.

Huang, X., Warren, J. T. and Gilbert, L. I. (2008). New players in the regulation of ecdysone biosynthesis. *Journal of genetics and genomics = Yi chuan xue bao* **35**, 1-10.

Huotari, J. and Helenius, A. (2011). Endosome maturation. *The EMBO journal* **30**, 3481-3500.

Ikonen, E. (2008). Cellular cholesterol trafficking and compartmentalization. *Nature reviews. Molecular cell biology* **9**, 125-138.

Jiang, C., Baehrecke, E. H. and Thummel, C. S. (1997). Steroid regulated programmed cell death during *Drosophila* metamorphosis. *Development* **124**, 4673-4683.

Jurgens, G., Wieschaus, E., Nusslein-Volhard, C. and Kluding, H. (1984). Mutations affecting the pattern of the larval cuticle in *Drosophila melanogaster*. *Roux's Archives of Developmental Biology* **193**, 283-295.

Kappler, C., Kabbouh, M., Hetru, C., Durst, F. and Hoffmann, J. A. (1988). Characterization of three hydroxylases involved in the final steps of biosynthesis of the steroid hormone ecdysone in *Locusta migratoria* (Insecta, Orthoptera). *Journal of steroid biochemistry* **31**, 891-898.

Koelle, M. R. (1992). Molecular analysis of the *Drosophila* ecdysone receptor complex. *PhD thesys. Stanford University, Stanford, CA.*

Koelle, M. R., Talbot, W. S., Segraves, W. A., Bender, M. T., Cherbas, P. and Hogness, D. S. (1991). The *Drosophila* EcR gene encodes an ecdysone receptor, a new member of the steroid receptor superfamily. *Cell* **67**, 59-77.

Kroemer, J. A. and Webb, B. A. (2005). Ikappabeta-related vankyrin genes in the *Campoletis sonorensis* ichnovirus: temporal and tissue-specific patterns of expression in parasitized *Heliothis virescens* lepidopteran hosts. *Journal of virology* **79**, 7617-7628.

Lee, T. and Luo, L. (1999). Mosaic analysis with a repressible cell marker for studies of gene function in neuronal morphogenesis. *Neuron* **22**, 451-461.

Li, S., Falabella, P., Kuriachan, I., Vinson, S. B., Borst, D. W., Malva, C. and Pennacchio, F. (2003). Juvenile hormone synthesis, metabolism, and resulting haemolymph titre in *Heliothis virescens* larvae parasitized by *Toxoneuron nigriceps*. *Journal of insect physiology* **49**, 1021-1030.

Lloyd, T. E., Atkinson, R., Wu, M. N., Zhou, Y., Pennetta, G. and Bellen, H. J. (2002). Hrs regulates endosome membrane invagination and tyrosine kinase receptor signaling in *Drosophila*. *Cell* **108**, 261-269.

Luo, L., Liao, Y. J., Jan, L. Y. and Jan, Y. N. (1994). Distinct morphogenetic functions of similar small GTPases: *Drosophila* Drac1 is involved in axonal outgrowth and myoblast fusion. *Genes & development* **8**, 1787-1802.

Malva, C., Varricchio, P., Falabella, P., La Scaleia, R., Graziani, F. and Pennacchio, F. (2004). Physiological and molecular interaction in the host-parasitoid system *Heliothis virescens-Toxoneuron nigriceps*: current status and future perspectives. *Insect biochemistry and molecular biology* **34**, 177-183.

Manning, L. and Doe, C. Q. (1999). Prospero distinguishes sibling cell fate without asymmetric localization in the *Drosophila* adult external sense organ lineage. *Development* **126**, 2063-2071.

Manseau, L., Baradaran, A., Brower, D., Budhu, A., Elefant, F., Phan, H., Philip, A. V., Yang, M., Glover, D., Kaiser, K. et al. (1997). GAL4 enhancer traps expressed in the embryo, larval brain, imaginal discs, and ovary of *Drosophila*. *Developmental Dynamics* **209**, 310-322.

Maxfield, F. R. and van Meer, G. (2010). Cholesterol, the central lipid of mammalian cells. *Current opinion in cell biology* **22**, 422-429.

McGrail, M. and Hays, T. S. (1997). The microtubule motor cytoplasmic dynein is required for spindle orientation during germline cell divisions and oocyte differentiation in *Drosophila*. *Development* **124**, 2409-2419.

McGuire, S. E., Le, P. T., Osborn, A. J., Matsumoto, K. and Davis, R. L. (2003). Spatiotemporal rescue of memory dysfunction in *Drosophila*. *Science* **302**, 1765-1768.

Milislav, D. (1950). Biology of *Drosophila*. 10 th ed. Cold Spring Harbor Laboratory. 1-2.

Mirth, C., Truman, J. W. and Riddiford, L. M. (2005). The Role of the Prothoracic Gland in Determining Critical Weight for Metamorphosis in *Drosophila melanogaster*. *Current Biology* **15**, 1796-1807.

Missotten, M., Nichols, A., Rieger, K. and Sadoul, R. (1999). Alix, a novel mouse protein undergoing calcium-dependent interaction with the apoptosis-linked-gene 2 (ALG-2) protein. *Cell death and differentiation* **6**, 124-129.

Mobius, W., van Donselaar, E., Ohno-Iwashita, Y., Shimada, Y., Heijnen, H. F., Slot, J. W. and Geuze, H. J. (2003). Recycling compartments and the internal vesicles of multivesicular bodies harbor most of the cholesterol found in the endocytic pathway. *Traffic* **4**, 222-231.

Moeller, M. E., Danielsen, E. T., Herder, R., O'Connor, M. B. and Rewitz, K. F. (2013). Dynamic feedback circuits function as a switch for shaping a maturation-inducing steroid pulse in *Drosophila*. *Development* **140**, 4730-4739.

Mulinari, S. (2008). From Cell Shape to Body Shape: Epithelial Morphogenesis in *Drosophila melanogaster*. *PhD thesys. Lund University, Sweden*.

Neubueser, D., Warren, J. T., Gilbert, L. I. and Cohen, S. M. (2005). molting defective is required for ecdysone biosynthesis. *Developmental biology* **280**, 362-372.

Nijhout, H. F. (1994). Genes on the wing. *Science* **265**, 44-45.

Nijhout, H. F. and Williams, C. M. (1974). Control of moulting and metamorphosis in the tobacco hornworm, *Manduca sexta*: Cessation of juvenile hormone secretion as a trigger for pupation. *J. Exp. Biol.* **61**, 493-501.

Niwa, R. and Niwa, Y. S. (2011). The Fruit Fly *Drosophila melanogaster* as a Model System to Study Cholesterol Metabolism and Homeostasis. *Cholesterol*.

Niwa, R., Matsuda, T., Yoshiyama, T., Namiki, T., Mita, K., Fujimoto, Y. and Kataoka, H. (2004). CYP306A1, a cytochrome P450 enzyme, is essential for ecdysteroid biosynthesis in the prothoracic glands of Bombyx and *Drosophila*. *The Journal of biological chemistry* **279**, 35942-35949.

Niwa, R., Namiki, T., Ito, K., Shimada-Niwa, Y., Kiuchi, M., Kawaoka, S., Kayukawa, T., Banno, Y., Fujimoto, Y., Shigenobu, S. et al. (2010). *Non-molting glossy/shroud* encodes a short-chain dehydrogenase/reductase that functions in the 'Black Box' of the ecdysteroid biosynthesis pathway. *Development* **137**, 1991-1999.

Nusslein-Volhard, C., Wieschaus, E. and Kluding, H. (1984). Mutations affecting the pattern of the larval cuticle in *Drosophila melanogaster*. *Roux's Archives of Developmental Biology* **193**, 267-282.

Odorizzi, G. (2006). The multiple personalities of Alix. *Journal of cell science* **119**, 3025-3032.

Ono, H., Rewitz, K. F., Shinoda, T., Itoyama, K., Petryk, A., Rybczynski, R., Jarcho, M., Warren, J. T., Marques, G., Shimell, M. J. et al. (2006). Spook and Spookier code for stage-specific components of the ecdysone biosynthetic pathway in Diptera. *Developmental biology* **298**, 555-570.

Oro, A. E., McKeown, M. and Evans, R. M. (1990). Relationship between the product of the *Drosophila* ultraspiracle locus and the vertebrate retinoid X receptor. *Nature* **347**, 298-301.

Parvy, J. P., Blais, C., Bernard, F., Warren, J. T., Petryk, A., Gilbert, L. I., O'Connor, M. B. and Dauphin-Villemant, C. (2005). A role for betaFTZ-F1 in regulating ecdysteroid titers during post-embryonic development in *Drosophila melanogaster*. *Developmental biology* **282**, 84-94.

Pennacchio, F. and Strand, M. R. (2006). Evolution of developmental strategies in parasitic hymenoptera. *Annu Rev Entomol* **51**, 233-258.

Pennacchio, F., Vinson, S. B. and Tremblay, E. (1993). Growth and development of *Cardiochiles nigriceps* Viereck (Hymenoptera, Braconidae) larvae and their synchronization with some changes of the hemolymph composition of their host,

Heliothis virescens (F.) (Lepidoptera, Noctuidae). *Archives of Insect Biochemistry & Physiology* **24**, 65-77.

Pennacchio, F., Malva, C. and Vinson, S. (2001). Regulation of host endocrine system by the endophagous braconid *Cardiochiles nigriceps* and its polydnavirus. In: Edwards JP, Weaver RJ (eds) Endocrine interactions of insect parasites and pathogens. BIOS Scientific, Oxford. 123-132.

Pennacchio, F., Tranfaglia, A. and Malva, C. (2003). Host-parasitoid antagonism in insects: New opportunities for pest control? *AGROFood industry hi-tech*, 53-56.

Pennacchio, F., Vinson, S., Tremblay, E. and Tanaka, T. (1994). Biochemical and developmental alterations of *Heliothis virescens* (F.) (Lepidoptera, Noctuidae) larvae induced by the endophagous parasitoid *Cardiochiles nigriceps* Viereck (Hymenoptera, Braconidae). *Arch Insect Biochem Physiol* **26**, 211-233.

Pennacchio, F., Sordetti, R., Falabella, P. and Vinson, S. (1997). Biochemical and ultrastructural alterations in prothoracic glands of *Heliothis virescens* (F.) (Lepidoptera: Noctuidae) last instar larvae parasitized by *Cardiochiles nigriceps* Viereck (Hymenoptera: Braconidae). *Insect biochemistry and molecular biology* **27**, 439-450.

Pennacchio, F., Falabella, P., Sordetti, R., Varricchio, P., Malva, C. and Vinson, S. B. (1998). Prothoracic gland inactivation in *Heliothis virescens* (F.) (Lepidoptera:Noctuidae) larvae parasitized by *Cardiochiles nigriceps* Viereck (Hymenoptera:Braconidae). *Journal of insect physiology* **44**, 845-857.

Petryk, A., Warren, J. T., Marques, G., Jarcho, M. P., Gilbert, L. I., Kahler, J., Parvy, J. P., Li, Y., Dauphin-Villemant, C. and O'Connor, M. B. (2003). Shade is the *Drosophila* P450 enzyme that mediates the hydroxylation of ecdysone to the steroid insect molting hormone 20-hydroxyecdysone. *Proceedings of the National Academy of Sciences of the United States of America* **100**, 13773-13778.

Provost, B., Varricchio, P., Arana, E., Espagne, E., Falabella, P., Huguet, E., La Scaleia, R., Cattolico, L., Poirie, M., Malva, C. et al. (2004). Bracoviruses contain a large multigene family coding for protein tyrosine phosphatases. *Journal of virology* **78**, 13090-13103.

Quicke, D. L. (1997). Parasitic wasps. *Chapman and Hall, London*.

Raffa, G. D., Cenci, G., Siriaco, G., Goldberg, M. L. and Gatti, M. (2005). The putative *Drosophila* transcription factor woc is required to prevent telomeric fusions. *Molecular cell* **20**, 821-831.

Rawlings, N. D. and Barrett, A. J. (1995). Families of aspartic peptidases, and those of unknown catalytic mechanism. *Methods in enzymology* **248**, 105-120.

Rewitz, K. F., Rybczynski, R., Warren, J. T. and Gilbert, L. I. (2006a). Developmental expression of *Manduca shade*, the P450 mediating the final step in molting hormone synthesis. *Molecular and cellular endocrinology* **247**, 166-174.

Rewitz, K. F., Styrishave, B., Lobner-Olsen, A. and Andersen, O. (2006b). Marine invertebrate cytochrome P450: emerging insights from vertebrate and insects analogies. *Comparative biochemistry and physiology. Toxicology & pharmacology : CBP* **143**, 363-381.

Riddiford, L. M. (1982). Changes in translatable mRNAs during the larval-pupal transformation of the epidermis of the tobacco hornworm. *Developmental biology* **92**, 330-342.

Riddiford, L. M., Truman, J. W., Mirth, C. K. and Shen, Y. C. (2010). A role for juvenile hormone in the prepupal development of *Drosophila melanogaster*. *Development* **137**, 1117-1126.

Rodenburg, K. W. and Van der Horst, D. J. (2005). Lipoprotein-mediated lipid transport in insects: analogy to the mammalian lipid carrier system and novel concepts for the functioning of LDL receptor family members. *Biochimica et biophysica acta* **1736**, 10-29.

Rogers, S., Wells, R. and Rechsteiner, M. (1986). Amino acid sequences common to rapidly degraded proteins: the PEST hypothesis. *Science* **234**, 364-368.

Roignant, J. Y., Carre, C., Mugat, B., Szymczak, D., Lepesant, J. A. and Antoniewski, C. (2003). Absence of transitive and systemic pathways allows cell-specific and isoform-specific RNAi in *Drosophila*. *RNA (New York, N.Y.)* **9**, 299-308.

Safranek, L. and Williams, C. M. (1989). Inactivation of the corpora allata in the final instar of the tobacco hornworm, *Manduca sexta*, requires integrity of certain neural pathways from the brain. *Biol. Bull.* **177**, 396-400.

Schubiger, M., Wade, A. A., Carney, G. E., Truman, J. W. and Bender, M. (1998). *Drosophila* EcR-B ecdysone receptor isoforms are required for larval molting and for neuron remodeling during metamorphosis. *Development* **125**, 2053-2062.

Shea, M. J., King, D. L., Conboy, M. J., Mariani, B. D. and Kafatos, F. C. (1990). Proteins that bind to *Drosophila* chorion cis-regulatory elements: a new C2H2 zinc finger protein and a C2C2 steroid receptor-like component. *Genes & development* **4**, 1128-1140.

Shi, M., Chen, Y. F., Huang, F., Liu, P. C., Zhou, X. P. and Chen, X. X. (2008). Characterization of a novel gene encoding ankyrin repeat domain from *Cotesia vestalis* polydnavirus (*Cv*BV). *Virology* **375**, 374-382.

Silverman, N. and Maniatis, T. (2001). NF-kappaB signaling pathways in mammalian and insect innate immunity. *Genes & development* **15**, 2321-2342.

Sinenko, S. A. and Mathey-Prevot, B. (2004). Increased expression of *Drosophila* tetraspanin, Tsp68C, suppresses the abnormal proliferation of ytr-deficient and Ras/Raf-activated hemocytes. *Oncogene* **23**, 9120-9128.

Stoltz, D. B., Krell, P., Summers, M. D. and Vinson, S. B. (1984). Polydnaviridae - a proposed family of insect viruses with segmented, double-stranded, circular DNA genomes. *Intervirology* **21**, 1-4.

Strand, M. R. (2010). Polydnaviruses. In: Insect Virology, Asgari, S. and K.N. Johnson (eds.). 216-241. Academic Press, Norwich, UK.

Strand, M. R. (2012a). Polydnavirus gene products that interact with the host immune system. In: Beckage NE, Drezen JM (eds) Parasitoid Viruses - Symbionts and Pathogens, Elsevier Inc: 149-161.

Strand, M. R. (2012b). Polydnavirus gene expression profiling: what we know now. In Beckage NE, Drezen JM (eds) Parasitoid Viruses - Symbionts and Pathogens, Elsevier Inc: 139-147.

Talbot, W. S., Swyryd, E. A. and Hogness, D. S. (1993). *Drosophila* tissues with different metamorphic responses to ecdysone express different ecdysone receptor isoforms. *Cell* **73**, 1323-1337.

Tanaka, T. and Vinson, S. (1991). Interactions of venoms with the calyx fluids of three parasitoids, *Chardiochiles nigriceps*, *Microplitis croceipes* (Hymenoptera: Braconidae) and *Campoletis sonorensis* (Hymenoptera: Ichneumonidae) in effecting a delay in pupation in *Heliothis virescens* (Lepidopteran: Noctuidae) *Ann. Entomol. Soc. Am.* **84**, 87.

Tanaka, T. and Nakamura, A. (2008). The endocytic pathway acts downstream of Oskar in *Drosophila* germ plasm assembly. *Development* **135**, 1107-1117.

Tata, J. R. (2002). Signalling through nuclear receptors. *Nature reviews. Molecular cell biology* **3**, 702-710.

Terashima, J., Takaki, K., Sakurai, S. and Bownes, M. (2005). Nutritional status affects 20-hydroxyecdysone concentration and progression of oogenesis in *Drosophila melanogaster*. *The Journal of endocrinology* **187**, 69-79.

Tettamanti, G., Grimaldi, A., Pennacchio, F. and de Eguileor, M. (2008). *Toxoneuron nigriceps* parasitization delays midgut replacement in fifth-instar *Heliothis virescens* larvae. *Cell and tissue research* **332**, 371-379.

Theilmann, D. A. and Summers, M. D. (1988). Identification and comparison of *Campoletis sonorensis* virus transcripts expressed from four genomic segments in the insect hosts *Campoletis sonorensis* and *Heliothis virescens*. *Virology* **167**, 329-341.

Thoetkiattikul, H., Beck, M. H. and Strand, M. R. (2005). Inhibitor kappaB-like proteins from a polydnavirus inhibit NF-kappaB activation and suppress the insect immune response. *Proceedings of the National Academy of Sciences of the United States of America* **102**, 11426-11431.

Thomas, H. E., Stunnenberg, H. G. and Stewart, A. F. (1993). Heterodimerization of the *Drosophila* ecdysone receptor with retinoid X receptor and ultraspiracle. *Nature* **362**, 471-475.

Torroja, L., Chu, H., Kotovsky, I. and White, K. (1999). Neuronal overexpression of APPL, the *Drosophila* homologue of the amyloid precursor protein (APP), disrupts axonal transport. *Current Biology* **9**, 489-492.

Tsuda, M., Seong, K. H. and Aigaki, T. (2006). POSH, a scaffold protein for JNK signaling, binds to ALG-2 and ALIX in *Drosophila*. *FEBS letters* **580**, 3296-3300.

Turnbull, M. and Webb, B. (2002). Perspectives on polydnavirus origins and evolution. *Advances in virus research* **58**, 203-254.

Varricchio, P., Falabella, P., Sordetti, R., Graziani, F., Malva, C. and Pennacchio, F. (1999). *Cardiochiles nigriceps* polydnavirus: molecular characterization and gene expression in parasitized *Heliothis virescens* larvae. *Insect biochemistry and molecular biology* **29**, 1087-1096.

Vinson, S. and Iwantsch, G. (1980). Host regulation by insect parasitoids. *Q. Rev. Bio.* **55**, 143-165.

Vinson, S. B. and Scott, J. R. (1974). Parasitoid egg shell changes in a suitable and unsuitable host. *Journal of ultrastructure research* **47**, 1-15.

Volkoff, A. N., Beliveau, C., Rocher, J., Hilgarth, R., Levasseur, A., Duonor-Cerutti, M., Cusson, M. and Webb, B. A. (2002). Evidence for a conserved polydnavirus gene family: ichnovirus homologs of the CsIV repeat element genes. *Virology* **300**, 316-331.

Warren, J. T., Wismar, J., Subrahmanyam, B. and Gilbert, L. I. (2001). *Woc* (*without children*) gene control of ecdysone biosynthesis in *Drosophila melanogaster*. *Molecular and cellular endocrinology* **181**, 1-14.

Warren, J. T., Yerushalmi, Y., Shimell, M. J., O'Connor, M. B., Restifo, L. L. and Gilbert, L. I. (2006). Discrete pulses of molting hormone, 20-hydroxyecdysone, during late larval development of *Drosophila melanogaster*: correlations with changes in gene activity. *Developmental dynamics : an official publication of the American Association of Anatomists* **235**, 315-326.

Warren, J. T., Petryk, A., Marques, G., Jarcho, M., Parvy, J. P., Dauphin-Villemant, C., O'Connor, M. B. and Gilbert, L. I. (2002). Molecular and biochemical characterization of two P450 enzymes in the ecdysteroidogenic pathway of *Drosophila melanogaster*. *Proceedings of the National Academy of Sciences of the United States of America* **99**, 11043-11048.

Warren, J. T., Petryk, A., Marques, G., Parvy, J. P., Shinoda, T., Itoyama, K., Kobayashi, J., Jarcho, M., Li, Y., O'Connor, M. B. et al. (2004). *Phantom* encodes the 25-hydroxylase of *Drosophila melanogaster* and *Bombyx mori*: a P450 enzyme critical in ecdysone biosynthesis. *Insect biochemistry and molecular biology* **34**, 991-1010.

Webb, B. A. (1998). Polydnavirus Biology, Genome Structure, and Evolution. In: Miller, L. K., and Ball L. A., The Insect Viruses. 105-134.

Webb, B. A. and Strand, M. R. (2005). The biology and genomics of polydnaviruses. *In Comprehensive Molecular Insect Science* **6**, 323-360.

Webb, B. A., Beckage, N. E., Hayakawa, Y., Krell, P. J., Lanzrein, B., Stoltz, D. B., Strand, M. R. and Summers, M. D. (2000). Family Polydnaviridae. *In Virus Taxonomy: Seventh Report of the International Committee on Taxonomy of Viruses*, 253-260.

Webb, B. A., Strand, M. R., Dickey, S. E., Beck, M. H., Hilgarth, R. S., Barney, W. E., Kadash, K., Kroemer, J. A., Lindstrom, K. G., Rattanadechakul, W. et al. (2006). Polydnavirus genomes reflect their dual roles as mutualists and pathogens. *Virology* **347**, 160-174.

Whitfield, J. B. (2002). Estimating the age of the polydnavirus/braconid wasp symbiosis. *Proceedings of the National Academy of Sciences of the United States of America* **99**, 7508-7513.

Whitfield, J. B. and Dangerfield, P. C. (1997). Subfamily Cardiochilinae. pp-176-183. In Warton, R. A., Marsh, P. M., and Sharkey, M. J. eds. Manual of the New World Genera of the family *Braconidae* (Hymenoptera). Special pubblications of the International Society of Hymenopterists. 439.

Wieschaus, E., Nusslein-Volhard, C. and Jurgens, G. (1984). Mutations affecting the pattern of the larval cuticle in *Drosophila melanogaster*. *Roux's Archives of Developmental Biology* **193**, 296-307.

Wigglesworth, V. B. (1955). The breakdown of the thoracic gland in the adult insect, *Rhodnius prolixus*. *J. Exp. Biol.* **32**, 181-214.

Wilder, E. L. and Perrimon, N. (1995). Dual functions of wingless in the *Drosophila* leg imaginal disc. *Development* **121**, 477-488.

Williams, R. L. and Urbe, S. (2007). The emerging shape of the ESCRT machinery. *Nature reviews. Molecular cell biology* **8**, 355-368.

Yanagawa, T. Y., Enya, S., Niwa, Y. S., Yaguchi, S., Haramoto, H., Matsuya, T., Shiomi, K., Sasakura, Y., Takahashi, S., Asashima, M. et al. (2011). The Conserved Rieske Oxygenase DAF-36/Neverland Is a Novel Cholesterol-metabolizing Enzyme. *J Biol Chem.* . **286**, 25756-25762.

Yao, T. P., Segraves, W. A., Oro, A. E., McKeown, M. and Evans, R. M. (1992). *Drosophila* ultraspiracle modulates ecdysone receptor function via heterodimer formation. *Cell* **71**, 63-72.

Yao, T. P., Forman, B. M., Jiang, Z., Cherbas, L., Chen, J. D., McKeown, M., Cherbas, P. and Evans, R. M. (1993). Functional ecdysone receptor is the product of *EcR* and *Ultraspiracle* genes. *Nature* **366**, 476-479.

Yoshiyama, T., Namiki, T., Mita, K., Kataoka, H. and Niwa, R. (2006). Neverland is an evolutionally conserved Rieske-domain protein that is essential for ecdysone synthesis and insect growth. *Development* **133**, 2565-2574.

Zerial, M. and McBride, H. (2001). Rab proteins as membrane organizers. *Nature reviews. Molecular cell biology* **2**, 107-117.

Zettervall, C. J., Anderl, I., Williams, M. J., Palmer, R., Kurucz, E., Ando, I. and Hultmark, D. (2004). A directed screen for genes involved in *Drosophila* blood cell activation. *Proceedings of the National Academy of Sciences of the United States of America* **101**, 14192-14197.

Zhou, L., Schnitzler, A., Agapite, J., Schwartz, L. M., Steller, H. and Nambu, J. R. (1997). Cooperative functions of the reaper and head involution defective genes in the programmed cell death of *Drosophila* central nervous system midline cells. *Proceedings of the National Academy of Sciences of the United States of America* **94**, 5131-5136.

Zinchuk, V. and Zinchuk, O. (2008). Quantitative colocalization analysis of confocal fluorescence microscopy images. *Curr Protoc Cell Biol*, Chapter 4; Unit 4.19.